



**University of
Sunderland**

Patel, Sharvil Pankaj (2007) Development of Immobilised Biopolymer Stationary Phases based on the Efflux Transporters. Doctoral thesis, University of Sunderland.

Downloaded from: <http://sure.sunderland.ac.uk/id/eprint/3756/>

Usage guidelines

Please refer to the usage guidelines at <http://sure.sunderland.ac.uk/policies.html> or alternatively contact sure@sunderland.ac.uk.

**Development of Immobilised
Biopolymer Stationary Phases based
on the Efflux Transporters**

S. P. PATEL

Ph.D

2007

Development of Immobilised Biopolymer Stationary Phases based on the Efflux Transporters

SHARVIL PANKAJ PATEL

A thesis submitted in partial fulfillment of the requirements of the
University of Sunderland for the degree of Doctor of Philosophy

This research programme was carried out in collaboration with the
National Institute of Aging, NIH, Baltimore, USA.

JULY 2007

TABLE OF CONTENTS

ABSTRACT	I
ACKNOWLEDGEMENTS	V
TABLE OF CONTENTS	VI
LIST OF FIGURES	XIII
LIST OF TABLES	XVII
ABBREVIATIONS	XIX
CHAPTER 1	1
1. GENERAL INTRODUCTION	2
1.1 Protein Affinity Chromatography	2
1.1.1 Principles and Development	2
1.1.2 The application of quantitative affinity chromatography to protein binding studies	15
1.1.3 The application of quantitative affinity chromatography using the nicotinic acetylcholine receptor (nAChR).	18
1.2 Aims and Objectives	19
CHAPTER 2	23
2. APPLICATION OF PROTEIN AFFINITY CHROMATOGRAPHY TO ANALYTICAL STUDIES	24
2.1 Use of affinity based chiral stationary phase α_1-AGP for the determination of ketamine and norketamine in human plasma	24

2.1.1	Introduction	24
2.1.1.1	<i>Preparation of AGP-CSPs</i>	25
2.1.1.2	<i>Bioanalytical Applications of AGP-CSPs</i>	26
2.1.2	Experimental	28
2.1.2.1	<i>Chemicals and reagents</i>	28
2.1.2.2	<i>Apparatus</i>	29
2.1.2.3	<i>Chromatographic conditions</i>	30
2.1.2.4	<i>Optimization of the mass selective detector (MSD) parameters</i>	30
2.1.2.5	<i>Preparation of stock solutions</i>	31
2.1.2.6	<i>Preparation of calibration curve and quality control standards</i>	31
2.1.2.7	<i>Extraction procedure</i>	32
2.1.2.8	<i>Validation</i>	32
2.1.2.9	<i>Application of the analytical method</i>	33
2.1.3	Results and Discussion	34
2.1.3.1	<i>Optimization of the chromatographic separation</i>	34
2.1.3.1.1	<i>Selection of the buffer in the mobile phase for an LC-MS application</i>	34
2.1.3.1.2	<i>Selection of the organic modifier in the mobile phase</i>	35
2.1.3.1.3	<i>Optimization of buffer pH</i>	36
2.1.3.2	<i>Optimization of the mass spectrometric detection</i>	38
2.1.3.3	<i>Extraction efficiency (% recovery)</i>	40
2.1.3.4	<i>Linearity and detection limits</i>	41
2.1.3.5	<i>Accuracy and precision</i>	42
2.1.3.6	<i>Stability</i>	43
2.1.4	Application to clinical samples	43
2.1.5	Conclusions	46
2.2	Use of immobilized $\alpha 3/\beta 4$ neuronal nicotinic acetylcholine receptor based chromatographic stationary phase in multidimensional on-line screening for ligands of $\alpha 3/\beta 4$ neuronal nicotinic acetylcholine receptor.	47
2.2.1	Introduction	47
2.2.1.1	<i>Neuronal nicotinic acetylcholine receptors</i>	49
2.2.1.2	<i>$\alpha 3\beta 4$ nAChR affinity chromatographic columns</i>	53
2.2.2	Materials and methods	54
2.2.2.1	<i>Materials</i>	54
2.2.2.2	<i>Chromatographic System</i>	55
2.2.2.3	<i>Preparation of the $\alpha 3/\beta 4$ Nicotinic Receptor Column</i>	56
2.2.2.4	<i>Chromatographic Procedures</i>	57
2.2.2.5	<i>Mass Spectrometry</i>	58

2.2.3	Results and Discussion	59
2.2.4	Conclusions	67
CHAPTER 3		68
3. P-GLYCOPROTEIN		69
3.1	Introduction	69
3.1.1	Structure of P-glycoprotein (ABC Transporter)	72
3.1.2	Mechanism of Pgp Transport	76
3.1.3	ATP and Substrate Binding sites	77
3.1.4	Substrate Recognition	81
3.1.5	Pgp mediated drug-drug interactions	84
3.1.6	Effects of chemotherapy on Pgp expression	85
3.1.7	Importance of Pgp in Drug Discovery	86
3.1.8	Role of P-Glycoprotein in pharmacokinetics and pharmacodynamics	88
3.1.9	Distribution of intestinal Pgp	89
3.1.10	Role of intestinal Pgp in drug absorption	89
3.1.11	Localization of Pgp in brain	90
3.1.12	Role of Pgp in brain uptake	90
3.1.13	Bioavailability & drug design	91
3.1.14	Comparison of <i>in-vitro</i> screening assays for Pgp	92
3.1.15	Aims & Objectives	95
3.2	Evaluation of doxorubicin toxicity in Pgp-(+)LCC6/MDR1 vs. Pgp(-) LCC6 human breast cancer cells.	96
3.2.1	Introduction	96
3.2.2	Cell culture	96
3.2.3	Experimental	97
3.2.4	Results & Discussion	98
3.2.5	Conclusion	101
3.3	Substrate accumulation of vinblastine in Pgp (+) LCC6/MDR1 vs. Pgp(-) LCC6 Human breast cancer cells.	101
3.3.1	Introduction	101
3.3.2	Experimental	103
3.3.3	Results & Discussion	103
3.3.4	Conclusion	105

3.4	Preparation of and frontal chromatographic studies with IAM based columns with Pgp(+) and Pgp(-) membranes	106
3.4.1	Introduction	106
3.4.2	Experimental	106
3.4.2.1	<i>Materials</i>	106
3.4.3	Preparation of Pgp(-) and Pgp(+) membranes	107
3.4.3.1	<i>Cell lines</i>	107
3.4.3.2	<i>Solubilization of the membranes</i>	107
3.4.4	Preparation of chromatographic column	108
3.4.5	Chromatographic system	109
3.4.6	General procedures	109
3.4.7	Results and Discussion	110
3.4.7.1	<i>Characterisation of the immobilized Pgp-IAM column</i>	110
3.4.8	Conclusion	114
3.5	Pgp PEEK Columns (Vanadate Trap)	115
3.5.1	Introduction	115
3.5.2	Experimental	117
3.5.2.1	<i>Preparation of membranes</i>	117
3.5.2.2	<i>Preparation of chromatographic column</i>	117
3.5.2.3	<i>Vanadate-trapping</i>	117
3.5.3	Results and Discussion	118
3.5.4	Conclusion	120
3.6	Caco-2 permeability measurements and stimulation of membrane-based ATPase activity.	121
3.6.1	Materials	121
3.6.2	Caco-2 assay	122
3.6.3	Membrane based ATPase assay	124
3.7	Preparation of open tubular (OT) based columns with Pgp(+) and Pgp(-) membranes and frontal chromatographic studies with radio-labelled markers.	125
3.7.1	Introduction	125
3.7.2	Materials	126
3.7.3	Preparation of Pgp(-) and Pgp(+) membranes	127
3.7.3.1	<i>Cell lines</i>	127
3.7.3.2	<i>Solubilization of the membranes</i>	127
3.7.4	Immobilization of the Pgp membranes on the open tubular capillary	128

3.7.4.1	<i>Preparation of the capillary</i>	128
3.7.4.2	<i>Immobilization using biotin-X</i>	129
3.7.4.3	<i>Reagent removal</i>	130
3.7.5	Chromatographic system	131
3.7.6	General procedures	131
3.7.7	Calculation of dissociation constants	132
3.7.8	Results and Discussion	133
3.7.8.1	<i>Characterization of the immobilized Pgp(+)-OT</i>	133
3.7.8.2	<i>Effect of ATP on the chromatographic properties of the Pgp(+)-OT column</i>	139
3.7.9	Conclusion	140
3.8	Rapid-frontal chromatography with mass spectrometric detection	142
3.8.1	Introduction	142
3.8.2	Chromatographic system	142
3.8.3	Chromatographic conditions	143
3.8.4	General procedures	143
3.8.5	Results and Discussion	144
3.8.5.1	<i>Comparison of rapid frontal chromatography using the Pgp(+)-OT and Pgp(-)-OT with Caco-2 permeability measurements and stimulation of membrane-based ATPase activity.</i>	144
3.9	Conclusion	154
CHAPTER 4		156
4. ORGANIC CATION TRANSPORTER (OCT)		157
4.1 Introduction		157
4.1.1	Overview	157
4.1.2	Conserved Amino Acids in the OCT-Family	160
4.1.3	Functional properties of expressed cation transporters	162
4.1.4	OCT1 and OCT2 type distribution	167
4.2 Drug Uptake studies for hOCT1 & MDCK cell lines		171
4.2.1	Experimental	171
4.2.1.1	<i>Materials</i>	171
4.2.1.2	<i>Method</i>	171

4.3	Preparation of IAM based columns with MDCK and hOCT1 membranes	172
4.3.1	Materials	172
4.3.2	Preparation of hOCT1(-) and hOCT1(+) membranes	173
4.3.2.1	<i>Cell lines</i>	173
4.3.3	Solubilization of the membranes	173
4.3.4	Immobilization of the solubilized membranes	174
4.4	Frontal chromatography with radio-labeled markers	175
4.4.1	Chromatographic system	175
4.4.2	Determination of binding affinities using frontal chromatography	175
4.4.3	Chromatographic studies:	176
4.4.4	Data analysis	176
4.5	Membrane Binding Assays	177
4.6	Pharmacophore – Methods	178
4.7	Results and Discussion	179
4.7.1	Characterization of the hOCT1 and MDCK cell lines	179
4.7.2	Characterization of the immobilized hOCT1(+)-IAM	180
4.7.3	Enantioselectivity on the hOCT1 column	189
4.7.4	Drug transport on the hOCT1 column	202
4.8	Conclusion	204
CHAPTER 5		206
5. CONCLUSION AND SUGGESTION FOR FUTURE WORK		207
CHAPTER 6		211
6. REFERENCES		212
CHAPTER 7		235
7. APPENDICES		236

7.1	Papers	236
7.2	Chapters	237
7.3	Abstracts & Presentations	237
7.4	Conferences	238

LIST OF FIGURES

- Figure 1. A typical ABC protein containing two transmembrane domains (TMs). 3
- Figure 2. The chemical structure of the monolayer that is covalently bound to the silica on the IAM-PC particles (12 micron, 300 Å pores). 8
- Figure 3. Schematic of a zonal chromatogram depicting the movement of the analyte through the chromatographic bed in concentration zones. 10
- Figure 4. Schematic of a frontal chromatogram showing a saturation binding curve of the marker ligand when placed in the mobile phase and passed through the chromatographic column. 11
- Figure 5. A representative non-linear regression plot of [concentration] M vs. [conc](V - V_{min}) that results from the data obtained from frontal chromatography which is used to derive the dissociation constant K_d and the number of active binding sites B_{max}. 14
- Figure 6. The relationship between the chromatographic retention, expressed as k', on a chiral stationary phase containing immobilized human serum albumin (HSA-CSP) and percent protein binding to free human serum albumin for a series of 18 benzodiazepines. 17
- Figure 7. Chemical structures of cationic drugs ketamine, norketamine and bromoketamine (anaesthetic agent shown to induce analgesia by non-opioid mechanism). 27
- Figure 8. Representative chromatogram of the low quality control plasma sample (LQC) containing 5 ng/ml of (R)-Ket, (S)-Ket, (R)-norKet and (S)-norKet and 100ng/ml of (R)-BrKet and (S)-BrKet. 37
- Figure 9. Representative chromatograms of drug-free plasma obtained using single ion monitoring for Ket at $m/z = 238.1$ (A), norKet $m/z = 224.1$ (B) and BrKet $m/z = 284.0$ (C). 39
- Figure 10. The chromatograms from the analysis of plasma samples from a patient obtained before the administration of Ket and 15 min after the administration of an infusion of 60 ng/ml. 44
- Figure 11. Plasma concentrations of the enantiomers of ketamine, (R)-Ket and (S)-Ket, in two patients before and after dosing period 1 and dosing period 2. 45

Figure 12. Transverse schematic representation of the muscle-type AChR showing the domains involved in the specific binding of non-competitive inhibitors from exogenous origin.	50
Figure 13. The multidimensional coupled-column chromatographic system used in this study.	55
Figure 14. A representative chromatogram from the chromatography of epibatidine on: a. the NR column alone; b. the multidimensional system produced after injection of a 1 μ M solution of epibatidine using SIM analysis at [M + H] 209.	62
Figure 15. The chromatogram from the chromatography of the Test Mixture on the multidimensional system. Compound list in	64
Figure 16. Schematic Model of Pgp showing two homologous halves.	74
Figure 17. Two ATP-binding domain(s), which are also called nucleotide-binding folds (NBFs) and are located on the cytoplasm side of the phospholipid bilayer.	78
Figure 18. Pgp transporter consisting of 655 amino acids. The Walker A and B motifs of the NBF are circled.	79
Figure 19. Plot of log [doxorubicin] (nM) vs. cell survival at different concentrations of cytotoxic drug doxorubicin for Pgp(+) cell line and the Pgp(-) cell line.	100
Figure 20. Molecular structure of vinblastin (Vinca alkaloid).	102
Figure 21. Vinblastine molecule bound to the ligand binding domain in the cavity of the Pgp transporter.	104
Figure 22. A. IAM chromatography packing material composed of single chain ether phospholipids containing ω -carboxyl groups in the alkyl chain immobilized on aminopropyl silica.	111
Figure 23. Comparison of the frontal chromatograms of 0.5 nM [3 H]-Vb (5ml) on the LCC6/MDR1 Pgp(+)-IAM-column (red), LCC6 Pgp(-)-IAM column (blue) and IAM column (green).	112
Figure 24. ATP dependant Pgp transport cycle showing Pgp transporter in its different transformational states.	116
Figure 25. Effect of vanadate trapping on a the retention of Vb on a Pgp(+)-IAM PEEK tubing column.	119
Figure 26. Schematic for the preparation of the open tubular column.	129

Figure 27. Structure of Ketoconazole and vinblastine know substrates of Pgp.	134
Figure 28. Frontal chromatographic study of the displacement of [³ H]-vinblastine by ketoconazole on the Pgp(+)-OT column.	136
Figure 29. Frontal chromatographic study of the retention of [³ H]-vinblastine on the Pgp(+)-OT column (chromatogram A) and Pgp(-) -OT column (chromatogram B).	138
Figure 30. The frontal chromatographic traces produced by A: loratadine, B: nicardipine, C: tamoxifen, on Pgp(+)-OT and Pgp(-)-OT.	151
Figure 31. Schematic of the secondary structure of the OCT1 protein.	159
Figure 32. [¹⁴ C]-TEA efflux studies carried out on hOCT1-MDCK (+) cell line and MDCK (-) cell line.	180
Figure 33. Comparison of the frontal chromatograms of 20 pM [³ H]-MPP on the hOCT1-column (red) and on the MDCK-column (hOCT1-(-)) (black) showing the front and plateau regions for each column.	182
Figure 34. The effect of the addition of increasing concentrations of nicotine on the chromatographic retention of 20 pM [³ H]-MPP ⁺ on the hOCT1(+)-IAM column from no nicotine in the mobile phase (black trace), to 10 μM cold nicotine in the mobile phase (blue trace) to 20 μM cold nicotine in the mobile phase (green trace).	184
Figure 35. The relationship between chromatographic retention volume expressed as (V - V _{min}) and increasing mobile phase concentrations of nicotine on the hOCT1(+)-IAM column.	185
Figure 36. Frontal affinity chromatography showing enantioselectivity for the enantiomers of verapamil.	190
Figure 37. The structure of the enantiomers of propranolol, atenolol, psuedoephedrine, α-methylbenzylamine and verapamil used in this study.	192
Figure 38. The chromatographic traces from the frontal competitive displacement of 10 pM [³ H]-MPP carried out using a stationary phase containing immobilized membranes obtained from the hOCT1-MDCK cell line that express a human organic cation transporter.	194
Figure 39. Determination of the binding affinity, K _d value, of (+)-(R)-propranolol for the immobilized human organic cation transporter calculated using Eqn. 1 and the effect of the addition of increasing concentrations of (+)-(R)-propranolol on the chromatographic retention of [³ H]-N-methyl 4-phenyl pyridinium.	195

Figure 40. The inhibition of the intercellular uptake of [¹⁴C]-tetraethyl ammonium by increasing concentrations of (-)-(S)-propranolol {■} or (+)-(R)-propranolol {Δ} in the hOCT1-MDCK cell line. (n = 3) 198

Figure 41. Preliminary pharmacophore that describes the enantioselective binding interactions observed in this study. 200

Figure 42. Drug uptake studies on the hOCT1(+) and MDCK cell lines where each cell line was treated with 1 μm of the following ligands: [³H]-propranolol, [³H]-verapamil, [³H]-dopamine, [³H]-MPP, [³H]-metamphetamine and [³H]-nicotine. 203

LIST OF TABLES

Table 1. Summary of validation statistics for ketamine	40
Table 2. Summary of validation statistics for norketamine	41
Table 3. The compounds used in this study, their respective affinities for the $\alpha 3/\beta 4$ nAChR defined as yes if the compound is reported to bind to the receptor and no if it is not reported to bind to the receptors and the observed retention times on the column containing immobilized $\alpha 3/\beta 4$ nAChR..	59
Table 4. Compounds eluting from the column containing immobilized $\alpha 3/\beta 4$ nAChR before 8 min and after 8 min..	65
Table 5. Fisher's Exact Test to determine, "Can the multidimensional system distinguish between ligands and non-ligands to the immobilized $\alpha 3/\beta 4$ nAChR using a retention time of 8 min as the selector?"	66
Table 6. A wide range of Pgp substrates, majority of which are known cardiovascular and anti-cancer drugs, depicting the broad substrate specificity of the Pgp transporter and showing the importance of Pgp in drug resistance.	82
Table 7. Cell Survival (%) at different concentrations of cytotoxic drug doxorubicin.	99
Table 8. Vinblastine accumulation was carried out on Pgp (+) and Pgp (-) cells and then measured by scintillation counting in disintegrations per minute (DPM).	105
Table 9. Comparison of K_d values determined on the Pgp-OT column with those obtained on the Pgp-IAM and membrane binding studies.	135
Table 10. Effect of ATP on the retention of ^3H -CysA for Pgp-(+) and Pgp(-) OT columns.	139
Table 11. Results from the Caco-2 permeability, ATPase membrane and chromatographic assays conducted in this study.	147
Table 12. Binding affinities expressed as K_d values (μM) calculated by frontal affinity chromatography using the immobilized hOCT1(+)-IAM column, compared to K_i 's calculated by uptake studies.	186
Table 13. The binding affinities (K_d) of the compounds used in this study for the immobilized human organic cation transporter obtained using frontal displacement chromatography with [^3H]-MPP ⁺ as the marker ligand.	196

Table 14. The calculated distances between the middle of the aromatic ring (Ar), the amine nitrogen atom (N) and the oxygen atom of the hydroxyl group (O) for the compounds used in this study (n = 3). 199

ABBREVIATIONS

ABC	ATP-binding cassette
TM, TMD	transmembrane domain
NBF	nucleotide binding folds
Pgp	P-glycoprotein
CSP	chiral stationary phase
ACTH	α chymotrypsin
TRYP	trypsin
IAM	immobilized artificial membrane
AGP	α_1 - acid glycoprotein
PC	phosphatidyl choline
K_d	dissociation constant
k'	retention time
CPM	counts per minute
B_{max}	no of active binding sites
nM	nanomolar
μ M	micromolar
HAS	human serum albumin
nAChR	nicotinic acetylcholine receptor
HTS	high throughput screening
GPCRs	G-protein coupled receptors
ORM	orosomuroid
LC-MS	liquid chromatography-mass spectrometry
Ket	ketamine
SIM	single ion monitoring
MSD	mass selective detector
norKet	norketamine
BrKet	bromoketamine
QC	quality control
LQC	low quality control
MQC	medium quality control
HQC	high quality control
SPE	solid phase extraction
α	enantioselectivity
FIA	flow injection analysis
LLOQ	lower limit of quantification
LOD	limit of detection
S/N	signal to noise ratio
CV	coefficient of variance
TID	trifluoromethyl-iodophenyldiazirine
CPZ	chlorpromazine
TPMP+	triphenylmethylphosphonium
PCP	phencyclidine
NCI	non-competitive inhibitor

$\alpha 3\beta 4$ -nAChR or $\alpha 4\beta 2$ nAChR	NR columns
FS	full scan
MDR1	multidrug resistant gene 1
MDR3	multidrug resistant gene 3
CNS	central nervous system
NBD	nucleotide binding domain
MRP1	multi resistant protein 1
L_0	linker region
BCRP	breast cancer resistant protein
ATP	adenosine triphosphate
QSAR	quantitative structure activity relationship
SNP	single nucleotide polymorphism
BBB	blood brain barrier
CYP	cytochrome P450
RH	relative humidity
Pgp	P-glycoprotein
Vb	vinblastine
DTT	dithiothreitol
CHAPS	3-[3-(cholamidopropyl)dimethylammonio]-1-propane sulfate
PMSF	phenyl methyl sulfonyl fluoride
Trisma	tris[hydroxymethyl]aminomethane
APTS	aminopropyltrimethoxy silane
Biotin-X	6-[(biotinoyl)amino] hexanoic acid
DMEM	delbecco's modified eagles medium
Caco-2	human colorectal adenocarcinoma cells
TEER	trans-epithelial electric resistance
SDS	sodium dodecyl sulphate
OT	open tubular
CysA	cyclosporine A
Bq	becquerel
BCA	bicinchoninic acid
NMN	N-methylnicotinamide
SLC	solute carrier
OCT	organic cation transporter
HEK	human embryonic kidney cells
kDa	kilodalton
hOCT	human organic cation transporter
TEA	tetra ethylammonium
MPP	1-methyl-4-phenylpyridinium
K_m	metabolism constant
K_i	inhibition constant
rOCT	rat organic cation transporter
TAA	tetraalkylammonium
Log P	partition coefficient
BLM	basolateral membrane

FBS	foetal bovine serum
MDCK	Madin-Darby canine kidney
MEM	minimum essential medium
HPLC	high performance liquid chromatography
pM	picomolar

Chapter 1

1. General Introduction

1.1 Protein Affinity Chromatography

1.1.1 Principles and Development

In the last decade considerable attention has been focused on the role played by drug transporters in a drug's therapeutic and toxic profiles. Because of their importance in pharmacokinetics and bioavailability, the screening of a lead drug candidate for interactions with drug transporters has been incorporated into the drug development process. Transporters also play a role in the development of multiple drug resistance and are targets for new drug discovery.

One superfamily of protein transporters is the ATP-binding cassette (ABC) class of proteins. They are the largest class of transporters, appear in every cell, and are arguably the most important family of membrane transport proteins. First identified over thirty years ago in prokaryotes, these proteins hydrolyze ATP in order to power the transportation of mostly hydrophobic compounds. An example of an ABC transporter can be seen in Figure 1.

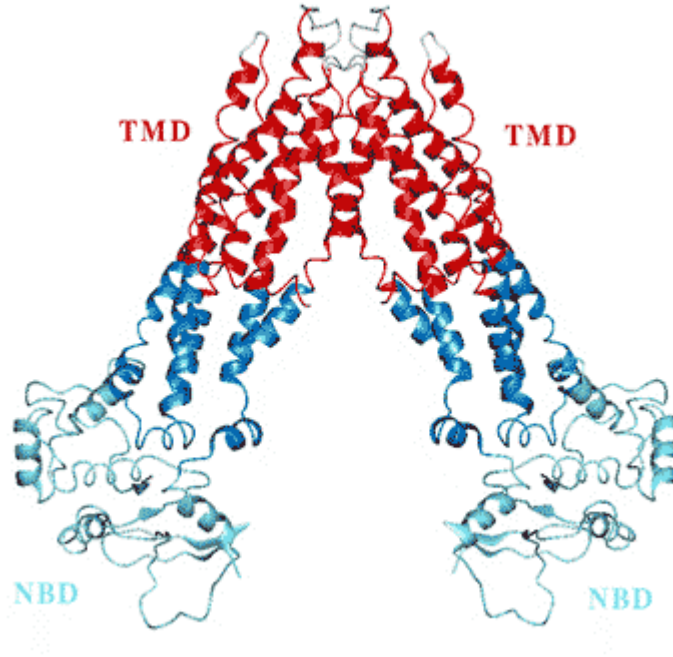


Figure 1. A typical ABC protein containing two transmembrane domains (TMs). Each domain consisting of α -helices which 'criss cross' the phospholipid bilayer, forming between between six to eleven (usually six), membrane-spanning regions. All ABC proteins also contain either two ATP-binding domain(s), which are also called nucleotide-binding folds (NBFs) and are located on the cytoplasm side of the phospholipid bilayer.

ABCs are mostly unidirectional, meaning they only function in one direction. In bacteria, they mainly pump essential compounds such as sugars, vitamins, metal ions, etc. into the bacteria. These transporters are called importers. In eukaryotes, ABCs mainly move compounds from within the cytoplasm to the outside of the cell or into a membrane bound organelle (endoplasmic reticulum, mitochondria, peroxisomes, etc.). These transporters are called exporters. ABC transporters are largely dispersed

throughout the genome and have an extremely wide variety of uses. For example lipid flippases work by flipping a lipid from the inner phospholipid membrane to the other phospholipid membrane.

P-glycoprotein (Pgp) is one of the most important and best characterized member of the ABC transporter family and has a high expression in various tissues. In addition, Pgp is also a pharmacological target because of its anatomical localization in relation to the sequence of drug movement, i.e. cellular uptake, intracellular distribution, metabolism and excretion.

Various approaches have been used for the study of Pgp function. However, it is difficult to classify test compounds as Pgp substrates and/or inhibitors by a single assay, as different experimental systems and test conditions produce different classifications. Also this process is very laborious and time consuming. The topic of the research programme therefore involves a new approach to the classification of drug candidates as Pgp substrates and/or inhibitors, as well as the investigation of the functionality of this membrane transporter.

The approach utilized in this work is based upon affinity chromatography. The mechanism of affinity separations is most often described by a “lock and key” analogy. Retention depends on complementarity of a ligand molecule (the “key”) and a specific binding site (the “lock”) with high affinity for the ligand. Typically the molecule containing the binding site is a protein, although some nucleic acid interactions may also be useful. The ligand can be a small molecule, a carbohydrate, another protein, a prosthetic group, a specific amino acid sequence in a protein, or a specific nucleotide

sequence. There are virtually an unlimited number of affinity separations that can be used, the only requirement being a strong and specific binding interaction that is in some way reversible.

In some cases the ligand is covalently bound to the stationary media. The affinity adsorbent thus constructed can be used to specifically scavenge proteins or other macromolecules containing a binding site from a sample which may be a complex mixture containing many other non-binding molecules. This strategy has been used to isolate proteins with binding sites for specific cofactors, enzyme inhibitors, cell-surface carbohydrates, and nucleic acid sequences, among other possibilities.

In other cases a protein with affinity for a specific ligand or sequence is covalently bound to the media and used to scavenge the ligand, or a molecule to which the ligand is covalently attached, from solution. This approach has much in common with the fundamental processes of drug action, absorption, distribution, excretion and receptor activation which are dynamic in nature and have similarities with the basic mechanisms involved in chromatographic distribution. Indeed, the same basic intermolecular interactions (hydrophobic, electrostatic, hydrogen bonding) determine the behaviour of chemical compounds in both biological and chromatographic environments. (Kaliszan & Wainer, 1997)

The relationships between pharmacological and chromatographic processes have been emphasized by the inclusion of a wide variety of proteins as active components of chromatographic systems, in the creation of protein-based stationary phases. The extreme complexity of biological systems limits rational design of an individual

chromatographic system that would directly mimic a total biological system. However, construction of the right protein-based stationary phase can readily yield a great amount of diversified, precise and reproducible data about key aspects of that system. The possibilities are only limited by the ability to create and use unique phases. In addition, the ability of enzymes and carrier proteins to act as chiral selectands has been extensively used in drug development, as well as adapted for use in the chromatographic sciences.

An example of the utility of the latter approach is the creation of *chiral stationary phases (CSPs)* through the immobilization of biopolymers on chromatographic backbones. These CSPs have been based upon enzymes and carrier proteins and used primarily in liquid chromatographic systems. The use of biopolymeric based CSPs has been particularly valuable in the quantification and separation of small chiral compounds on an analytical scale (Lough & Wainer 2002; Wainer 1993)

In general, two approaches have been used in the construction of biopolymer-based CSPs – covalent immobilization and entrapment/adsorption. The enzymes α -chymotrypsin (ACHT), trypsin (TRYP) and cellobiohydrolase I have been covalently attached to silica supports (Marle *et al.*, 1992, 1991; Jadaud *et al.*, 1989, Thelohan *et al.* 1989). ACHT and TRYP have been entrapped in the interstitial spaces of an immobilized artificial membrane stationary phase (IAM) (Chui & Wainer 1992, Kolbah & Wainer 1993), while ACHT has been adsorbed on LiChrospher phases (Marle *et al.* 1992). The carrier protein phases have been synthesized using entrapment followed by cross-linking as in the case of α_1 acid glycoprotein (AGP) (Wainer 1989) or through

covalent immobilization used when immobilizing serum albumin (Hage & Austin 2000, Domenici *et al.*, 1990).

Biopolymeric based CSP's have also found a use in pharmacological applications. The immobilization of proteins has also been widely studied and a variety of covalent and non-covalent immobilization techniques have been developed. In addition, the experimental approaches to the isolation and purification of receptors from biological matrices have been extensively studied and discussed.

It has been demonstrated in recent work that these techniques can be used to immobilize transporter proteins such as the P-glycoprotein transporter (Pgp) (Zhang *et al.* 2000), carrier proteins such as human serum albumin (HSA) (Noctor *et al.* 1993) and receptor proteins such as nicotinic acetylcholine receptors (Moaddel *et al.* 2002). The nicotinic receptor and Pgp were immobilized via hydrophobic insertion into the interstitial spaces of an immobilized artificial membrane (IAM) stationary phase (Figure 2). The IAM is comprised of silica particles (12 μm id with 300 Å pores) to which phospholipid analogues, with functional head groups, have been covalently coupled in a monolayer.

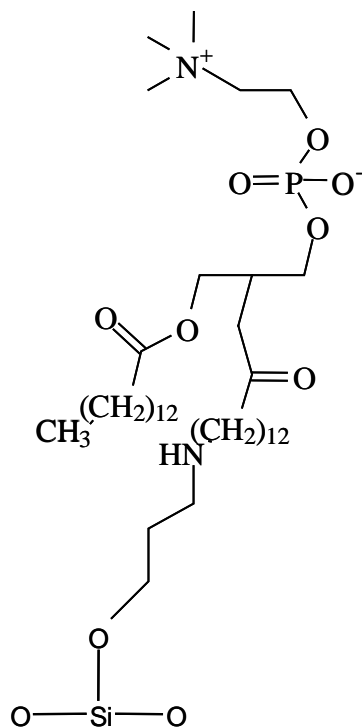


Figure 2. The chemical structure of the monolayer that is covalently bound to the silica on the IAM-PC particles (12 micron, 300 Å pores).

The specific feature of IAM beads is its resemblance to a hydrophobic environment that allows immobilization of membrane proteins and receptors. The IAM stationary phase used in these studies was commercially available from Regis Technologies (Morton Grove, IL, U.S.A.) as the IAM-phosphatidyl choline (IAM-PC) stationary phase.

The stationary phases were characterized using zonal and frontal chromatographic experiments. Binding affinities (expressed as dissociation constants, K_d 's) were determined using the stationary phases and in some cases a mixtures of ligands were resolved according to their relative affinities. The immobilized proteins retained their ability to bind and/or transport ligands and were suitable for determining the

pharmacological activities of the tested ligands. Thus, it is conceivable to envision the creation of a wide variety of immobilized-receptor phases.

The protein based stationary phases can be employed for quantitative affinity chromatography, a theoretical approach to the use of protein-based stationary phases as probes of ligand-protein and protein-protein interactions. The two predominant methods for the analysis are zonal affinity chromatography and frontal affinity chromatography. In the case of zonal affinity chromatography a small sample volume is injected into the mobile phase and the analyte (or analytes) move through the column in concentration zones. The shape of the chromatographic peak produced by this process represents an equilibrium process defined by the association and dissociation rate constant while the retention volume represents the total of specific and non-specific interactions of the solute with the stationary phase. Refer to Figure 3.

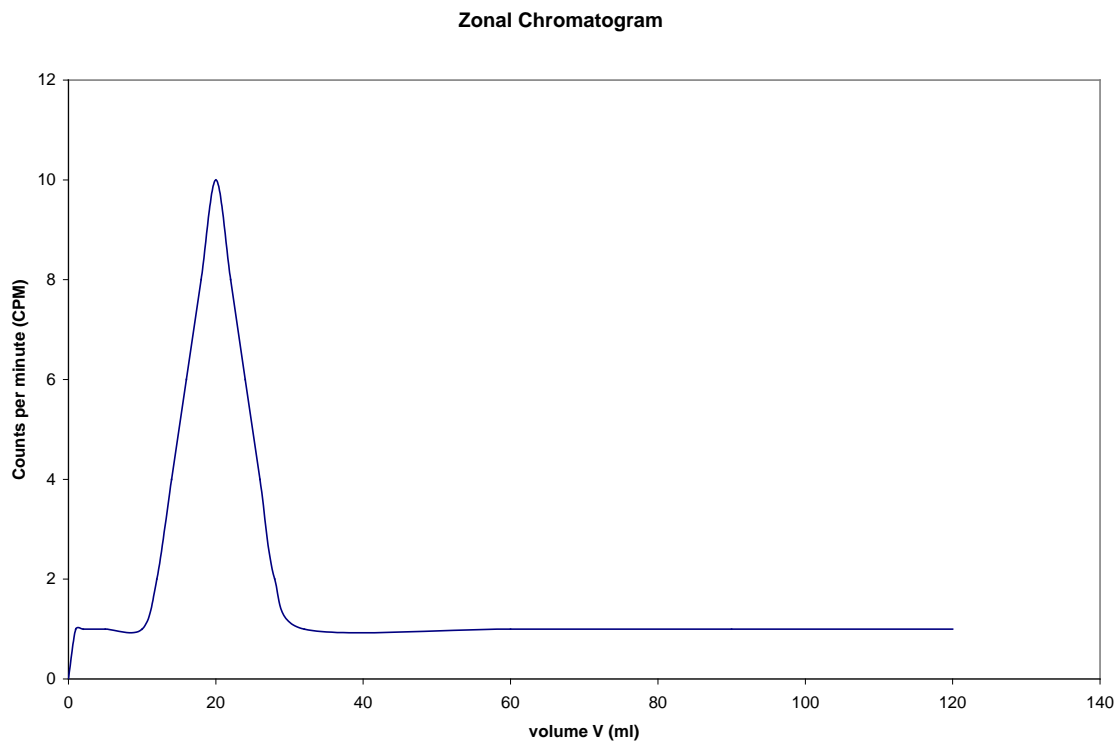


Figure 3. Schematic of a zonal chromatogram depicting the movement of the analyte through the chromatographic bed in concentration zones. The process represents an equilibrium process defined by the association and dissociation rate constant. The retention time k' , can be measured as the time at which the counts per minute (e.g. if radioactivity detection was being used) are at the peak (maximum).

This technique can also be used to study the binding of drugs and other solutes on immobilized protein columns, to determine drug-drug protein binding interactions and in the development of quantitative structure-retention relationships that describe these binding processes. Information on the kinetics of solute-protein interactions can also be obtained if appropriate data are collected on the width and retention of solute peaks under various flow rate conditions.

In frontal affinity chromatography a larger sample volume is required than zonal elution. A marker ligand is placed in the mobile phase and passed through the column. The frontal regions are composed of the relatively flat initial portion of the chromatographic traces, which represent the nonspecific and specific binding of the marker to the cellular membranes and the target (Figure 4). The saturation of the target by the marker produces a steep rise in the chromatographic trace, which ends, or plateaus, when the target is saturated.

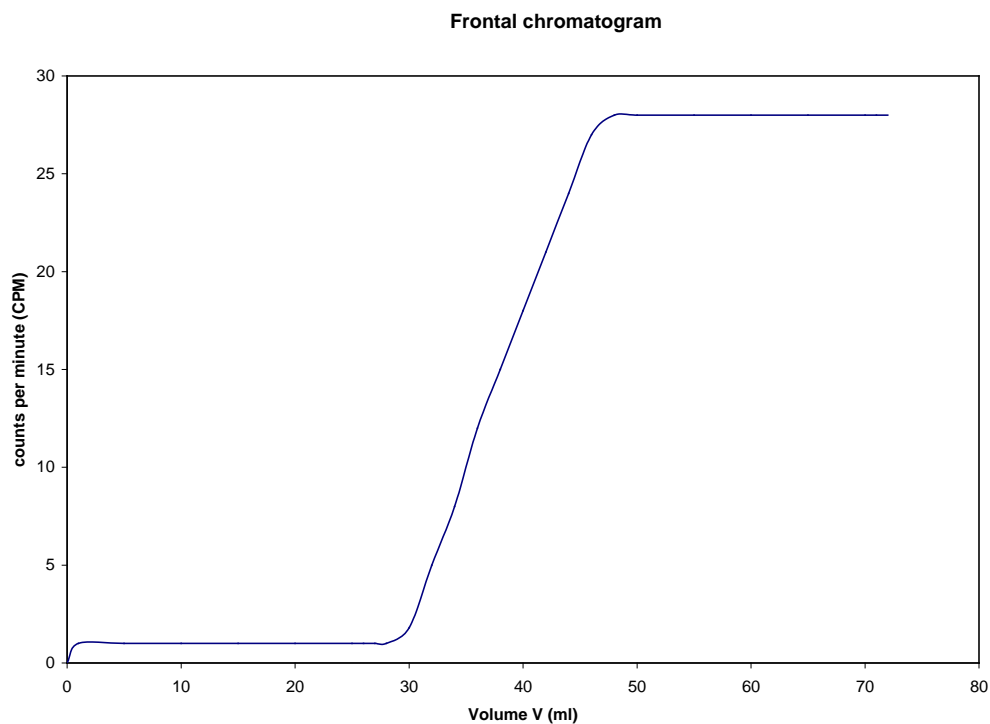


Figure 4. Schematic of a frontal chromatogram showing a saturation binding curve of the marker ligand when placed in the mobile phase and passed through the chromatographic column. The plot looks like the familiar sigmoidal dose-response curve or is described as a rectangular hyperbola or a binding isotherm curve.

Frontal affinity chromatography can be used to calculate the dissociation constant K_d and the number of active binding sites B_{max} .

The K_d value is used to describe how tightly a ligand (such as a drug) binds to a protein. Such binding is usually non-covalent, i.e., no chemical bonds are made or broken. Since the binding is usually described by a two-state process



the corresponding dissociation constant is defined

$$K_d = \frac{[P][L]}{[C]}$$

where [P], [L] and [C] represent the concentrations of the protein, ligand and bound complex, respectively. The K_d has the units of concentration (M), and corresponds to the concentration of ligand [L] at which the binding site on the protein is half occupied, i.e., when the concentration of protein with ligand bound [C] equals the concentration of protein with no ligand bound [P]. The smaller the dissociation constant, the more tightly bound the ligand is; for example, a ligand with a nanomolar (nM) dissociation constant binds more tightly than a ligand with a micromolar (μ M) dissociation constant.

K_d and B_{max} values can be obtained from frontal chromatographic data using one of two models, a) linear regression model or b) non-linear regression model. (Gottschalk *et al.*, 2002)

For the linear regression model, the association constants of the competitive ligands (CL), K_{CL} , as well as the number of the active and available binding sites of immobilized receptors, B_{max} , were calculated using the following equations [(1) and (2)]

$$(V_{max}-V)^{-1}=(1+[M]K_M)(V_{min}[B_{max}]K_M)^{-1}+(1+[M]K_M)^2(V_{min}[B_{max}]K_MK_{CL})^{-1}[\text{drug}]^{-1} \quad (1)$$

$$(V-V_{min})^{-1}=(V_{min}[B_{max}]K_{CL})^{-1}+(V_{min}[B_{max}])^{-1}[M] \quad (2)$$

where, V is the retention volume of the marker ligand (M); V_{max} the retention volume of M at the lowest concentration and in the absence of drugs; V_{min} the retention volume of M when the specific interaction is completely suppressed. The value of V_{min} is determined by running M in a series of concentration of drugs and plotting $1/(V_{max}-V)$ versus $1/[CL]$ extrapolating to infinite $[CL]$. From the above plot and a plot of $1/(V-V_{min})$ versus $[M]$, dissociation constant values, K_d , for M and CL can be obtained as can the number of active binding sites on the immobilized protein $[B_{max}]$.

In the non-linear regression model the relationship between displacer concentration and retention volume can be established using Equation 3 and can be used to determine the K_d value of the displacer and the number of active binding sites, B_{max} .

$$[X] (V - V_{min}) = B_{max} [X] (K_{dx} + [X])^{-1} \quad (3)$$

where: V is retention volume of drug (displacer); V_{\min} , the retention volume of drug (displacer) when the specific interaction is completely suppressed (this value can be determined by running the drug with a high concentration of displacer).

An example of a non-linear regression model is shown in Figure 5, where $[X] (V - V_{\min})$ is plotted vs $[X]$. The plateau represents the B_{\max} where all the sites are saturated and 50% of the B_{\max} represents the K_d .

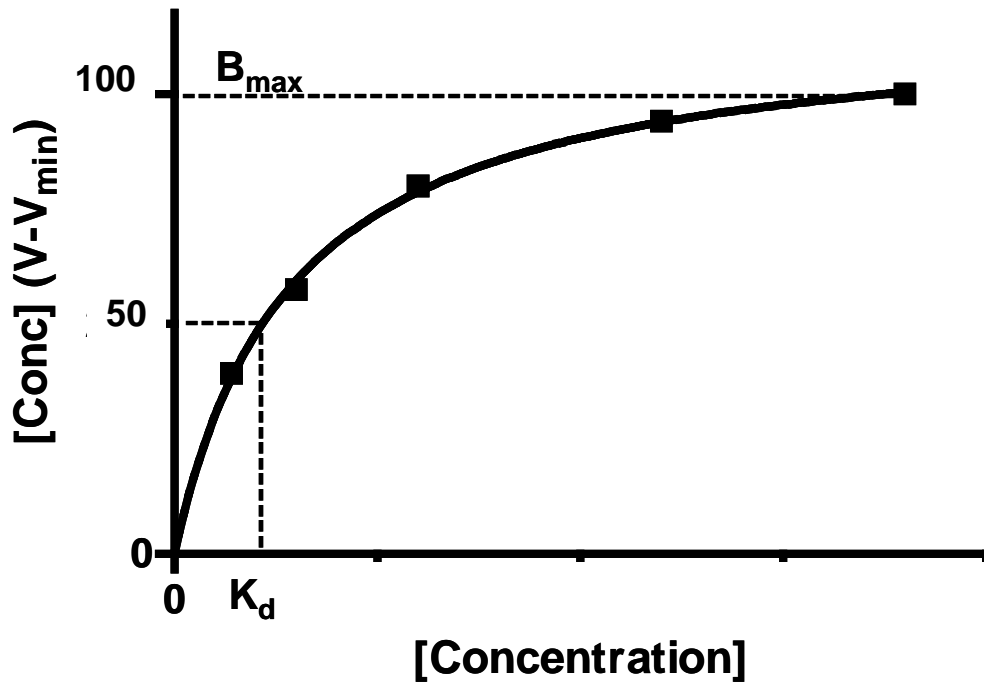


Figure 5. A representative non-linear regression plot of [concentration] M vs. [conc](V- V_{\min}) that results from the data obtained from frontal chromatography which is used to derive the dissociation constant K_d and the number of active binding sites B_{\max} .

In affinity chromatography various isotherm equations may arise according to the chemical system considered. For the interaction of the solute and the immobilized ligand, non equilibrium conditions must be taken into account. The association constants measured between the solute and the immobilized ligand are hardly comparable to the solvated conditions. Thus the trend is then to produce immobilized ligands with affinity properties as close as possible to those of the free ones, to decrease the nonspecific interactions of the support itself. Frontal affinity chromatography decreases the nonspecific interactions between the solute and the immobilized ligand as it saturates the column. Thus for measuring the equilibrium constants of complicated systems frontal elution is a powerful tool, since the amount of interacting biopolymers/compounds at equilibrium is easily related to the chromatographic data.

1.1.2 The application of quantitative affinity chromatography to protein binding studies

The interaction of small solutes with proteins is important in many biological processes. Examples include the action of enzymes upon substrates and the binding of hormones with their receptors. The binding of drugs and other compounds with serum proteins is yet another example of such a process. Protein binding in blood is important in determining the eventual activity and fate of drugs once they have entered the circulation. These interactions, in turn, help control the distribution, rate of excretion, and toxicity of drugs in the body. In addition, the presence of direct or indirect competition between two drugs or a drug and endogenous compound (e.g. fatty acid)

for the same binding proteins can be an important source of drug–drug interactions or drug displacement effects. For all of these reasons, it is important to have a good understanding of how pharmaceutical agents bind to serum proteins and of how these interactions are affected by other substances.

Zonal chromatographic techniques have been used with the human serum albumin chiral stationary phases (HSA-CSP) for the direct determination of the percent of a compound bound to HSA (Noctor *et al.* 1993). A series of benzodiazepines and a series of coumarin derivatives were chromatographed on the HSA-CSP and the retention time of each compound (expressed as k') was compared to the percent of the compound bound to HSA determined by ultrafiltration techniques. The values were correlated by plotting $k'/(k' + 1)$ versus percent bound to HSA to make the plot linear and correlation factors of 0.999 were obtained for both series (Figure 6).

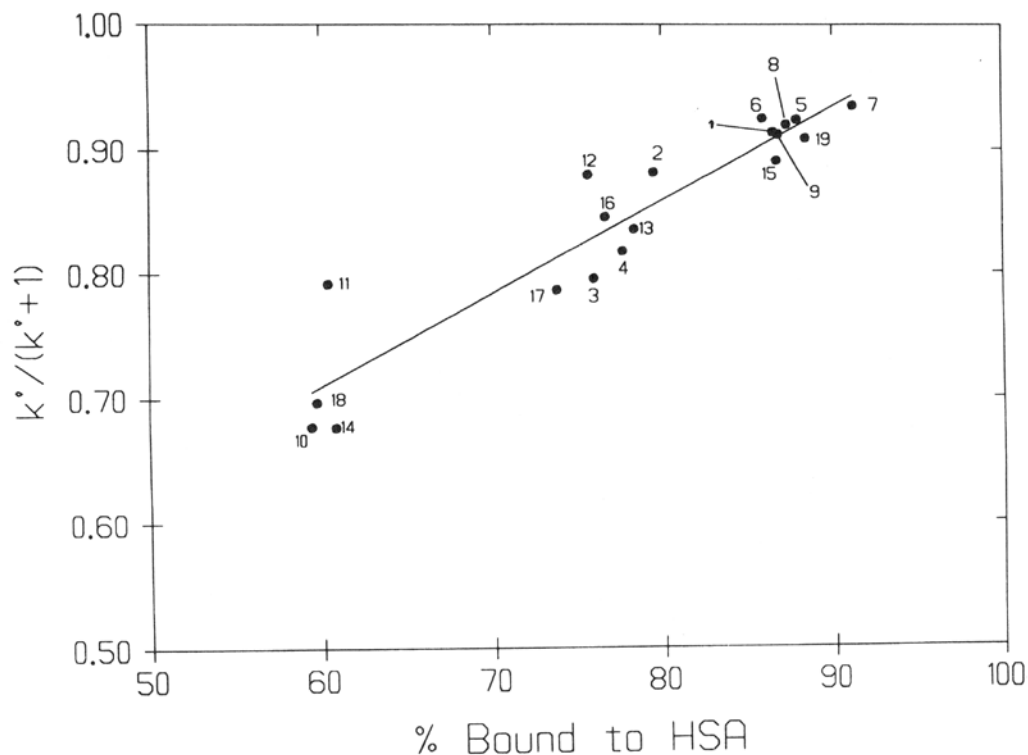


Figure 6. The relationship between the chromatographic retention, expressed as k' , on a chiral stationary phase containing immobilized human serum albumin (HSA-CSP) and percent protein binding to free human serum albumin for a series of 18 benzodiazepines, see Noctor *et al.*, 1993, for experimental conditions and identity of compounds.

A third series of triazole derivatives was also studied, but no correlation was observed. This result reflected the fact that the members of this series did not significantly bind to HSA (percent binding for all triazoles was less than 40%) and were not retained on the HSA-CSP (all k' 's were less than 0.70). The data indicated that the HSA-CSP could be used to determine whether compounds bind or do not bind to the protein.

Frontal chromatography on the HSA-CSP has also been used to determine the extent of binding to the protein (Loun & Hage, 1992). In this study, the association constants for *R*-warfarin and L-tryptophan were determined. The calculated values for *R*-warfarin and L-tryptophan were 2.47×10^5 and $1.10 \times 10^4 \text{ M}^{-1}$, respectively, which did not significantly differ from the results obtained by equilibrium dialysis or zonal elution techniques.

1.1.3 The application of quantitative affinity chromatography using the nicotinic acetylcholine receptor (nAChR).

The nAChR has been immobilized on the IAM liquid chromatographic stationary phase and used in frontal affinity chromatography experiments to determine receptor-binding affinities (K_d values). The K_d values determined chromatographically were comparable to those found using standard membrane affinity binding techniques. Frontal affinity chromatography could also be used to detect differences in the binding affinity of a compound between nAChR subtypes. (Moaddel *et al.*, 2002, 2003).

Zonal chromatography results demonstrated that the immobilized nAChR stationary phases can be used for the on-line screening for ligands to the nAChR. The nAChR columns can be used to identify both competitive and non-competitive ligands to this receptor. (Moaddel & Wainer, 2003).

Thus the possibility of the extensive use of immobilized liquid chromatographic stationary phases containing drug targets in on-line high through-put screening (HTS) is extremely encouraging. Successful development of stationary phases containing immobilized receptors, transporters and enzymes will lead to their use for on-line pharmacological studies and as rapid screens for the isolation and identification of lead drug candidates from complex biological or chemical mixtures. The usefulness of this approach is only limited by the ability to identify potential targets and the construction of the appropriate chromatographic system (Baynham *et al.*, 2002).

1.2 Aims and Objectives

Membrane bound receptors and trans-membrane transporters and ion channels are difficult to characterize and to utilize in drug discovery unless you have a marker ligand. It will be particularly important in characterizing orphan receptors, ion channels and transporters. To put things into focus, G-protein coupled receptors (GPCRs) are the target for over 50% of the marketed drugs. The human genome contains about 1,000 genes which encode for approximately 10,000 GPCRs, however only a few 100 GPCRs have been characterized. Clearly there is a growing need to develop methods which would help in the process of screening for various drugs and identification of suitable lead candidates. Also it is very difficult to classify test compounds as transporters and inhibitors by a single assay because different experimental systems and test conditions produce different classifications. A well defined strategy should be used to identify potential inhibitors and substrates of these transporters.

Recently the use of affinity chromatography, which is based upon target biopolymers in a flow system, has been considered as a valuable method in identifying substrates for different biopolymers. This method can rapidly determine a compound's affinity for biopolymers and whether it is an inhibitor/substrate of the transporter. This is a key element in drug discovery and drug development programs. Therefore the method can be used as a pre-screen to identify all substrates and inhibitors, which could be subsequently moved onto a more expensive and time consuming functional assays to determine functional activity.

Accordingly, the aim of this research programme was to develop novel methodology to enable the study of the interaction of drugs and related compounds with these transporters, in a rapid and facile manner.

The initial studies were designed to develop practical experience in the application of affinity chromatography. These studies included the use of an immobilized α_1 acid glycoprotein (AGP) column to achieve the enantioselective separation of the drug ketamine. The second study was designed to explore the use of online affinity chromatography in the isolation of ligands to an immobilized nicotinic acetyl choline receptor (nAChR).

The final and primary objective of this program was to characterize the Pgp and hOCT1 transporters and immobilize these cellular membranes on a chromatographic backbone.

These stationary phases would then be used in frontal affinity chromatographic studies to determine the binding affinities $\{K_d \text{ values}\}$ of various Pgp and OCT substrates/inhibitors and lead to identification of competitive, allosteric and enantioselective interactions in ligand binding to these transporters. This would help to ascertain whether competitive binding experiments on the Pgp and hOCT1 columns could be a rapid method for the identification of synergistic pairs for specific clinical targets.

Also an aim of this programme was to attempt to use these immobilized biopolymeric stationary phases in on-line pharmacological studies and as a rapid screen for the isolation and identification of lead drug candidates from complex biological mixtures. A further objective was to study its application in determining apparent equilibrium constants (association constants, dissociation constants, binding constants) using very small amounts of biopolymer and ligand.

Also these affinity chromatographic methods could be of particular relevance in monitoring interactions between exogenous or endogenous compounds in binding to different drug receptors. This might lead to the understanding of their pharmacological and/or toxicological activities. A further objective was to screen varied drugs for their drug-protein interaction and to develop a pharmacophore (structural feature in a molecule that is recognized at a receptor site and is responsible for the molecule's biological activity) which would depict the possible interactions of the active site of

these transporters. Also possible enantioselectivity studies would be carried out to identify for any enantioselectivity of the transporters active site.

Chapter 2

2. Application of Protein Affinity Chromatography to Analytical Studies

2.1 Use of affinity based chiral stationary phase α_1 -AGP for the determination of ketamine and norketamine in human plasma

2.1.1 Introduction

Human α_1 -acid glycoprotein (AGP) is also known as orosomucoid (ORM). This is a 41- to 43-kDa glycoprotein with a pI of 2.8 to 3.8 and a high carbohydrate content of 45% (Kremer *et al.*, 1988, Fournier *et al.*, 2000). The peptide portion of this protein has 183 amino acids in a single polypeptide chain with two disulfide bridges. The carbohydrate portion has five to six highly sialylated complex-type-N-linked glycans that are attached to the peptide chain. AGP has a high solubility in water and polar organic solvents.

AGP is one of the plasma proteins synthesized by the liver and is mainly secreted by the hepatocytes, although extrahepatic AGP gene expression has also been reported (Kremer *et al.*, 1988). The hepatic production of these proteins, also known as “acute phase proteins,” is increased in response to various types of stress, such as physical trauma or unspecific inflammatory stimuli.

The biological function of AGP remains unknown. However, a number of possible physiological activities have been studied, such as immunomodulating effects. Due to its low pI value, AGP is the major plasma protein responsible for the binding of cationic

drugs (Chui *et al.*, 1992). As will be seen later, this property has made AGP supports the most versatile of all the serum protein-based chiral stationary phases.

2.1.1.1 Preparation of AGP-CSPs

An AGP chiral stationary phase (AGP-CSP) was initially synthesized by coupling this protein to epoxide-activated silica (Hermansson *et al.*, 1983). The silica (LiChrospher Si 300) was activated using 3-glycidoxypropyltrimethylsilane and mixed with a solution of AGP dissolved in pH 8.5, 0.1 M borate buffer containing 0.2 M sodium chloride. The resulting AGP-CSP contained about 35 mg of AGP per gram silica.

The first commercially available form of AGP-CSP (i.e., EnantioPac) was prepared by first ionically binding AGP to diethylaminoethyl silica. This protein was then cross linked using a process that involved the oxidation of the terminal alcohol groups to aldehydes, Schiff base formation, and reduction to form amine groups (Wainer *et al.*, 1989). This process yielded an immobilized coating of approximately 180 mg protein per gram of silica. The resulting column is a useful CSP but has a short lifetime. A second-generation column (i.e., Chiral AGP) was later produced with better chromatographic performance and stability.

2.1.1.2 Bioanalytical Applications of AGP-CSPs

Because of the broad applicability of AGP-CSPs and their use with aqueous mobile phases, columns based on these phases have been used in many bioanalytical studies. The AGP-CSP can be used alone or in a multidimensional system. The latter approach involves the use of an achiral column (usually as a precolumn) for the separation of compounds such as a parent drug and its metabolites based upon structural differences; this is followed by an enantioselective separation on the AGP-CSP. However, the growing use of liquid chromatography/mass spectrometry (LC-MS) and selective ion monitoring has reduced the need for multidimensional systems, with the required chiral separations now often being accomplished using just the AGP-CSP. Bioanalytical methods based on AGP-CSPs have been developed for disopyramide (Hermansson *et al.*, 1984), atenolol (Enquist *et al.*, 1989), verapamil and norverapamil (Chu *et al.*, 1989), citalopram (Haupt *et al.*, 1996), mepivacaine (Vletter *et al.*, 1996), and thiopentone (Jones *et al.*, 1996).

Looking at the success of AGP-CSP in the enantioselective separation of wide variety of basic, neutral and acidic chiral compounds and its use in bioanalytical applications, the AGP-CSP was used to develop and validate the enantioselective separation of ketamine and norketamine from plasma samples.

Ketamine (Ket) is a dissociative anaesthetic agent that has also been shown to induce analgesia by non-opioid mechanisms (White *et al.*, 1980; Oye *et al.*, 1992; Klepstad *et*

al., 1990). Ket is a chiral molecule that is commercially available as a racemic mixture, i.e. a 50:50 mixture of its enantiomers, (R)-Ket and (S)-Ket. (Figure 7)

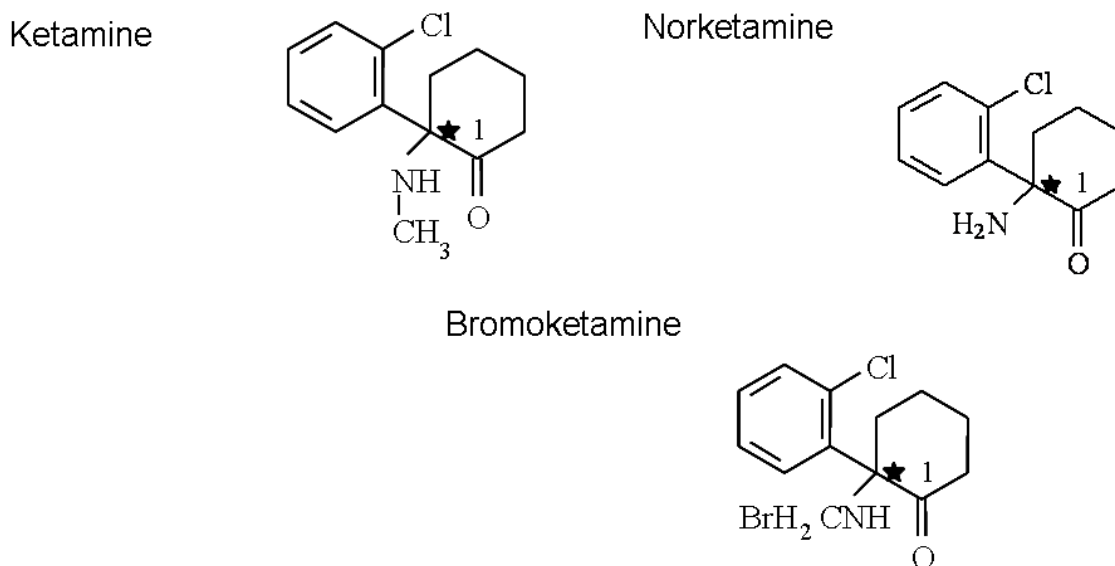


Figure 7. Chemical structures of cationic drugs ketamine, norketamine and bromoketamine (anaesthetic agent shown to induce analgesia by non-opioid mechanism). * indicating the chiral centre.

However, (R)- and (S)-Ket have significantly different pharmacodynamic activities (White *et al.*, 1982; Reich *et al.*, 1989) as the therapeutic potency of (S)-Ket is 2 to 4 times greater than the (R)-enantiomer (Marietta *et al.*, 1977; White *et al.*, 1985) and (S)-Ket is a more potent analgesic agent than the (R)-Ket. (Oye *et al.*, 1992)

Ket is currently undergoing trials as an analgesic agent for the treatment of neuropathic pain. The clinical protocol utilized in this study involved a continuous infusion of racemic-Ket designed to reach plasma concentrations of 60 to 120 ng/ml. It was

assumed that the study would produce Ket and norKet plasma levels at or below the previously reported lower limits of detection. Thus, the objective of this study was to develop and validate a highly sensitive enantioselective bioanalytical method to analyze the plasma samples associated with this clinical study.

The aim therefore is to develop a sensitive enantioselective liquid chromatographic assay with mass spectrometric detection (LC-MS) and validate for the simultaneous determination of plasma concentrations of (R)- and (S)-ketamine, and (R)- and (S)-norketamine. The compounds need to be extracted from human plasma using solid phase extraction method and then directly injected into the LC-MS for detection and quantification. Enantioselective separations could be achieved on a liquid chromatographic chiral stationary phase based upon immobilized α 1-acid glycoprotein (the Chiral AGP column).

2.1.2 Experimental

2.1.2.1 Chemicals and reagents

(+)-(S)-Ketamine, [(S)-Ket]; (-)-(R)-ketamine, [(R)-Ket]; (+)-(S)-norketamine, [(S)-norKet]; (-)-(R)-norketamine. [(R)-norKet]; (R,S)-ketamine, [(R,S)-Ket]; (R,S)-norketamine, [(R,S)- norKet] and (R,S)-Bromoketamine, [(R,S)-BrKet] were a kind gift from Dr. Thomas Wolfe from Parke-Davis Pharmaceutical Research (Ann Arbor, MI, USA). HPLC grade 2-propanol was purchased from Fisher Scientific (Fair Lawn, NJ, USA). HPLC reagent grade ammonium acetate was obtained from J.T.Baker

(Phillippsburg, NJ, USA). Ultra-pure water was obtained using a Milli-Q water purification system (Millipore, Milford, MA, USA). Pooled drug-free human plasma was received from the Apheresis Unit, National Institute on Aging (Balltimore, MD USA). The extraction cartridges were Oasis HLB 1ml, 30 mg and Oasis MCX 3 ml, 60 mg (Waters Corporation, Milford, MA, USA) and Bond Elut-C18, 1 ml, 50 mg (Varian, Harbor City, CA USA).

2.1.2.2 Apparatus

The analytical system consisted of a Series 1100 Liquid Chromatography/ Mass Selective Detector, LC/MSD (Agilent Technologies, Palo Alto, CA, USA) equipped with a vacuum de-gasser (G 1322 A), a binary pump (1312 A), an autosampler (G1313A), a thermostated column compartment (G1316 A); a mass selective detector, MSD (G1946 B) supplied with atmospheric pressure ionization electrospray (API-ES) and an on-line nitrogen generation system (Whatman, Haverhill, MA, USA). The chromatographic system was interfaced to a 250 MHz Kayak XA computer (Hewlett-Pakard, Palo Alto, CA, USA) using ChemStation software (Hewlett-Packard). The extractions were performed using a 12-Port Vacuum Manifold, PrepSep TM from Fisher Scientific (Fair Lawn, NJ, USA).

2.1.2.3 Chromatographic conditions

The enantioselective separations of (R)- and (S)-Ket, (R)- and (S)-norKet and (R)- and (S)-BrKet were accomplished using a guard Chiral-AGP column (10 x 2.0 mm i.d., 5 μm) and an analytical column Chiral-AGP (100 x 4.0 mm i.d., 5 μm) purchased from Advanced Separation Technologies (Whippany, NJ, USA). The mobile phase consisted of 2-propanol: ammonium acetate buffer [10 mM, pH 7.6 (adjusted with ammonium hydroxide)], 6:94 (v/v). The flow rate was 0.5 ml/min, the injection volume was 20 μl and the column temperature was kept at 25 °C.

Mass spectra were recorded using a full scan in positive ion mode, with a scan range from m/z 100 to 600. Single ion monitoring (SIM) was used to quantitate the target compounds. The chromatograms were monitored at $m/z = 238.1$ (Ket), $m/z = 224.1$ (norKet) and $m/z = 284.0$ (BrKet).

2.1.2.4 Optimization of the mass selective detector (MSD) parameters

The sensitivity of the Ket and norKet signals was primarily dependent on the MSD experimental parameters. In order to identify the optimized condition, the following MSD parameters were investigated: fragmentation voltage (50 - 80 V), capillary voltage (1000 - 3000 V), nebulizer pressure (40 - 55 psig) and drying gas temperature (200 - 350 °C).

2.1.2.5 Preparation of stock solutions

Concentrated stock solutions of (R,S)-Ket [1.00 mg/ml], (R,S)-norKet [1.00 mg/ml] and (R,S)-BrKet [0.40 mg/ml] were prepared in ultra-pure water, placed in capped polypropylene tubes, wrapped in aluminum foil and stored at -20°C . Spiking standard solutions for the calibration curve and quality control samples (QCs) were made by serial dilutions with ultra-pure water starting with their respective concentrated stock solution. These spiking standards were placed in capped polypropylene tubes, wrapped in aluminum foil and stored at 4°C .

2.1.2.6 Preparation of calibration curve and quality control standards

The determinations of Ket and norKet were based on the internal standard method, using BrKet as internal standard. Calibration and QC standards were prepared daily by adding $50\ \mu\text{l}$ of the corresponding spiking standard solution containing Ket, norKet and BrKet to $450\ \mu\text{l}$ drug-free plasma. The 7-point calibration curve ranged from 1.0 to 125.0 ng/ml (1.0, 5.0, 25.0, 50.0, 75.0, 100.0, 125.0 ng/ml) for each ketamine and norketamine enantiomer and a constant concentration of 100.0 ng/ml for each bromoketamine enantiomer. The QC standards were 5.0 ng/ml {low quality control (LQC)}, 50.0 ng/ml {medium quality control (MQC)}, and 100.0 ng/ml {high quality control (HQC)}. The concentrations are given per enantiomer.

2.1.2.7 Extraction procedure

Sample extraction was performed using solid phase extraction (SPE). To 15 ml conical polypropylene capped tubes, were added 450 μ l aliquots of plasma samples and 50 μ l internal standard. The resulting solutions were made alkaline by the addition of 0.5 ml of ammonium acetate buffer [10 mM, pH 9.5], vortex-mixed for 2 min, and centrifuged at 1250 x g (4 °C) for 15 min. The plasma samples were then added to preconditioned 1 ml solid phase extraction cartridges (Oasis HLB). The cartridges were conditioned with 1 ml of methanol followed by 1 ml of water and then 1 ml of ammonium acetate buffer [10 mM, pH 9.5]. After addition of the plasma, the conditioned cartridges were washed with 1 ml of water and the retained compounds were eluted with 0.5 ml methanol. The methanol eluents were transferred to 300- μ l autosampler vials and 20 μ l aliquots were injected onto the LC-MSD system.

2.1.2.8 Validation

The intra- and inter-day validation studies for precision and accuracy were performed in quintuplicate with QC standards at 5.0, 50.0 and 100.0 ng/ml per enantiomer. The analyses were carried out over a period of 3 days for the interday validation. The curves were constructed by plotting the peak height ratio (R)-Ket / (R)-BrKet, or (S)-Ket / (S)-BrKet, or (R)-norKet / (R)-BrKet or (S)-norKet / (S)-BrKet against its concentration.

Extraction efficiencies (% recovery) of (R,S)-Ket , (R,S)-norKet and (R,S)-BrKet were determined by comparing peak heights for the QC standards to the peak heights resulting from the chromatography of standard solutions containing the equivalent final concentrations.

Accuracy was determined by comparing the observed concentrations of the QC standards calculated from the calibration curve to their nominal concentrations.

The specificity of the method for each analyte was examined by individually screening Ket, norKet and BrKet after spiking in pooled human plasma.

2.1.2.9 Application of the analytical method

The validated method was applied to the analysis of plasma samples obtained from a clinical study on Ket in pain management (Protocol A00-M91-00), conducted in the Anesthesia Research Unit, McGill University Medical Center (Montreal, Quebec, CA). After signing consent form, the patients received infusion of Ket (Ketalar®, Park-Davis) delivered using a computer-controlled pump (Stanpump, Harvard 22 Basic Syringe Pump®, Harvard Apparatus, South Natick, MA, USA). The target plasma concentrations set on the pump for the Ket infusions were 0 ng/ml (baseline), 60 ng/ml (dose 1) and 120 ng/ml (dose 2), during three testing periods of 15 min each. Blood samples were collected at the end of the baseline period and at the beginning and the

end of dose 1 and dose 2 periods. Plasma was obtained by centrifugation and the samples were frozen at -80 °C until analysis.

2.1.3 Results and Discussion

2.1.3.1 Optimization of the chromatographic separation

Enantioselective separations on an immobilized α 1-acid glycoprotein chiral stationary phase (AGP-CSP) are affected by the buffer concentration, the type and concentration of organic modifiers and the pH of the mobile phase (Yanagihara *et al.*, 2000). Each of these parameters was systematically studied in the development of the enantioselective separation. Temperature also plays a role in separations on a CSP. However, in this study, the temperature was maintained at 25 °C and this parameter was not adjusted.

2.1.3.1.1 Selection of the buffer in the mobile phase for an LC-MS application

The buffer selected for this study was ammonium acetate because of its compatibility in LC-MS applications. Buffer concentrations of 10 and 20 mM were investigated and there was no significant influence of buffer concentration on the enantioselective separation. Therefore, a 10 mM concentration of ammonium acetate was chosen for the study.

2.1.3.1.2 Selection of the organic modifier in the mobile phase

The mobile phase concentration of 2-propanol was varied between 3 and 10% and it was found that the enantioselective separations of Ket, norKet and BrKet were highly dependent on the 2-propanol content. The optimum enantioselective separations of the three compounds were achieved with a 2-propanol : buffer ratio of 3:97 (v/v). Under these conditions, the observed enantioselectivities (α 's) were 1.14 (Ket), 1.71 (norKet) and 1.34 (BrKet). However, the analysis took 35 min. When the mobile phase concentration of 2-propanol was raised to 10%, the analysis took only 13 min. However, while the observed α 's were acceptable for norKet and BrKet, 1.27 and 1.13, respectively, the enantioseparation of Ket was essentially lost ($\alpha = 1.03$). The best balance between enantioselectivity and analysis time was found with a mobile phase composed of 2-propanol : buffer, (6:94, v/v). Under these conditions the observed α 's were 1.09 (Ket), 1.46 (norKet) and 1.22 (BrKet) and the analysis time was 18 min. This mobile phase composition was used in the remaining optimization studies.

The addition of acetonitrile to the mobile phase has been shown to often improve the enantioselectivity (Wainer *et al.*, 1993). In this study, the addition of acetonitrile (0.5 to 1.0 %, v/v) to the mobile phase had no significant effect on the chromatography, although there was a slight decrease in retention time (0.25 to 0.5 min difference). The mobile phase selected for the validation and clinical studies did not contain acetonitrile.

2.1.3.1.3 Optimization of buffer pH

The effect of pH on the enantioselective separation of Ket and norKet was studied using the previously determined mobile phase composition of 2-propanol : ammonium acetate buffer [10 mM], (6:94, v/v). The pH of the buffer was varied over the range 4.0 to 7.0, in intervals of 0.5 units and from pH 7.0 to pH 8.5 in 0.1 intervals. At all pH values, an enantioselective separation was observed for norKet and BrKet. At pH 7.0 and higher, baseline enantioselective separations were achieved with observed α 's of 1.33-1.86 (norKet) and 1.16 – 1.57 (BrKet).

An adequate enantioseparation of Ket was harder to achieve. From pH 4.0 to 6.5 no enantioselective separation of (R,S)-Ket was observed. Between pH 7.0 and pH 7.5, the observed α for Ket ranged from 1.04 (pH 7.0) to 1.09 (pH 7.5) with a maximum resolution (RS) of 0.69 obtained at pH 7.5. Between pH 7.6 and pH 8.5, the observed α increased from 1.17 to 1.37, the RS values from 0.83 to 1.90.

On the basis of these studies, the pH of the buffer was set at 7.6. Although the best chromatographic separations were achieved at pH 8.5, the stability of the AGP-CSP is reduced when the pH of the mobile phase is > 7 {Instruction Manual Chiral-AGP, ChromTech AB}. Thus, the selected pH was a compromise between chromatographic separation and column life.

Based upon these results, the mobile phase composition for the validation and clinical study were set at 2-propanol : ammonium acetate buffer [10 mM, pH 7.6], (6:94, v/v).

Under these conditions, the analysis was completed in less than 20 min. The relative retentions (k') of (S)-Ket and (R)-Ket were 9.0 and 10.5, respectively and the observed enantioselectivity (α) was 1.17 (Figure 8A), for (S)-norKet and (R)-norKet the k 's were 5.2 and 8.2, respectively, and the observed α was 1.58 (Figure 8B), while for BrKet the k 's for (S)-BrKet and (R)-BrKet were 9.8 and 12.8, respectively, and the observed α was 1.31 (Figure 8C). The enantiomeric elution orders were established by chromatographing the separate enantiomers.

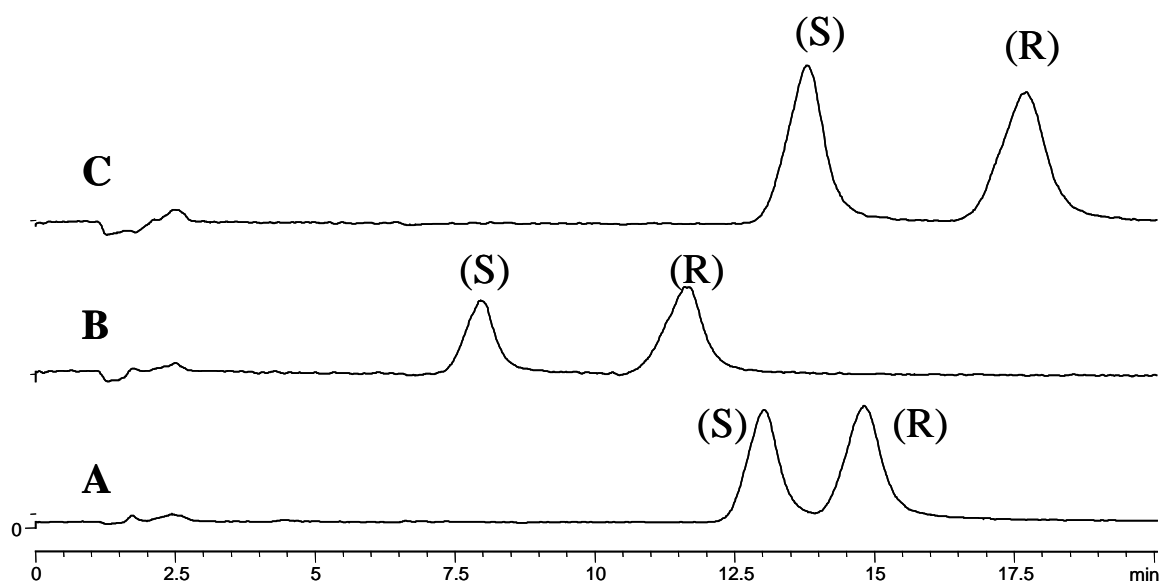


Figure 8. Representative chromatogram of the low quality control plasma sample (LQC) containing 5 ng/ml of (R)-Ket, (S)-Ket, (R)-norKet and (S)-norKet and 100ng/ml of (R)-BrKet and (S)-BrKet; where: A: the chromatographic trace obtained using single ion monitoring at $m/z = 238.1$ (Ket); B: the chromatographic trace obtained using single ion monitoring at $m/z = 224.1$ (norKet); and C: the chromatographic trace obtained using single ion monitoring at $m/z = 284.0$ (BrKet).

Previous Ket assays utilizing the AGP-CSP had reported a rapid deterioration of the CSP (Svensson *et al.*, 1996). Under the described chromatographic conditions, the method was stable and reproducible, allowing us to analyze over 350 plasma standards and patient samples on a single analytical AGP column with replacement of the guard AGP column after an average of 100 plasma samples analysed.

2.1.3.2 Optimization of the mass spectrometric detection

The chromatograms were monitored using single ion monitoring for Ket at $m/z = 238.1$, for norKet at $m/z = 224.1$ and BrKet at $m/z = 284.0$ (BrKet). Each compound was injected individually and a full scan mass spectra was obtained and the signals were monitored at each of the specific m/z values. The specific ion data was collected on three separate channels and analyzed. The results of these studies demonstrated that there were no overlaps in the mass spectra of the compounds at the m/z values chosen for the monitoring. In addition, the analysis of drug-free blank plasma at these m/z values detected no interfering peaks (Figure 9).

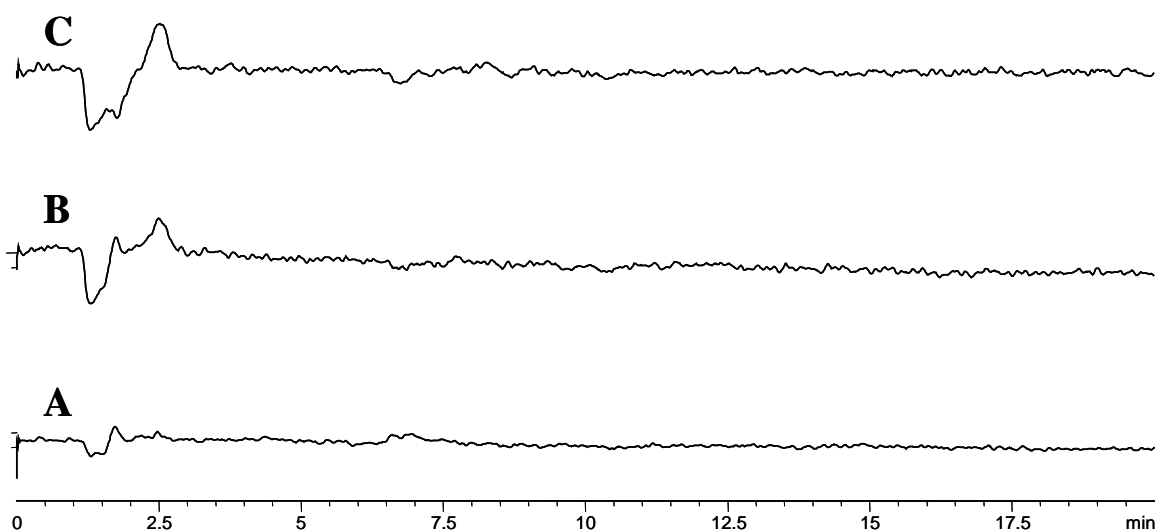


Figure 9. Representative chromatograms of drug-free plasma obtained using single ion monitoring for Ket at $m/z = 238.1$ (A), norKet $m/z = 224.1$ (B) and BrKet $m/z = 284.0$ (C).

The optimization of the mass spectrometer parameters was carried out using flow injection analysis (FIA) in which Ket and norKet standard solutions [50 ng/ml] were injected every two minutes. The Ket and norKet signals were optimized by the evaluation of changes in their peak height at their respective m/z value in response to changes in fragmentor voltage, capillary voltage, nebulizer pressure and drying gas temperature. The peak height of (R,S)-Ket and (R,S)-norKet varied with the fragmentor voltage and the optimum response was obtained at 60 V. The value for the fragmentor voltage was set to 60 V and the other parameters were evaluated. In this way, the optimum conditions based on the maximum peak height were: drying gas flow-rate, 11.0 L/min; nebulizer pressure, 40 psig; drying gas temperature, 350°C and capillary voltage, 1000 V.

2.1.3.3 Extraction efficiency (% recovery)

During the development of the extraction method, 3 SPE cartridges were tested. The cation exchange cartridges (Oasis MCX, 3 ml / 60 mg) gave low recoveries in the range 60-75% for the 3 compounds as did the Bond Elute C-18 (1 ml / 30 mg), which yielded recoveries of 59-65%. The best recoveries were obtained using the Oasis HLB (1 ml / 30 mg) where the recoveries ranged from 95.0% to 99.6%, Table 1 and Table 2.

Table 1. Summary of validation statistics for ketamine

	LQC		MQC		HQC	
	R	S	R	S	R	S
Conc.(ng/ml)	5.0	5.0	50.0	50.0	100.0	100.0
<i>Intra-day</i>						
N	5	5	5	5	5	5
Mean	4.9	5.0	48.5	48.4	97.4	97.3
S.D.	0.1	0.1	1.8	1.4	3.2	3.3
%CV	1.6	2.2	3.8	2.8	3.2	3.4
<i>Inter-day</i>						
N	15	15	15	15	15	15
Mean	5.0	5.0	50.0	49.8	99.8	99.8
S.D.	0.3	0.4	2.4	2.3	3.7	4.9
%C.V.	5.8	7.5	4.8	4.5	3.7	4.9
Accuracy (%)	100.2	100.8	99.9	99.6	99.8	99.8
Recovery (%)	95.0	95.5	98.0	98.6	99.5	99.6

Table 2. Summary of validation statistics for norketamine

	LQC		MQC		HQC	
	R	S	R	S	R	S
Conc.(ng/ml)	5.0	5.0	50.0	50.0	100.0	100.0
<i>Intra-day</i>						
N	5	5	5	5	5	5
Mean	5.0	4.7	49.5	48.9	97.2	97.1
S.D.	0.2	0.2	0.6	0.9	2.7	2.9
%CV	3.0	4.0	1.2	1.8	2.8	2.9
<i>Inter-day</i>						
N	15	15	15	15	15	15
Mean	5.1	5.1	49.9	49.5	99.9	99.4
S.D.	0.2	0.4	3.1	2.7	6.6	5.9
%C.V.	3.9	7.2	6.3	5.5	6.7	5.9
Accuracy (%)	101.4	102.2	99.7	99.0	99.9	99.4
Recovery (%)	99.3	99.2	99.0	99.0	99.5	99.0

2.1.3.4 Linearity and detection limits

Calibration curves were generated by weighted (1/x) least squares linear regression. The linear relationships between peak height ratio and drug-enantiomer concentrations in the range of 1 to 125 ng/ml were described by the following equations: $y = 0.0315x + 0.0058$, $r^2 = 1$ {(R)-Ket}; $y = 0.027x - 0.0018$, $r^2 = 0.9994$ {(S)-Ket}; $y = 0.1259x +$

0.0419, $r^2 = 0.9995$ {(R)-norKet}; $y = 0.0688x + 0.0062$, $r^2 = 0.9993$ {(S)-norKet}. The data were based on 9 replicates of a 7-point calibration curve.

The chromatogram of the LQC (5.0 ng/ml per enantiomer of Ket and norKet) is presented in Fig. 2. The lower limit of quantification (LLOQ) is the concentration of the drug, in the matrix, which could be determined with a percentage accuracy within acceptable limits (80-100%). LLOQ per enantiomer for Ket and norKet was 1.0 ng/ml ($n = 15$) with an acceptable precision and accuracy for each enantiomer as follows: (R)-Ket 8.6% and 97.8%, for (S)-Ket 9.2% and 97.4%, for (R)-norKet 7.5% and 98.8% and for (S)-norKet 8.7% and 99.3%. The lower limit of detection (LOD) was defined as the concentration of the compound at which the signal versus noise ratio (S/N) was equal to 3. For each enantiomer, the LOD for Ket and norKet was 0.25 ng/ml.

2.1.3.5 Accuracy and precision

Accuracy and precision of the method for Ket and norKet were evaluated from quintuplicate analysis of each QC standards levels (LQC, MQC and HQC) repeated for 3 days. The calculated accuracy was 100.0 % for (R)-Ket , 100.1 % for (S)-Ket, 100.3 % for (R)-norKet and 100.2 % for (S)-norKet (Tables 1 and 2).

The intra-day and inter-day precision of the method, determined as % of coefficient of variance (%CV) for the LQC, MQC and HQC for Ket and norKet were $\leq 5.8\%$ for (R)-Ket, $\leq 7.5\%$ for (S)-Ket, $\leq 6.7\%$ for (R)-norKet and $\leq 7.2\%$ for (S)-norKet. The

results of the validation studies demonstrated that the method had excellent accuracy, recovery and precision.

2.1.3.6 Stability

Hijazi *et al.*, 2001, have previously reported that Ket and norKet were stable in aqueous solutions at -80°C for at least 6 months, and that plasma samples could be transported at 4°C within 2 days and can be stored at -20°C for 10 weeks without any change in the concentrations of Ket and norKet. The results from this study were consistent with the observation by Hijazi *et al.*, 2001 as no significant degradation of the Ket and norKet standards or plasma samples was observed.

2.1.4 Application to clinical samples

The validated method has been applied to the analysis of plasma samples obtained from a clinical study on Ket in pain management. A representative chromatogram of a patient plasma sample obtained before administration of the drug and 15 min after the end of dose 1 (where the target plasma concentrations was 60 ng/ml) is presented in Figure 10.

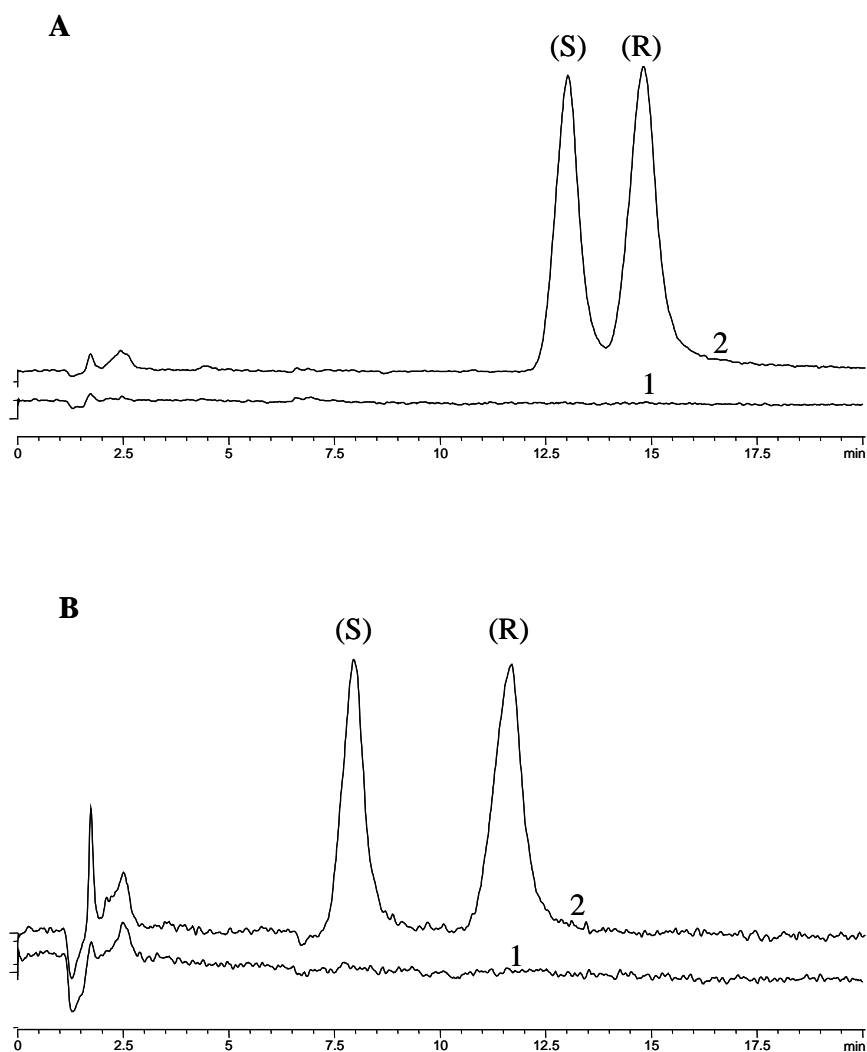


Figure 10. The chromatograms from the analysis of plasma samples from a patient obtained before the administration of Ket and 15 min after the administration of an infusion of 60 ng/ml, where: A: the chromatographic traces obtained using single ion monitoring at $m/z = 238.1$ (Ket), trace 1 – before administration, trace 2 - after administration; B: the chromatographic trace obtained using single ion monitoring at $m/z = 224.1$ (norKet), trace 1 – before administration, trace 2 - after administration. The calculated concentrations were: (S)-Ket 27.1 ng/ml, (R)-Ket 28.9 ng/ml, (S)-norKet 3.4 ng/ml, (R)-norKet 2.5 ng/ml.

The measured concentrations were: S-Ket 27.1 ng/ml, R-Ket 28.9 ng/ml, S-norKet 3.4ng/ml, (R)-norKet 2.5 ng/ml. The plasma concentrations of (R)-Ket and (S)-Ket in two patients measured before and after doses 1 and 2 are presented in

Figure 11.

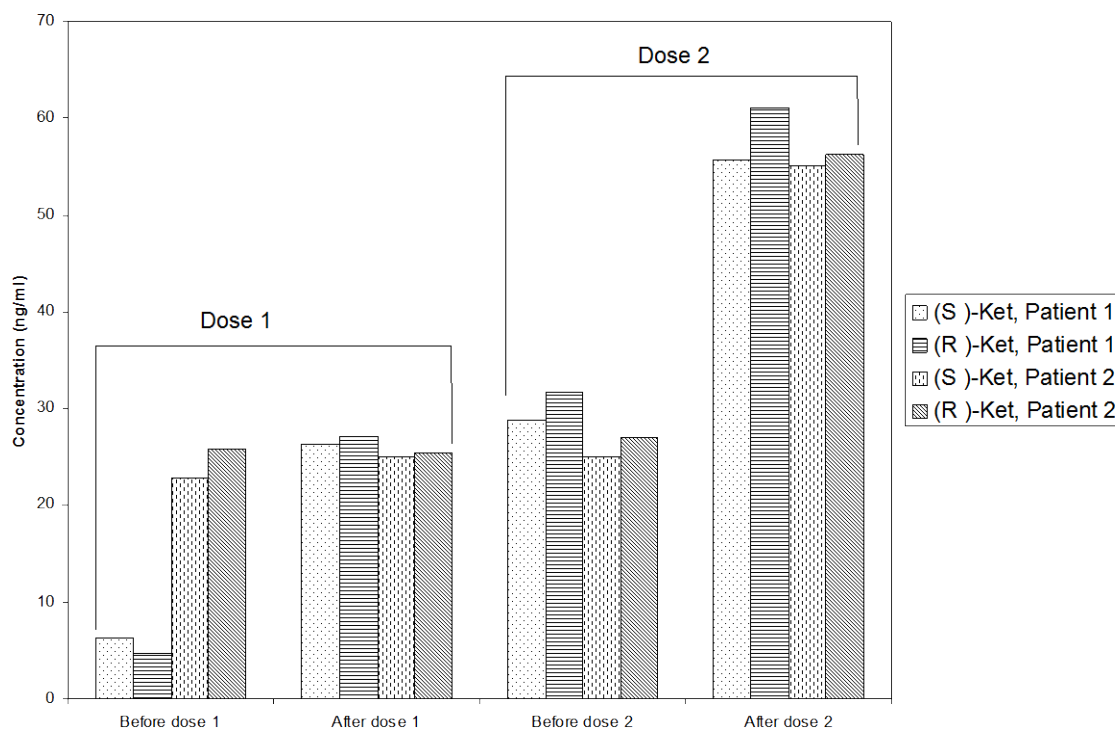


Figure 11. Plasma concentrations of the enantiomers of ketamine, (R)-Ket and (S)-Ket, in two patients before and after dosing period 1 and dosing period 2, see Experimental Section for description of the clinical protocol.

In these two patients, the norKet levels were below our limit of detection during the first dosing period. At the start of dosing period 2, norKet was undetectable in patient 1 and 1.0 ng/ml of (R)-norKet was observed in patient 2, while at the end of dosing period 2 (R)-norKet and (S)-norKet were measured in the plasma from patient 1 (2.7 and 1.0 ng/ml, respectively) and patient 2 (2.7 and 2.8 ng/ml, respectively).

2.1.5 Conclusions

The results of these studies demonstrated that an immobilized protein based liquid chromatographic column could be used to separate and quantify enantiomeric compounds. The enantioselective binding of Ket and NorKet to the immobilized α_1 AGP was the same as that determined with free protein. In addition, the bioanalytical assay conducted was a simple, sensitive and reproducible method for the enantioselective and simultaneous determination of Ket and norKet in human plasma by LC-MS. The assay had greater sensitivity than previously reported methods and a run time of less than 20 min. Thus, the data indicated that this approach, i.e. using immobilized protein affinity chromatography, can be used to probe pharmacologically relevant binding interactions.

2.2 Use of immobilized $\alpha 3/\beta 4$ neuronal nicotinic acetylcholine receptor based chromatographic stationary phase in multidimensional on-line screening for ligands of $\alpha 3/\beta 4$ neuronal nicotinic acetylcholine receptor.

2.2.1 Introduction

While the work described in section 2.1 was an illustrative example as to how protein affinity chromatography and LC-MS are useful tools for the determinations of chiral drugs and biological fluids, they can also be used in the study of drug-protein interactions. This can go beyond the use of common commercially available protein stationary phases such as AGP and HSA to other important proteins which require further studies. One such protein type is the nicotinic acetylcholine receptors. Affinity chromatography is a valuable method for rapid determination of a compound's affinity for biopolymers immobilized on stationary phase and whether it is an inhibitor/substrate of the biopolymer. The study of the interactions of drugs with these biopolymers can be used as a pre-screen to identify all substrates/inhibitors, which could be then moved to a more expensive and time consuming functionally assay to determine functional activity.

The health risks associated with tobacco and tobacco smoke have been clearly defined and well publicized. As a result, one aspect that is often-overlooked, is the fact that the tobacco plant and tobacco smoke contain more than 4,000 compounds (Gundish *et al.*, 2005), many of which may possess beneficial pharmacological and therapeutic properties. This possibility has been suggested by the observed physiological effects

associated with smoking that include alertness, reduced anxiety, muscle relaxation and analgesia (Buccafusco *et al.*, 2004), as well as specific disease-related effects, which have been observed in Alzheimer's disease, Parkinson's disease and schizophrenia. (Gundish *et al.*, 2005; Newhouse *et al.*, 2004)

Although tobacco and tobacco smoke have been shown to contain compounds that inhibit a number of different targets such as monoamine oxidases (Herraiz *et al.*, 2005), the therapeutic responses associated with tobacco smoking have been assumed to be primarily due to the interaction of nicotine with neuronal nicotinic acetylcholine receptors (nAChRs). This assumption was derived from a number of clinical observations including improved cognitive responses and memory in Alzheimer's patients who had received intravenous, subcutaneous or trans-dermal doses of nicotine, the lower than expected incidence of Parkinson's disease in smokers and the prevalence of cigarette smoking among patients with schizophrenia (Newhouse *et al.*, 2004). These observations have led to the initiation of drug discovery programs which have the development of nAChR agonists as the primary focus. (Buccafusco *et al.*, 2004; Holladay *et al.*, 1997)

Although current drug discovery programs are primarily concentrated on the development of nAChR agonists, nAChR antagonists have been in clinical use for over 60 years, e.g., d-tubocurarine, a competitive inhibitor of peripheral nAChRs, was introduced into clinical anesthesia and surgical muscle relaxation in 1942 (Tassonyi *et al.*, 2002). The growing interest in nAChR antagonists was reflected in a recent review

by Dwoskin and Crooks, which identified these agents as “a new direction for drug discovery.” (Dwoskin *et al.*, 2001). A possible pharmacological basis for this approach is the observation that nAChR agonists rapidly desensitize the receptors, which essentially inhibits their function. Thus, if inhibition and not excitation is the actual therapeutic effect, competitive inhibitors or agonists that result in rapid desensitization should work equally well. (Dwoskin *et al.*, 2001)

2.2.1.1 Neuronal nicotinic acetylcholine receptors

nAChRs are a family of ligand gated ion channels found in the central and peripheral nervous systems that regulate synaptic activity. The receptor is composed of five separate trans-membrane proteins (subunits), each containing a large extra-cellular N-terminal domain, four membrane spanning alpha helices (M1, M2, M3, and M4) and a small extracellular C-terminal. domain, Figure 12 (Karlin *et al.*, 2002).

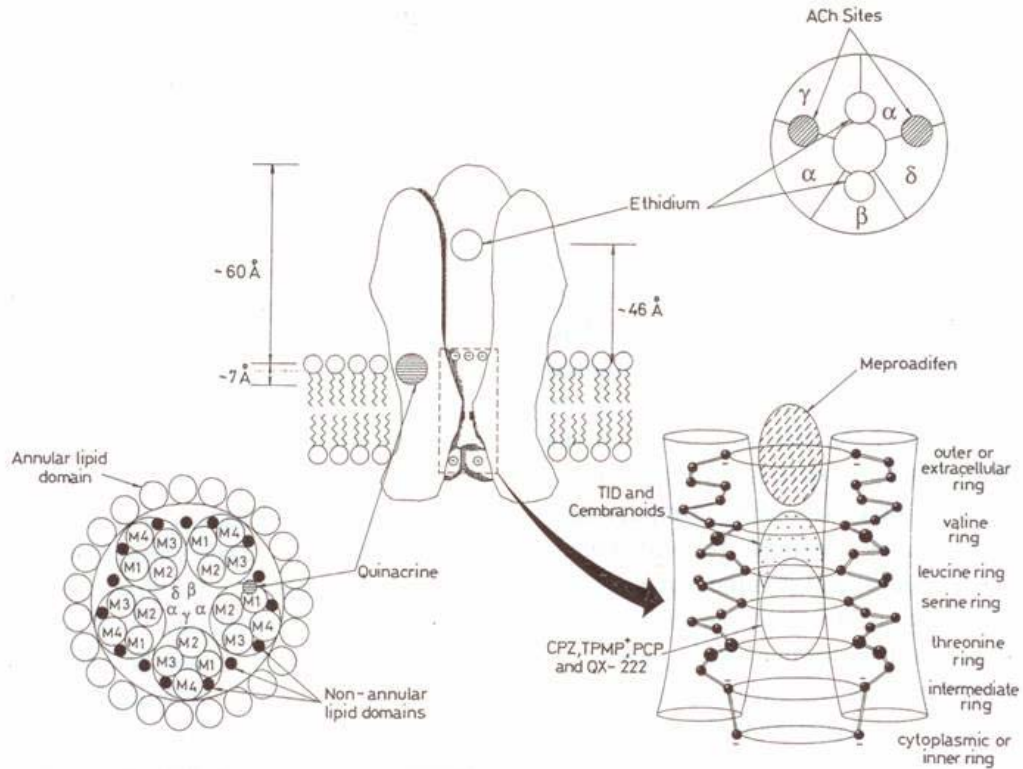


Figure 12. Transverse schematic representation of the muscle-type AChR showing the domains involved in the specific binding of non-competitive inhibitors from exogenous origin. Top and right panel: Schematic representation of a section of the AChR at ~ 46 Å from the membrane surface viewed from the synaptic cleft. The ethidium locus can be putatively located in the AChR vestibule between both acetylcholine (ACh) binding sites. The ethidium site includes either a region near the $\alpha\gamma$ interface, being this α subunit the one that bears the high-affinity ACh binding site, or a portion of the β subunit. Bottom and left panel: Schematic representation of a section of the AChR at the lipid-aqueous interface viewed from the synaptic cleft. The amino acid chain from each subunit (α, β, γ and δ) crosses the lipid membrane four times (M1-M4). The perimeter of the AChR is surrounded by ~ 45 lipid molecules, i.e., the annular lipid domain. The 23 empty circles around the AChR represent the phospholipid head

groups on the extracellular leaflet of the lipid bilayer. The small black circles between subunits and between domains M1/M4 and M3/M4 represent the possible locations for non-annular lipid domains. The high-affinity quinacrine binding site is located at the α M1 transmembrane domain, near the β subunit. Bottom and right panel: Schematic representation of two M2 transmembrane domains of the AChR subunit. The amino acid side chains from both α M2 domains represent the transmembrane α M2 domains represent the transmembrane α -helix. A consensus exists that the interaction of certain residues from the α subunit (shown here as filled spheres), in addition to the respective homologous amino acids from the other subunits (not shown for simplicity), form a series of stratified rings disposed from the extracellular to the intracellular side in the following manner: outer or extracellular, valine, leucine, serine, threonine, intermediate, and cytoplasmic or inner ring. In addition, some of them are involved in the binding of the so-called luminal non-competitive inhibitors. In particular, the binding site for the local anesthetic mepradifen is located close to the mouth of the ion channel, probably at the negatively-charged outer or extracellular ring. The binding site for cembranoids and trifluoromethyl-iodophenyldiazirine (TID) is related to both the valine and the leucine ring. Finally, the binding site for chlorpromazine (CPZ), triphenylmethylphosphonium (TPMP⁺), the local anesthetic QX-222, and phencyclidine (PCP) includes the leucine, the serine, and the threonine ring. Reprinted from Arias *et al.*, 1998.

The five subunits are oriented around a central pore (Hucho *et al.*, 1996; Albuquerque *et al.*, 1997) and the resulting transmembrane ion channel is formed by a pentameric arrangement of the M2 helical segments contributed by each of the five subunits (Changeux *et al.*, 1992) (Figure 12). To date, twelve neuronal subtypes of the nicotinic receptor have been identified thus far ($\alpha 2$ - $\alpha 10$) and ($\beta 2$ - $\beta 4$). Typically, three $\alpha 2$ - $\alpha 6$ combine with two β subunits to form functional heteromeric subtypes of the nicotinic receptors. These can combine to form a variety of subtypes including the $\alpha 3\beta 4$, $\alpha 3\beta 2$, $\alpha 2\beta 4$, $\alpha 4\beta 2$, $\alpha 4\beta 4$, with the $\alpha 4\beta 2$ being the most targeted therapeutically. The $\alpha 7$ - $\alpha 9$ differ from the rest of the family in that they only combine with themselves to form functional homomeric subtypes, including the $\alpha 7$, $\alpha 8$, $\alpha 9$ and $\alpha 10$ nicotinic receptors, with the $\alpha 7$ nicotinic receptors being the most targeted therapeutically.

The agonist binding site of the neuronal nicotinic receptor is located at the interface of the α and β subunits. The agonist must bind simultaneously to the two agonist binding sites of the nicotinic receptor to elicit a pharmacological response. This is the predominant target for most therapeutic drugs in development today. In addition to the agonist binding site, another site of increasing importance is the non-competitive inhibitor (NCI) binding site, where the NCIs bind. NCIs inhibit nAChR function by a rapid reversible channel blockade or a shorten channel opening time (Yamakura *et al.*, 2000) and include mecamylamine (Lloyd *et al.*, 1999), ketamine (Hernandez *et al.*, 2000), and dextromethorphan (Furuya *et al.*, 1999). In most cases, the non-competitive inhibitory properties of a compound at the nAChR are not its primary pharmacological function. Indeed, whether or not a compound functions as a NCI is usually determined

after observation of unexpected pharmacological effects. For example, ketamine is an anesthetic that competitively blocks the N-methyl-D-aspartate receptor (Hernandez *et al.*, 2000). However, ketamine also acts as a NCI at nAChRs and this activity may be responsible for some of the drugs side effects. (Hernandez *et al.*, 2000; Zhang *et al.*, 1998)

2.2.1.2 $\alpha 3\beta 4$ nAChR affinity chromatographic columns

Currently, high throughput screening for competitive agonist and antagonists involve competitive binding affinity experiments using recombinant receptor systems and radiolabelled marker ligands (Holladay *et al.*, 1997). An alternative method for the screening of compounds for competitive and non-competitive inhibitory properties is the determination of binding affinities to the nAChR by frontal chromatography. One approach to the direct measurement of absolute and relative binding affinities at the nAChR is affinity chromatography using nAChR affinity columns.

Liquid chromatographic columns containing immobilized $\alpha 3\beta 4$ -nAChR or $\alpha 4\beta 2$ -nAChR (NR columns) have been previously reported and used to determine the binding affinities of competitive agonists and antagonists (Wainer *et al.*, 1999; Xiao *et al.*, 1998). The initial studies with these columns involved displacement chromatography with a single marker ligand and a single displacer.

In the current studies, a NR column containing an immobilized $\alpha 3\beta 4$ -nAChR stationary phase has been coupled to a C₁₈ reversed-phase column and a mass spectrometer. In this manner, the NR column could be used to initially sort a mixture of compounds through their affinity to the $\alpha 3\beta 4$ -nAChR using chromatographic retention as the marker. In these studies, the eluent was directed to waste for the first 8 min of the run and then directed onto the C₁₈ column. The compounds contained in the eluent were compressed at the head of the C₁₈ column, then resolved using a step-gradient and ultimately identified using a mass spectrometer. The results of the study indicate that the coupled NR column – C₁₈ column system can be used for the rapid on-line screening of mixtures for potential ligands to the $\alpha 3\beta 4$ -nAChR.

2.2.2 Materials and methods

2.2.2.1 Materials

Nicotine, epibatidine, nornicotine, anabasine, acetylcholine, benzamidine, butyrlcholine, caffeine, glutamic acid, 3-hydroxytyramine, naltrexone, ketamine, norketamine, 2,3-dihydroxybenzoic acid, epinephrine, norepinephrine, cytosine and 4-dimethylaminopyridine were purchased from Sigma Chemical Co. (St. Louis, MO, USA). Tris HCl and cholic acid sodium salt were also purchased from Sigma Chemical Co. HPLC grade methanol, ammonium acetate and 0.1 M ammonium hydroxide solution were purchased from Fisher scientific (Pittsburgh, PA, USA). All water used for preparing solutions was supplied by a Nanopure reverse osmosis water purification system (Barnstead, Dubuque, IA, USA).

2.2.2.2 Chromatographic System

The coupled-column chromatographic system used in these studies is presented in Figure 13.

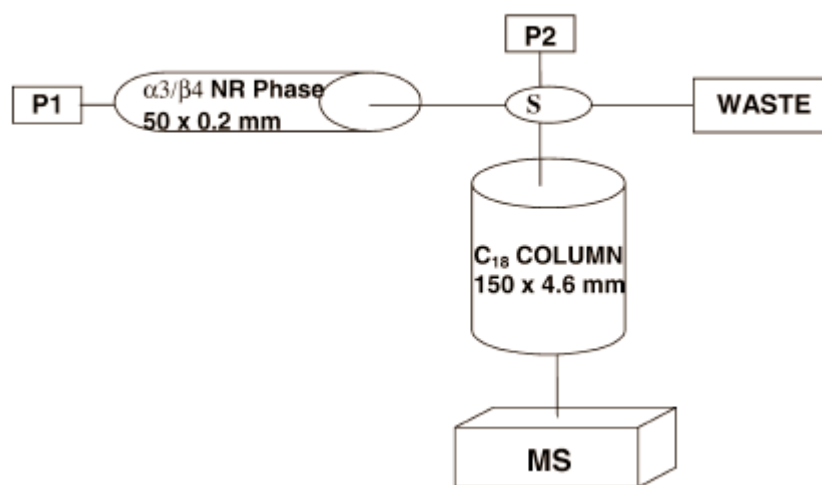


Figure 13. The multidimensional coupled-column chromatographic system used in this study composed of a HP-1100 chromatography system (Agilent Technologies, Palo Alto, CA, USA), which consisted of a binary gradient pump (P1), autosampler, column oven, switching valve and a MS detector. The column containing the immobilized nicotinic receptors was connected on-line to a reversed-phase Zorbax C₁₈ column (150 x 4.6 mm i.d., 5 μ m, obtained from Agilent). A Rheodyne LabPRO switching valve (Ronert Park, CA, USA) was used to connect the two columns. A second isocratic HP pump (P2) was used to supply the mobile phase to the C₁₈ column. Mass spectrometry experiments were conducted using a Agilent technologies Mass Selective Detector (MSD) operating in positive ion electrospray (ES+) mode.

The system was composed of a HP-1100 chromatography system (Agilent Technologies, Palo Alto, CA, USA), which consisted of a binary gradient pump (P1), autosampler, column oven, switching valve and a diode array detector. The column containing the immobilized nicotinic receptors was connected on-line to a reversed-phase Zorbax C18 column (150 x 4.6 mm i.d., 5 μ m, obtained from Agilent). A Rheodyne LabPRO switching valve (Ronert Park, CA, USA) was used to connect the two columns. A second isocratic HP pump (P2) was used to supply the mobile phase to the C18 column. Mass spectrometry experiments were conducted using an Agilent technologies Mass Selective Detector (MSD) operating in positive ion electrospray (ES+) mode.

2.2.2.3 Preparation of the α 3/ β 4 Nicotinic Receptor Column

The nicotinic receptor (NR) column was prepared as previously described (Wainer *et al.*, 1999; Xiao *et al.*, 1998). In brief: Cells from the KX α 3/ β 4R2 cell line (Glennon *et al.*, 1994) were suspended in Tris-HCl, [50 mM, pH 7.4] (buffer A), homogenized for 30 sec with Brinkmann Polytron, and centrifuged at 35,000 x g for 10 min at 4 °C. The pellet was resuspended in 6 ml of 2% cholate in buffer A and stirred for 2 h. The mixture was centrifuged at 35,000 x g for 30 min, and the supernatant containing NR - cholate solution was collected.

The IAM liquid chromatographic stationary phase (200 mg, IAM-PC stationary phase, Regis Chemical Co., Morton Grove, IL, USA) was suspended in 4 ml of the obtained detergent solution containing proteins. The mixture of IAM-detergent-receptor was stirred for 1 h at room temperature. The suspension was dialyzed against 2 x 1L buffer A for 24 h at 4 °C. The IAM liquid chromatographic support was then washed with buffer A, centrifuged and the solid collected.

The IAM liquid chromatographic support containing the NR was packed into a HR5/2 glass column (Pharmacia Biotech, Uppsala, Sweden) to form a chromatographic bed of 20 mm x 5 mm i.d. The NR column was then placed in the chromatographic system and used as described below.

2.2.2.4 Chromatographic Procedures

An ammonium acetate buffer [10 mM, pH 7.4] {Buffer} was used throughout the study. The pH of the Buffer was adjusted to 7.4 with 0.1 M ammonium hydroxide. The Buffer was used to prepare separate 1 µM stock solutions for each compound used in the study. A 100 µl aliquot of each stock solution was added to a 10-ml test tube and the Test Mixture was briefly vortex-mixed. The stock solutions and Test Mixture were stored at 4°C until use.

Separations on the NR column were achieved using a mobile phase consisting of Buffer / methanol, 95/5 (v/v), at a flow rate of 0.2 ml/min and a column temperature of 35°C.

The retention times of each test compound was determined by injecting a 50 μ l aliquot of each stock solution onto the chromatographic system. The retention times of the compounds were monitored by single ion monitoring at the appropriate m/z.

When the Test Mixture was injected onto the chromatographic system, the eluent from the NR column was directed through the switching valve to waste for the first 8 min of the chromatographic run. At t = 8 min, the switching valve was rotated and the eluent from the NR column was directed onto the C18 column. At t = 20 min, the switching valve was rotated and the eluent from the NR column was again directed to waste.

At t = 20 min, the second pump (P2) was engaged and a mobile phase consisting of Buffer / methanol, 40/60 (v/v) was pumped through the C18 column at a flow rate of 1.0 ml/min. The eluent from the C18 column was directed into the mass spectrometer. At t = 30 min, the mobile phase was changed to Buffer / methanol, 95/5 (v/v), the flow rate reduced to 0.2 ml/min and the mass spectrometer turned off.

2.2.2.5 Mass Spectrometry

Mass spectrometry experiments were performed using an Agilent MSD single quadrupole mass spectrometer in positive ion electrospray mode, data was recorded using Chem Station (version 6.3) software. The Capillary voltage was set at 2.5 kV and the fragmentor at 50 V. The mass spectrometer drying gas temperature was 3500C, with

nitrogen supplied as the nebulising gas (11 l/min). Single Ion Monitoring (SIM) and Full Scan (FS) modes were employed for these experiments.

2.2.3 Results and Discussion

The retention times of the compounds used in this study are presented in Table 3.

Table 3. The compounds used in this study, their respective affinities for the $\alpha 3/\beta 4$ nAChR defined as yes if the compound is reported in Refs. (Holladay *et al.*, 1997; Lloyd *et al.*, 1999; Hernandez *et al.*, 2000; Xiao *et al.*, 1998) to bind to the receptor and no if it is not reported to bind to the receptors in Refs. (Holladay *et al.*, 1997; Lloyd *et al.*, 1999; Hernandez *et al.*, 2000; Xiao *et al.*, 1998) and the observed retention times on the column containing immobilized $\alpha 3/\beta 4$ nAChR..

No.	Compound	Affinity for $\alpha 3/\beta 4$ Nicotinic Acetylcholine Receptor	Retention time (min)
1	Anabasine	No	2.1
2	Acetylcholine	Yes	4.7
3	Benzamidine	No	6.3
4	Butyrlcholine	No	6.0
5	Caffeine	No	2.7
6	Cystisine	No ($\alpha 2/\beta 4$ ligand)	4.8
7	2,3-Dihydroxybenzoic acid	No	3.2
8	4-Dimehtylaminopyridine	Yes ($\alpha 1$ ligand)	9.5
9	Epibatidine	Yes	13.1
10	Epinephrine	No	2.1
11	Glutamic acid	No	2.1
12	3-Hydroxytyramine	No	7.1
13	Ketamine	Yes (NCI)	8.3
14	Naltrexone	No	9.8
15	Nicotine	Yes	10.3
16	Norepinephrine	No	2.1
17	Norketamine	Yes (NCI)	8.5
18	Nornicotine	Yes	8.8

For compounds with no known affinity for the $\alpha 3/\beta 4$ nAChR the retention times ranged from 2.1 min to 7.1 min, except for naltrexone, which eluted at 9.8 min. This result is most probably due to the compound's hydrophobicity. However, preliminary studies with naltrexone indicate that this compound may be a NCI of the $\alpha 3/\beta 4$ nAChR, albeit with an EC₅₀ of >100 μ M (Kellar, personal communication). It is unclear what naltrexone's affinity for the $\alpha 3/\beta 4$ nAChR contributes to the observed retention.

Cytisine is a marker ligand for the $\alpha 3/\beta 4$ nAChR and has displayed no significant affinity for the $\alpha 3/\beta 4$ nAChR (Holladay *et al.*, 1997). Previous studies with NR columns composed of either the $\alpha 3/\beta 4$ nAChR or the $\alpha 3/\beta 4$ nAChR have demonstrated that NR columns can be used to distinguish between the activities of the two nAChR subtypes (Xiao *et al.*, 1998). The fact that the retention time of cytisine was 4.8 min on a NR column containing immobilized $\alpha 3/\beta 4$ nAChR is consistent with the previously reported selectivity of immobilized nAChR subtypes.

The compounds with a known affinity for the $\alpha 3/\beta 4$ nAChR eluted with retention times between 8.3 min and 13.1 min except for acetylcholine, which eluted at 4.7 min, Table 3. Epibatidine has the longest retention of the test compounds, 13.1 min, which is consistent with the fact that, of the compounds tested, it has the highest affinity for the $\alpha 3/\beta 4$ nAChR, $K_d = 0.30$ nM (Xiao *et al.*, 1998). The affinity of nicotine for the $\alpha 3/\beta 4$ nAChR is 300-fold less than epibatidine, $K_d = 90$ nM (Xiao *et al.*, 1998), and the compound eluted 2.8 min before epibatidine at 10.3 min. Nornicotine has a 20-fold

lower affinity than nicotine for the $\alpha 3/\beta 4$ nAChR and the compound eluted from the NR column at 8.8 min. In whole cell studies, the affinity of acetylcholine has been reported at 3-fold lower than nicotine (Holladay *et al.*, 1997). There are reported assays for the determination of the binding affinity of acetylcholine to the isolated $\alpha 3/\beta 4$ nAChR. However, the reason for the short retention time of this compound on the NR column is unknown.

The results indicate that in most cases, magnitude of the chromatographic retention on the NR column is a reflection of binding affinity for the $\alpha 3/\beta 4$ nAChR. This suggests that the NR column could be used for the direct resolution of a mixture of compounds into $\alpha 3/\beta 4$ nAChR ligands and non-ligands. However, the chromatogram of epibatidine illustrates that the chromatographic efficiency of the NR column is extremely poor, Figure 14a.

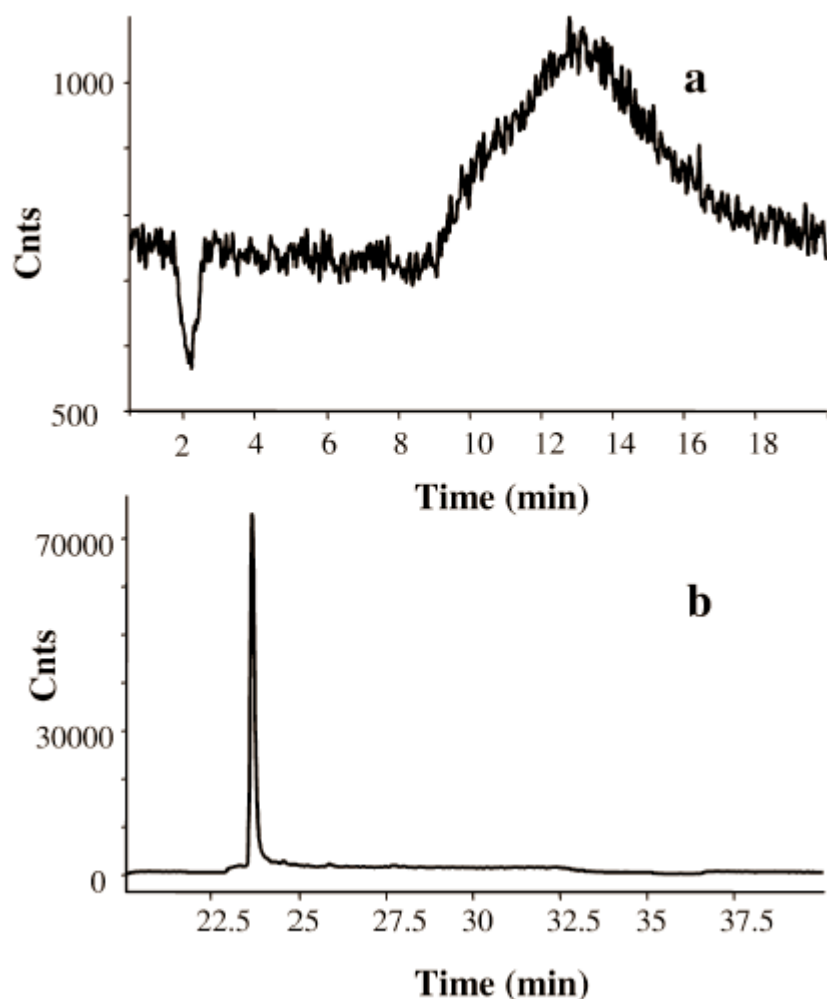


Figure 14. A representative chromatogram from the chromatography of epibatidine on: a. the NR column alone; b. the multidimensional system produced after injection of a 1 μM solution of epibatidine using SIM analysis at $[M + H] 209$. An ammonium acetate buffer (10mM, pH 7.4) was used for the study.

Indeed, co-injection of epibatidine and nicotine produced a chromatogram with no significant resolution of the two compounds even though their peak retention times were 2.8 min apart and their affinities differed by 300-fold {data not shown}. In addition, the chromatogram of epibatidine presented in Figure 14a , was produced after

the injection of a 1 μ M solution using SIM analysis at M+H 209.1. Due to the poor peak shape, this concentration was near the limit of detection on the mass spectrometer.

Clearly, the selectivity of the system was hindered by the poor chromatographic efficiency. One way of overcoming the chromatographic inefficiency of the NR column is to couple it to a more efficient column. In the resulting multi-dimensional system, the NR column would separate nicotinic receptor ligands from non-ligands and the second column, in this case a C₁₈ column, would separate the nicotinic receptor ligands from each other. The effect of coupled NR-C₁₈ column system on the chromatogram of epibatidine is presented in Figure 14b. The overall retention time of epibatidine from injection onto the NR column to mass spectrometric detection was 23.7 min. In addition, peak compression on the C₁₈ column increased the sensitivity of the method. The chromatogram in Figure 14b was produced by a 200 nM solution of epibatidine and demonstrates that the sensitivity of the analysis has been significantly increased.

In order to test the hypothesis that the coupled NR-C₁₈ system could be used to screen mixtures for ligands to the α 3/ β 4 nAChR, the compounds listed in Table 3 were combined to form a Test Mixture. Based on the individual chromatographic results, a cut-off time of 8 min was chosen, i.e. after injection onto the NR column, the eluent was directed to waste from 0 to 8 min and then, at the 8 min mark, the eluent was directed onto the C₁₈ column. After 20 min, the C₁₈ column was taken off-line from the NR

column and the compounds compressed on the column were eluted into the mass spectrometer.

The Test Mixture was chromatographed using the conditions described above. The eluent from the C₁₈ column was monitored in full scan mode and the resulting chromatogram is presented in Figure 15.

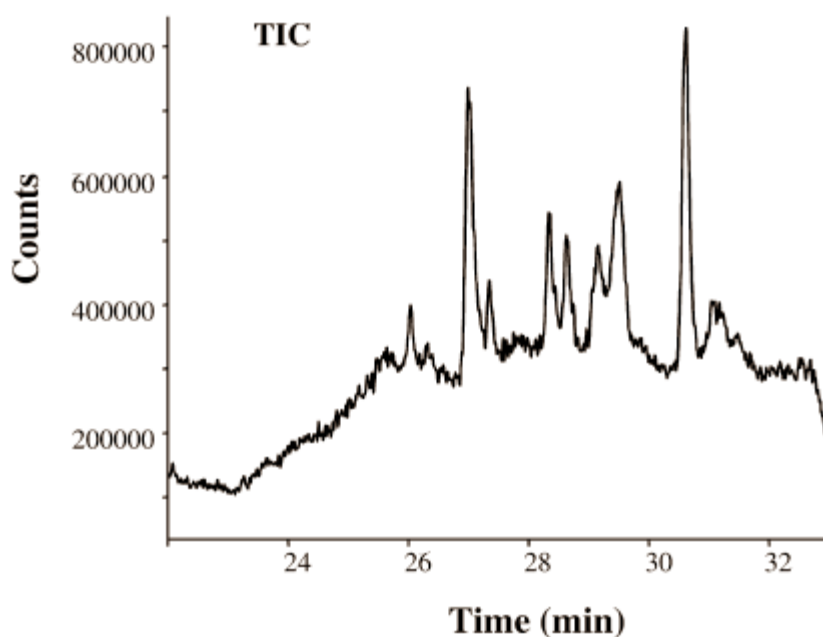


Figure 15. The chromatogram from the chromatography of the Test Mixture on the multidimensional system. Compound list in

Table 3 was combined to form a test mixture. Based on individual chromatographic results the cut-off time of 8 min was chosen, i.e. after injection onto the NR column, eluent was directed to waste from 0 to 8 min and then, at the 8 min mark, the eluent was directed to the C₁₈ column. After 20min, the compounds on the C₁₈ column were eluted into the mass spectrometer.

The compounds in the eluent were identified from their (M+H) masses and the eluent from the C₁₈ column contained 7 of the 18 compounds from the Test Mixture, Table 4.

Table 4. Compounds eluting from the column containing immobilized $\alpha 3\beta 4$ nAChR before 8 min and after 8 min. The data shows that any compound eluting before 8 min don't have affinity for the $\alpha 3\beta 4$ nAChR and the compounds eluting after 8 min have affinity for $\alpha 3\beta 4$ nAChR.

Compounds Eluted at t < 8 min	Compounds Eluted at t ≥ 8 min
Anabasine	Nornicotine
Acetylcholine	Nicotine
Benzamidine	Epibatidine
Butyrlcholine	Naltrexone
Caffeine	Ketamine
Glutamic acid	Norketamine
3-Hydroxytyramine	Dimethylaminopyridine
2,3-DHBA	
Epinephrine	
Norepinephrine	
Cytisine	

Of the 7 compounds 6 were known $\alpha 3\beta 4$ nAChR ligands and the seventh was naltrexone, which may be a NCI.

The sensitivity and specificity of the multidimensional system was investigated by performing a Fisher's Exact Test using GraphPad InStat software {Version 5.05, GraphPad Software, Inc, San Diego, CA, USA}. The question addressed was, "can the multidimensional system distinguish between ligands and non-ligands to the immobilized $\alpha 3\beta 4$ nAChR using a retention time of 8 min as the selector?" The results of the test are presented in Table 5 and indicate that sensitivity, specificity, positive and negative predictive values of the system are extremely significant.

Table 5. Fisher's Exact Test to determine, "Can the multidimensional system distinguish between ligands and non-ligands to the immobilized $\alpha 3\beta 4$ nAChR using a retention time of 8 min as the selector?" The two-sided P value is 0.0025 (extremely significant) and the row/column association is statistically significant.

Variable	Value	95 % Confidence Interval
Sensitivity	0.9091	0.5874 to 0.9977
Specificity	0.8571	0.4210 to 0.9964
Positive predictive value	0.9091	0.5874 to 0.9977
Negative predictive value	0.8571	0.4210 to 0.9964
Likelihood ratio	6.364	

2.2.4 Conclusions

Thus the study showed that a cell line expressing the $\alpha 4\beta 4$ nAChR which was used to create an affinity column containing immobilized $\alpha 3\beta 4$ nAChR coupled to a C_{18} column which was useful for the on-line screening of mixtures for $\alpha 3\beta 4$ nAChR ligands. The method was reproducible, the NR column was stable (the column used in these studies has been used for over 1 y) and relatively quick as the total analysis time from injection onto the NR column to identification of the compounds was 32 min. In addition, the NR column was also able to identify NCI of the $\alpha 3\beta 4$ nicotinic receptor subtype. Thus the results demonstrate that a stationary phase containing immobilized membranes can be used to identify substrate/inhibitors of an expressed receptor/transporter.

Chapter 3

3. P-Glycoprotein

3.1 Introduction

Having demonstrated that a stationary phase containing immobilized membranes can be used to identify substrate/inhibitors of an expressed receptor/transporter the next and principal phase of the programme was to adapt this methodology to other target biopolymers such as P-glycoprotein which over the last decade has been focused upon for its role in drug resistance in cancer treatments.

Resistance to chemotherapy is a critical issue in the management of breast cancer patients. When breast cancer is detected and treated early in the disease process and followed by adjuvant chemotherapy there is a decrease in the annual odds of recurrence by 24% and death by 15 % (Early Breast Cancer Trialists' Collaborative Group 1998). However, advanced breast cancer remains, largely an incurable disease. In advanced stage, the high percentage of non-responders to chemotherapy and of failures following initial response highlights the critical role played by drug resistance mechanisms in breast cancer management. Conversely, the significant number of initial responses and the impact on survival, especially in early disease, suggest that, at least initially, a limited number of mechanisms of resistance are involved. Thus, among solid cancers, breast cancer represents perhaps one of the best fields for the study of clinical drug resistance and of its reversal.

In the last decade considerable attention has been focussed on the role that membrane transporter proteins play in drug resistance. Of particular interest are the transporters

belonging to the ATP binding cassette protein super-family (ABC-transporter proteins), (a superfamily of genes which encode the ABC transporter proteins). ABC transporter proteins are one of the largest and most ancient families with representatives in all extant phyla from prokaryotes to humans. ABC transporters are transmembrane proteins that function in the transport of a wide variety of substrates across extra- and intracellular membranes, including metabolic products, lipids, sterols and drugs. These proteins are classified as ABC transporters based on the sequence and organization of their ATP-binding domains, also known as nucleotide binding folds (NBFs). The ABC transporter, P-glycoprotein (Pgp) is of particular interest as it has been observed that there is a strong association of Pgp with response rates to chemotherapy and an increase in Pgp expression after chemotherapy is coupled with a decrease in the response to further treatment.

Different groups have described a multidrug resistant phenotype characterized by resistance to the cytotoxic effect of multiple unrelated drugs, such as *Vinca* Alkaloids (antimiotic and anti-microtubule agents which are these days produced synthetically and used as drugs in cancer therapy and as immunosuppressive drugs, examples are vinblastine, vincristine etc.), epipodophyllotoxins, anthracyclines and actinomycin D, following cell selection with just one of these drugs (Biedler & Riehm, 1970; Juliano & Ling, 1976). This process was accompanied by decreased intracellular concentration of the target drugs due to their active efflux from cells (Riehm & Biedler, 1971; Dano, 1972; Dano, 1973; Ling and Thompson 1974). Later, it was defined that the same mechanism also confers resistance to taxanes (a class of alkaloids produced from plants

of the genus Taxus which inhibit the microtubule function and have been used to produce various chemotherapy drugs, examples include paclitaxel and docetaxel).and can also cause intracellular drug redistribution (Bellamy, 1996).

The protein responsible for this phenotype has been identified as Pgp, a 170 KDa plasma membrane glycoprotein (Juliano & Ling, 1976). Pgp is an energy-dependent efflux transporter driven by ATP hydrolysis. In humans, two members of the Pgp gene family multi drug resistant gene 1 and multidrug resistant gene 3 (MDR1 and MDR3) have been identified. The Pgp encoded by this gene functions as a drug efflux transporter. The gene MDR1 in humans was isolated and cloned in the 1980's (Roninson *et al.*, 1984, Gros *et al.*, 1986, Roninson *et al.*, 1986). Human MDR3 Pgp is believed to be active in phospholipid transport.

Pgp is the most extensively studied member of the ATP-binding cassette protein family. Pgp and other members of this family function as biological barriers by expelling toxins and xenobiotics from cells. *In vitro* and *in vivo* studies have demonstrated that Pgp plays a significant role in both drug absorption and disposition. Because of its localization, Pgp appears to play a significant role in the bioavailability of oral drugs by reducing the absorption through the intestinal lumen and in the penetration of drugs into the central nervous system (CNS) as well as a minor role in the excretion of drugs out of hepatocytes and renal tubules into the adjacent luminal space.

3.1.1 Structure of P-glycoprotein (ABC Transporter)

Since the identification of Pgp, major efforts have been made to elucidate the structure of the protein in order to gain better insight into its mechanism of action. The cloning of genes and structure-function analysis of the protein by genetic and biochemical studies have contributed to a better understanding of this transporter. Pgp is a part of a larger family of proteins called the ATP Binding Cassette (ABC) protein superfamily, which in humans is known to include forty eight ABC proteins {www.med.rug.nl/mdl/humanabc.htm}.

The ABC superfamily has been described in previous reviews (Klein *et al.* 1999, Dean *et al.* 2001), and based on sequence homology, ABC proteins can be grouped into seven different subfamilies (A-G). All ABC proteins share an ATP binding domain of 200-250 amino acids (Nucleotide Binding Domain, NBD). The NBD unit includes two short, conserved peptide motifs, the Walker A motif and Walker B motif, which are involved in ATP binding, and a third conserved sequence, located between the other two, that has been called the ‘ABC signature’, and is unique to the NBD unit.

Many of the ABC proteins are *transporters* and are characterized by the basic structural module “*TMD-NBD*” (or *NBD-TMD*) consisting of one ABC unit and a hydrophobic transmembrane domain (*TMD*). The *TMD* is usually composed of six transmembrane segments (helices). To be functional, ABC transporters require a minimum of two modules, *i.e.*, two *TMDs* and two *NBD* units. ABC proteins can be classified according to the number and arrangement of the basic structural modules. In ‘full transporters’ the

two *TMD-NBD* units are part of the same polypeptide chain: $(TMD-NBD)_2$. Some full transporters, *e.g.*, several members of the ABC-C subfamily, including multi drug resistant protein 1 (MRP1) (ABCC1), have a $TMD_0L_0(TMD-NBD)_2$ format. This format includes a third membrane domain (TMD_0), with transmembrane helices connected through a linker region (L_0) to the $(TMD-NBD)_2$ double module (Klein *et al.*, 1999, Borst *et al.*, 2000). The structure of ‘half transporters’ comprises only one *TMD-NBD* or *NBD-TMD* module; their activity requires aggregation in multi-protein complexes. Full transporters are usually located in the plasma membrane and half transporters in intracellular membranes, the half-transporter breast cancer resistance protein (BCRP) being one exception (Rocchi *et al.*, 2000).

Pgp is composed of two homologous and symmetrical halves (cassettes), each of which contains six transmembrane domains that are separated by an intracellular flexible linker polypeptide loop with an ATP-binding motif. Interestingly, the two halves of human Pgp have only 43% of the amino acids in alignment, suggesting that the two halves might have either evolved independently or have undergone major intron movement after a duplication event. Pgp appears approximately cylindrical in electron cryomicroscopy studies, with a diameter of about 10 nm, a depth (perpendicular to the plasma membrane) of about 8 nm and two lobes of about 3 nm each projecting from the cytoplasmic end (Rosenberg *et al.*, 1997). The Pgp molecule has a central pore that, in the resting phase, is conical in shape. The base of the cone, which is open to the extracellular space, is 5 nm wide (Rosenberg *et al.*, 1997, Loo & Clarke 2001a) (Figure 16).

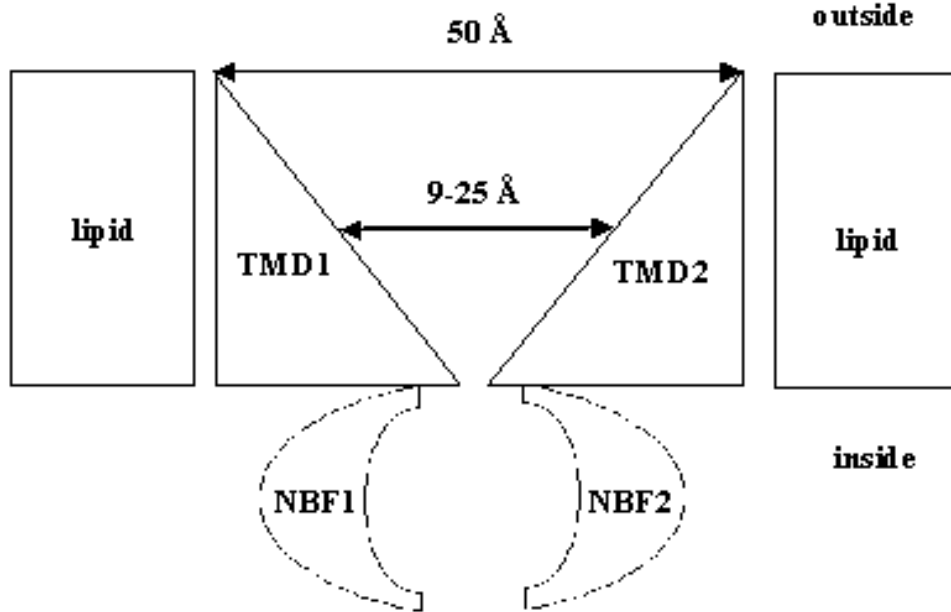


Figure 16. Schematic Model of Pgp showing two homologous halves. Each half consisting of one transmembrane domain (TMD) and one nucleotide binding fold (NBF). The central pore, in the resting phase, is conical in shape. The base of the cone, which is open to the extracellular space, is 50 Å wide. The diameter of the pore at the midlevel is 9-25 Å and the cytoplasmic end which corresponds to the apex of the cone is virtually closed. Pgp substrate binding area is located around the centre of the pore. (adapted from Loo TW & Clarke DM, 2001a)

The diameter of the pore is 0.9-2.5 nm at midlevel through the cell membrane and its cytoplasmic end corresponds to the apex of the cone and is virtually closed (Loo & Clarke, 2001a). The Pgp substrate binding area is located around the midlevel of the pore (Loo & Clarke, 1997; Loo & Clarke, 1999a; Loo & Clarke, 2000). The results of cysteine scanning mutagenesis and crosslinking studies are consistent with a “cyclone

model” of Pgp, whereas the two homologous halves of Pgp are arranged in the cell membrane in an antiparallel fashion, with transmembrane segments 4-6 and 10-12 more directly contributing to delimit Pgp’s central pore (Loo & Clarke, 1999b).

The Pgp transporter exhibits ATPase activity and translocates different substrates across a cell membrane and/or between various cell compartments. Transport of substrates is ensured by a tight molecular coupling of the *TMDs* to the *NBD* units, and a positive cooperation of the two *NBD* units. Site directed mutagenesis and antibody mapping studies suggests that the two cassettes of Pgp interact cooperatively to form a single functional unit. This was proven by cDNA (strong, cloned copies of otherwise fragile mRNA, which is the essential messenger element of the genes in the DNA which help in coding for the proteins) coding of each individual halves of the Pgp cloned into separate plasmids, which did not show any drug stimulated ATPase activity for each cassette. The hypothesis of a single functional unit for further supported in the study in which the key lysine and cysteine residues in the Walker A motifs of the ATP-binding domains were substituted by methionine and alanine, respectively (Takeda *et al.*, 2001). The results clearly demonstrated that if one ATP-binding domain was not functional, then there was no ATP hydrolysis even when ATP was bound to the other ATP-binding domain.

In addition to the ATP binding domains, the intracellular flexible linker loops also play a key role in the ATPase activity. Deletion of the central core of the intracellular flexible linker region of Pgp resulted in a protein without functional ATPase transport

activity. Collectively this data strongly suggested that the two cassettes of Pgp interact as a single transporter and that the flexible linker region is important for the correct interaction of the two cassettes.

3.1.2 Mechanism of Pgp Transport

Several mechanistic models have been proposed to describe the mechanism of drug transport activity. The initial hypothesis was that hydrophobic membrane-spanning regions and hydrophilic elements of Pgp form an aqueous transmembrane pore through which drugs are transported from the cytosol to the extracellular media. However, another model suggests that Pgp might extrude drug directly from the cell membrane even before they enter the cytoplasm. Recently it has been proposed that Pgp intercepts lipophilic drugs as they move through the lipid membrane and flips the drugs from the inner leaflet to the outer leaflet and into the extracellular medium. This model is consistent with the notion that the lipophilicity of a drug is important in its interaction with Pgp (Leonessa & Clarke, 2003).

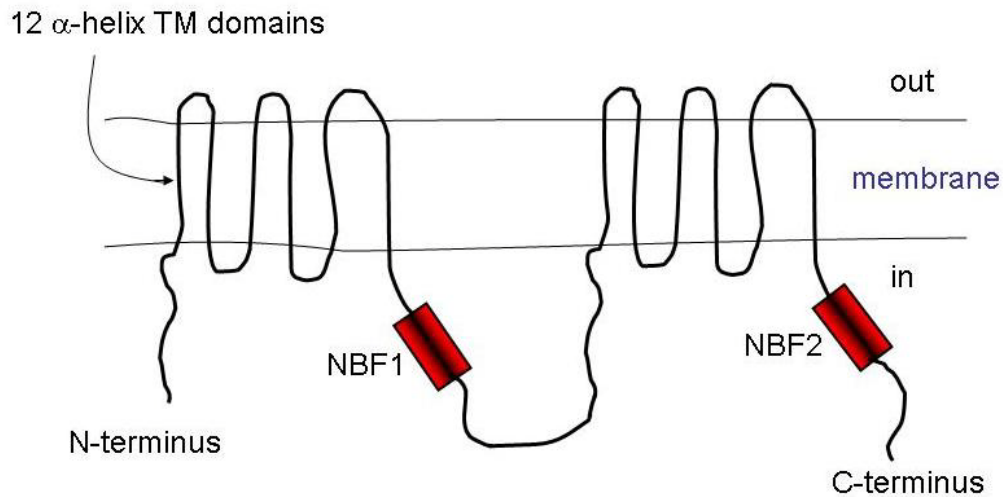
Raviv and Higgins have suggested a similar model where the Pgp substrates most likely diffuse from the inner leaflet of the cell membrane (hydrophobic vacuum cleaner model) (Raviv, 1990; Higgins, 1992), and between Pgp's transmembrane helices to the Pgp's substrate binding area located inside the pore, where they interact mostly with non-polar amino acids (Loo & Clarke, 1997; Loo & Clarke, 1999a; Loo & Clarke, 2000). Interaction with the binding site in the presence of ATP induces ATP hydrolysis,

followed by a rearrangement of the protein conformation: movement of Pgp's N-terminal and C-terminal halves in opposite directions closes the pore (Loo & Clarke, 2002), while rotation of the transmembrane α helices (Loo & Clarke, 2001b) may contribute to decrease the affinity of the site for the substrates. Ultimately, the substrate is pushed either to the extra-cellular phase ("hydrophobic vacuum cleaner" model) or to the membrane's outer leaflet ("flippase model").

3.1.3 ATP and Substrate Binding sites

There are two ATP-binding domains of Pgp, located in the cytosol side, each of which, contains three regions, (Gottesman & Pastan, 1993): Figure 17.

MDR1 (P-glycoprotein)



NBF = nucleotide binding fold

Figure 17. Two ATP-binding domain(s), which are also called nucleotide-binding folds (NBFs) and are located on the cytoplasm side of the phospholipid bilayer. These folds are divided into parts or motifs, called Walker A and Walker B, which are separated by approximately 90-120 amino acids. In addition, there is a third motif (called LSGGQ motif, C motif, or "signature" motif) located after the Walker B motif. Unlike the Walker A and Walker B motifs, which are found in other proteins which hydrolyze ATP, the signature motif is unique to ABC transporters. These folds form the "cassettes" which the protein family is named after. The transmembrane domains and nucleotide-binding folds are often arranged in the order NH^{3+} -TM-NBF-TM-NBF- COO^- .

Walker A motif (sequences of amino acids residues from 427-435^a, 1070-1078^b)

Walker B motif (sequences of amino acids residues from 531-542^a, 1172-1182^b)

Signature C motif (sequences of amino acids residues from 551-556^a, 1196-1201^b)

^a First ATP-binding domain

^b Second ATP-binding domain

Walker A and B can be seen in Figure 18.

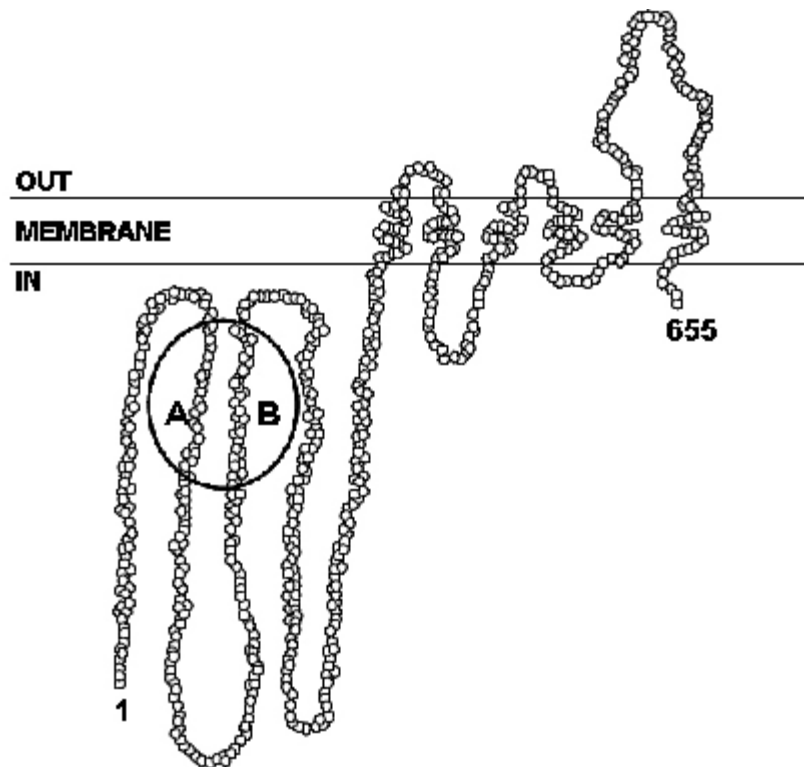


Figure 18. Pgp transporter consisting of 655 amino acids. The Walker A and B motifs of the NBF are circled.

Recently it has been reported that a highly conserved lysine residue within the Walker A motif of histidine permease, an ABC transporter, is directly involved with the binding of ATP, and a highly conserved Asp residue within the Walker B motif serves to bind the Mg^{2+} ion. Loss of activity is observed during mutation of any one of these residues,

thus suggesting that the ATP-binding sites may be restricted to the Walker A motifs of Pgp (Hung *et al.*, 1998).

Senior and Gadsby (1997) conducted vanadate-trapping studies to propose a so-called alternate ATP-binding site model, which showed that although both ATP-binding sites are capable of binding ATP, only one site participates in the catalysis at a given time, and the conformation of this catalytic site precludes the other site from hydrolyzing ATP.

Unlike the ATP-binding sites that are restricted to the Walker A motifs of ATP-binding domains, many substrate-binding sites have been identified throughout the transmembrane domains (TM) of Pgp. Using photoaffinity probes two substrate binding sites were found in TM6 and TM 12 (Greenberger 1993; Bruggemann *et al.*, 1989). In addition to these regions, a region that includes TM7 and TM8 has also been reported to be photolabelled specifically by an analogue of paclitaxel (Wu *et al.*, 1998) However, mutational studies also suggest that amino acid substitutions that affect substrate specificity are scattered throughout Pgp including TM1, TM4, TM6, TM10, TM11 and TM12 (Ueda *et al.*, 1998). Recently Taguchi *et al.*, (1997a, 1997b) suggested that three amino acids (His61, Gly64 and Leu65) in TM1 are involved in the formation of a binding pocket that plays a key role in determining the suitable substrate size for Pgp. Mutational analysis has also shown the importance of the intracellular linker loops in substrate recognition.

In summary, these results suggest that drug-binding sites are scattered throughout the Pgp molecule, including the TM, intracellular loops and even the ATP-binding domains.

3.1.4 Substrate Recognition

One of the most intriguing aspects of Pgp is that a single integral membrane protein can recognize and transport so many drugs with a wide array of chemical structures, ranging from a small molecular weight of 250 atomic mass unit (amu) (cimetidine) to a large molecular weight of 1202 amu (cyclosporin) (Pan *et al.*, 1994, Wu *et al.*, 1995). Although most of the drugs transported by Pgp are basic or uncharged, there are many exceptions. The only common feature is that most of the Pgp substrates are hydrophobic in nature, perhaps suggesting that the partitioning into the lipid membrane of cells is the first step for the interaction of a substrate with the active site of Pgp. Some representative Pgp substrates are presented in Table 6.

Table 6. A wide range of Pgp substrates, majority of which are known cardiovascular and anti-cancer drugs, depicting the broad substrate specificity of the Pgp transporter and showing the importance of Pgp in drug resistance. (Leonessa & Clarke, 2003)

Anthracyclines (doxorubicin, daunomycin, epirubicin)

Acridines (Amsacrine)

Azatoxins (Azatoxin)

Benzoxheptalene compounds (colchicines)

Benzothiazepines (diltiazem)

Dihydropyridines (azidopine, nicardipine)

Epipodophyllotoxins (etoposide)

Isoquinolines (cepharantine)

Macrolides (FK506)

Organometallic cations (^{99m}TC -sestamibi)

Peptides (actinomycin D, bleomycin, cyclosporin A, valinomycin)

Phenothiazines (chlorpromazine)

Phenylalkylamines (verapamil, tiapamil)

Pyrrolo-indoles (mitomycin C)

Quinolines (Chloroquine, Quinidine)

Rhodamines (Rhodamine 123)

Steroids (aldosterone, corticosterone, cortisol, dexamethasone, testosterone)

Taxanes (taxol, taxotere)

Vinca Alkaloids (vincristine, vinblastine)

Other (digoxin, Hoechst 33342, etc.)

Significant efforts have been made to establish structure-activity relationships (QSAR's) (Quantitative structure-activity relationships are mathematical relationships linking chemical structure and pharmacological activity in a quantitative manner for a series of compounds. Methods which can be used in QSAR include various regression and pattern recognition techniques) for Pgp substrates. Initially, it was assumed that a basic nitrogen atom was necessary for the interaction of substrates with Pgp, for example, studies of colchicine and its analogues suggested that the nitrogen atom of the acetamido group at the seventh position, was essential for Pgp recognition (Tang-Wai *et al.*, 1993). However, compounds lacking a nitrogen atom, such as cortisol, aldosterone and dexamethasone, are also good Pgp substrates (Ueda *et al.*, 1992).

Studies have shown that both lipophilicity and number of hydrogen bonds of compounds are probably the most important parameters in determining the affinity of compounds to Pgp (Chiba *et al.*, 1998; Ecker *et al.*, 1999). The higher the lipophilicity or the larger the number of hydrogen bonds, the better the Pgp transporter substrate.

Similarly it was also suggested that both lipophilicity and number of hydrogen bonds are important determinants for substrate and Pgp interactions (Seelig and Landwojtowicz, 2000). This indicates that partitioning into lipid membrane is the rate determining step for the interaction of a substrate with Pgp. It was also suggested that dissociation rate of the Pgp substrate complex is controlled by the number of hydrogen bonds. Seelig (1998) also studied the structure of hundred Pgp substrates and proposed that in addition to lipophilicity and number of hydrogen bonds, some essential structural

elements are required for an interaction with Pgp. The recognition elements of substrates are formed by two or three electron donor (hydrogen-bonding acceptor) groups with a fixed separation: $2.5 \pm 0.3\text{\AA}$ or $4.6 \pm 0.6\text{\AA}$. Additionally, the surface area and amphiphilic characteristic of the substrate also appear to play a significant role in determining its Pgp activity (Osterberg & Norinder, 2000).

Although a wealth of information on the relationship between physicochemical properties of substrates and Pgp activity has been generated in recent years, a clear structure-activity relationship for the prediction of Pgp substrates has not yet been established. The lack of a clear structure-activity relationship for substrate recognition is attributed mainly to the structural complexity of Pgp (Chiba *et al.*, 1996).

3.1.5 Pgp mediated drug-drug interactions

The interaction between Pgp substrates does not always follow simple kinetics. The type of interactions can be classified into four major categories,

- Competitive Inhibition, where two substrates act on the same site of Pgp and that only one or the other can bind at any one time.
- Non-competitive Inhibition, where the two substrates are able to bind simultaneously to Pgp at two distinct sites that are functionally independent.

- Cooperative Interactions, where the binding interactions occur when the binding of a second compound to the protein increases the affinity of a marker ligand.
- Anti-Cooperative Interactions, where the binding interactions occur when the binding of a second compound to the protein decreases the affinity of a marker ligand.

The complexity of the molecular mechanism for Pgp inhibition hinders the ability to predict potential Pgp mediated drug-drug interactions either quantitatively or qualitatively. Indeed one possible reason for the failure of the co-administration of Pgp modulators and anticancer agents to improve therapeutic profiles of the chemotherapeutic agents could be that the modulators also inhibit the Pgp protective function of normal cells, leading to cytotoxicity.

3.1.6 Effects of chemotherapy on Pgp expression

Both the processes of induction and of selection could be involved in an effect of chemotherapy on Pgp expression. *In vitro* studies have shown that treatment of neoplastic cells with chemotherapeutic agents can induce the expression of Pgp (Chaudary & Roninson, 1993). This induction appears to be independent of whether the anticancer drugs are substrates for Pgp, and may be part of a response to different stress stimuli, including irradiation, genotoxic stress and inflammation (Sukhai & Piquette-Miller, 2000). Conversely, treatment with anticancer drugs to which Pgp confers

resistance would be expected to enrich cancer in Pgp+ cells by a process of selection and should be specific for drugs that are MDR1 substrates.

3.1.7 Importance of Pgp in Drug Discovery

The elucidation of the 2.9 billion-letter nucleotide base pair sequence of the human genome is a key resource for any kind of drug discovery. Recent reports, in which 313 genes were screened in individuals of diverse ethnic origins indicated that polymorphisms would be observed at a rate of one single nucleotide polymorphism (SNP) in every 185 nucleotides, and individualized therapy based on the genome sequence of each individual would pave the way for modern medicines (Stephens *et al.*, 2001). Therefore, for this individualized pharmacotherapy (tailor - made pharmacotherapy), the genetic polymorphisms of drug metabolizing enzymes and drug transporters have been extensively investigated and established as a key factor responsible for interindividual differences in pharmacokinetic and pharmacodynamic profiles. It is estimated that approximately 500-1200 genes code transporters and, as this area of research is still in its infancy, the importance of this fact is only now beginning to be understood.

Pgp (MDR1) plays the most important role among these transporters, since the biological fate of a number of structurally unrelated drugs is defined by the MDR1 gene. To date, a total of 28 SNPs have been found at 27 positions on the MDR1 gene. A polymorphism in exon 26 at position 3435, a silent mutation, has been found to be of

key importance due to its effects on MDR1 expression and pharmacokinetic activity. In addition, recent investigations have raised the possibility that MDR1 and related transporters play a fundamental role in regulating apoptosis (mechanism of programmed cell death necessary to remove cells whose DNA has been damaged to the point at which cancerous change is liable to occur) and immunology, and are related to susceptibility to certain diseases, suggesting the possibility of disease diagnosis based on MDR1 genotyping.

Panwala *et al.*, (1998) indicated that *mdr1a*^{-/-} knock-out mice were susceptible to a severe and spontaneous intestinal inflammation under specific pathogen free conditions. These observations suggested that susceptibility to inflammatory bowel diseases depended on MDR1 expression and function, and therefore on MDR1 genotype. Also, it was noted that several drugs central to the therapy are substrates of MDR1.

Also there is increasing evidence that the risk of HIV related infections is linked to MDR1 expression and function. Lee *et al.*, (2000) showed that HIV viral production is greatly reduced when MDR1 was over-expressed, suggesting that the cells with high levels of MDR1 expression are relatively resistant to HIV infections. Additionally, since retroviral drugs are substrates of MDR1, therapeutic outcome of treating HIV infections also depends on the MDR1 genotype. In addition, susceptibility to renal cell carcinoma is consistent with the hypothesis that a lower MDR1 expression level offers less protection from the accumulation of carcinogenic materials in the renal tubules, and

therefore the development of the diseases in other tissues with MDR1 expression might be related to the level of MDR1 expression and function.

3.1.8 Role of P-Glycoprotein in pharmacokinetics and pharmacodynamics

Although the physiological function of Pgp is still not fully understood, the role of this efflux transporter in pharmacokinetics is becoming increasingly appreciated. In humans, Pgp is found on the apical surface of columnar epithelial cells of small and large intestines, the biliary canalicular membrane of hepatocytes, the apical surface of epithelial cells of the proximal tubules of kidney and the apical surface of endothelial cells in blood capillaries of the brain (Thiebaut *et al.*, 1987; Cordon-Cardo *et al.*, 1990). Because of its strategic localization, Pgp transport functionally can limit cellular uptake of drugs from the blood circulation into the brain and placenta, and from the gastrointestinal lumen into the enterocyte. On the other hand, this transporter can also enhance the elimination of drugs from hepatocytes, renal tubules and intestinal epithelial cells into the adjacent luminal space. Therefore, it is very important to distinguish the localization of Pgp in cells in relation to drug movement-either uptake of drugs into cells or excretion of drugs out of cells. It has been well established that MDR1 confers an intrinsic resistance to normal tissues by exporting unnecessary or toxic exogenous substances or metabolites out of the body. Therefore, the expression of Pgp (MDR1) throughout the body affects the pharmacokinetic profiles of drugs, which are its substrates.

3.1.9 Distribution of intestinal Pgp

Immunohistological studies with human jejunum and colon using MRK16 antibody revealed that high levels of Pgp are observed in the apical surface of columnar epithelial cells (Thiebaut *et al.*, 1987). The distribution of Pgp is also not uniform along the length of the intestine, appearing to increase progressively from the stomach to the colon with a low level in the stomach, with an intermediate level in the jejunum and a high level in the colon (Fojo *et al.*, 1987). The uneven distribution of intestinal Pgp seems to have a significant impact on the absorption of Pgp substrates, as has been demonstrated in a clinical study with cyclosporin (Fricker *et al.*, 1996).

3.1.10 Role of intestinal Pgp in drug absorption

Evidence of the involvement of intestinal Pgp in drug absorption was first shown *in vitro* with Caco-2 cells in which Pgp was highly expressed. The B (Basolateral)-to-A (Apical) transport of substrates like vinblastine and docetaxel was 10 and 20 fold, respectively, greater than the A-to-B transport, and the A-to-B transport was further enhanced in the presence of verapamil and MRK16 by blocking the Pgp efflux function (Hunter *et al.*, 1993a; 1993b). Similar studies were carried out for intestinal transport of cyclosporin and demonstrated that Pgp played an important role in drug absorption by limiting drug transport from intestinal lumen (Augustijns *et al.*, 1993).

3.1.11 Localization of Pgp in brain

Localization of Pgp in the brain has been a widely disputed topic that has become the centre of much controversy in recent years. Beaulieu *et al.*, (1997) provided very convincing evidence for Pgp being predominately localized in the luminal membrane of endothelial cells of rat brain capillaries facing blood circulation. Also the co-enrichment of Pgp and glucose transporter 1 in brain capillary luminal membranes compared with whole brain membrane preparations strongly suggests that Pgp is expressed predominantly in the luminal membrane of brain endothelial cells. Western blot analysis has also revealed higher expression level of Pgp in endothelial cells compared to astrocytes (Barrand *et al.*, 2001). Collectively, these results consistently suggest that brain Pgp is predominantly expressed on the apical surface of endothelial cells of capillaries.

3.1.12 Role of Pgp in brain uptake

Tsuji *et al.*, (1992), were the first to give experimental evidence that Pgp is involved in drug transport in the blood brain barrier (BBB). Kinetic studies have shown that efflux transport of vincristine (substrate of Pgp) from bovine brain endothelial cells was inhibited by verapamil, resulting in a significant increase in intracellular drug concentration. Similar results were also reported by Tatsuta *et al.*, (1992). The unidirectional transport of vincristine from the basolateral side to the apical side was demonstrated in the polarized monolayer of mouse epithelial cells. Similarly, efflux transport of cyclosporin was also observed in cultured endothelial cells of bovine and

mouse brain capillaries (Tsuji *et al.*, 1993 & Shirai *et al.*, 1994). Immunostaining with Pgp antibody (MRK16) also demonstrated an exclusively apical localization of Pgp in human brain endothelial cells (Biegel *et al.*, 1995). These *in vitro* studies have provided evidence of functional involvement of Pgp in the BBB penetration of drugs. Also it has been shown from *mdr1a* and *mdr1a/1b*-knockout mice studies that the brain is more sensitive to changes in Pgp function than other tissues. Therefore, Pgp inhibitors should be used with more caution to avoid potential neurotoxicity.

3.1.13 Bioavailability & drug design

Generally, drug transporters such as MDR1 and drug metabolizing enzymes like cytochrome P450s (CYPs) are the two major biological factors, which affect the pharmacokinetics (oral bioavailability) of drugs. Recently it has been demonstrated that Pgp and CYP3A4 (a member of the cytochrome P450 mixed-function oxidase system, which arguably is the most important enzyme involved in the metabolism of xenobiotics in the body. It is involved in oxidation of the largest range of substrates of all the CYPs and present in the largest quantity of all CYPs in the liver) share a significant overlap in substrate specificity (Wandel *et al.* 1999). Owing to this finding it could be said that the disappointing therapeutic effects of Pgp inhibitors in cancer therapy are due to the fact that high concentrations of Pgp inhibitors would also produce CYP3A4 inhibition. The duality of effects of these Pgp inhibitors on both Pgp and CYP3A4 would result in multiple effects at different tissue sites so that inhibition of Pgp will increase tumor

concentration, increase oral absorption, and increase central nervous system penetration. In addition, inhibition of CYP3A4 would further enhance oral absorption and decrease hepatic metabolism with consequent further increase in plasma concentration. Thus the therapeutic/toxic effects of the change will depend on whether CYP3A4 is involved in activation or detoxification of the drugs in question. A less potent Pgp inhibitor but one with minimal or no CYP3A4 inhibitory effect would be more desirable. The development of potent Pgp selective agents that minimize the risk of CYP3A4-mediated metabolic interactions with the anticancer drug regimen, would produce improved therapeutic specificity and efficacy.

3.1.14 Comparison of *in-vitro* screening assays for Pgp

Several *in vitro* screening assays have been used to identify and classify compounds as Pgp substrates or inhibitors. For example, drug stimulated ATPase activity can be determined by monitoring the release of inorganic phosphate by a colorimetric reaction (Sarkadi *et al.*, 1992; Urbatsch *et al.*, 1994). However this assay cannot distinguish between substrates and inhibitors and also only measures activity indirectly. Another approach is the use of fluorescent indicators (Nelson *et al.*, 1998; Wang *et al.*, 2001) where inhibition of Pgp leads to cellular accumulation of a fluorescent dye, such as rhodamine¹²³ (Eytan *et al.*, 1997) or calcein AM (Tiberghien *et al.*, 1996). These fluorometric assays can also be automated with sufficient suitability for high throughput screening. However, unambiguous identification of inhibitors or substrates of Pgp may

be difficult due to the presence of multiple binding sites. Not only does it not directly measure transport but also it needs to be run in conjunction with monolayer efflux assay, to prevent false negative results.

Kinetic data indicating non-competitive interactions between substrates and inhibitors of Pgp (Litman *et al.*, 1997; Pascaud *et al.*, 1998), as well as photoaffinity labeling studies (Dey *et al.*, 1997), suggest the presence of at least two distinct binding sites. The two sites have distinct but overlapping substrate specificities and exhibit positive cooperativity. Also a third drug-binding (non-transporting) site with positive allosteric properties for drug transport has been reported (Shapiro *et al.*, 1998). Thus, inhibition data obtained from Pgp interaction studies may depend on the kind of substrate used, as suggested for drug interactions at CYP3A4 (Korzekwa *et al.*, 1998).

Clearly then it is very difficult to classify test compounds as transporters and inhibitors by a single assay because different experimental systems and test conditions produce different classifications. A well defined strategy should be used to identify potential inhibitors and substrates of Pgp. Possibly an indirect fluorescence assay could be used as a primary screen followed by ATPase or transcellular transport assay to distinguish substrates and inhibitors. The results can be further confirmed at later stages of drug development by a direct transport assay, followed by *in vivo* experiments (e.g. Pgp knock-out mice) (A knockout mouse is a genetically engineered mouse one or more of whose genes have been made inoperable. Knockout is a route to learning about a gene that has been sequenced but has an unknown or incompletely known function. Mice are

the laboratory animal species most closely related to humans in which, the knockout technique can be easily performed, so they are a favorite subject for knockout experiments, especially with regard to genetic questions that relate to human physiology).

Recently the use of bio-affinity chromatography, which is based upon target biopolymers in a flow system has been considered as a valuable method in identifying substrates for different biopolymers. This method can be used to rapidly determine a compound's affinity for biopolymers and whether it is an inhibitor/substrate of the transporter. This is a key element in drug discovery and drug development programmes. Therefore the method can be used as a prescreen to identify all substrates and inhibitors, which could be subsequently moved onto a more expensive and time consuming functional assays to determine functional activity.

Wainer *et al.*, (2000) recently developed a chromatographic approach utilizing stationary phases containing membranes from cells expressing the Pgp transporter. These cellular membranes were immobilized on a liquid chromatography stationary phase containing an "immobilized artificial membrane" (IAM) stationary phase, to form Pgp-IAM phases. The Pgp-IAM phases were used in frontal affinity chromatographic studies to determine the binding affinities { K_d values} of Pgp substrates and inhibitors and to identify competitive, allosteric and enantioselective interactions in ligand binding to Pgp. In their study showing the enantioselective binding of mefloquine enantiomers to Pgp using a Pgp-IAM stationary phase they suggested that competitive binding

experiments on the Pgp-IAM columns could be a rapid method for the identification of synergistic pairs for specific clinical targets (Wainer *et al.*, 2001).

3.1.15 Aims & Objectives

Building upon the experience gained in related research studies (Chapter 2) involving immobilized protein that took place in the initial phase of this research programme, the general aim was to develop suitable chromatographic platforms for Pgp investigations which have reproducible and with acceptable run times and appropriate detections systems. The first phase was to evaluate the cell lines for Pgp expression and activity.

3.2 Evaluation of doxorubicin toxicity in Pgp-(+) LCC6/MDR1 vs. Pgp-(-) LCC6 human breast cancer cells.

3.2.1 Introduction

In the past years, a number of experimental agents, including vinblastine, verapamil, cyclosporin, and trifluoperazine, have been studied with various efficacies in reversing multi drug resistant phenotype in cancer cells. The application of these compounds is, however, very limited due to their unfavorable toxicities and/or their significant effects on the metabolism and pharmacokinetics of the concurrently administered chemotherapeutic agents (Hegewisch, 1996; Tan, 2000). However the general aim of this experiment was to confirm the functionality of the Pgp-positive LCC6/MDR1 cell line through comparison with the Pgp-negative LCC6 cell line by studying the effect of the cytotoxicity of doxorubicin on the effect of cell growth.

3.2.2 Cell culture

The parental MDA-MB-435 cells were originally provided by Dr Janet Price (MD Anderson Cancer Center, Houston, Texas, USA), and were established from a pleural effusion in a 31 year old Caucasian woman with metastatic breast cancer (Cailleau *et al.*, 1974, 1978). The patient had received no prior systemic therapy. MDA-MB-435 is one of the few human breast cancer cell lines that produces reproducible lung metastases from solid tumours (Price *et al.*, 1990; Meschter *et al.*, 1992). The MCF-7^{ADR} clone 5 cells are a cloned population of MCF-7^{ADR}, and were kindly provided by

M. Johnson (Lombardi Cancer Center, Georgetown University, Washington DC, USA). MDA-MB-435, MCF-7^{ADR} clone 5, MDA-435/LCC6 and MDA435/LCC6^{MDR1} (multi drug resistant gene 1) cells were routinely maintained in improved minimal essential medium (IMEM; Biofluids, Rockville, Maryland, USA) containing phenol red and supplemented with 5% foetal calf serum.

3.2.3 Experimental

LCC6 and LCC6/MDR1 cells were plated in 96 well plates (2 plates per cell line) with 1200 cells / 100 µl media per well, in 60 wells. The plates were incubated at 37°C in 5% CO₂ atmosphere and 90% relative humidity (RH) for 72 h. The cells were then treated with 200 µl of varying concentrations of doxorubicin (0, 3, 8, 20, 51, 128, 320, 800 & 2000 nM) in media and incubated for 24 h. The treatment was stopped and the media was exchanged with 200 µl of fresh growth media and re-incubated at 37°C for further 72 h. The cell cultures were then fixed / stained by exchanging spent media with 75 µl of crystal violet solution (0.5 % in 25 % methanol) per well. The plates were then rinsed with water and dried. After drying, the crystal violet attached to wells was re-dissolved in sodium citrate 0.1 M in 50% ethanol. Absorbance was evaluated using an ELISA reader spectrophotometer at 540 nm and the resulting data were used to evaluate the amount of cells. The absorbance directly correlates with cell number in this assay.

3.2.4 Results & Discussion

In order to study the effect of cytotoxic drug doxorubicin on Pgp cell growth it was decided to adopt the experimental approach of investigating the comparative effects of a range of eight different concentrations of doxorubicin on cell growth in the two cell lines. More specifically, the approach would be to evaluate cell growth in terms of crystal violet staining of cells grown in 96-well plates, six days after initial seeding.

The cell survival curves were obtained for each cell line at varied concentrations of doxorubicin (Table 7). The toxicity of each drug was expressed as an IC_{50} , defined as the concentration inhibiting cell density by 50% at the end of the treatment. The IC_{50} for LCC6 and LCC6/MDR1 were 16.33 nM and 341.20 nM respectively. Since Pgp transporter is an efflux pump which transports substrates out of the cell. The results indicated that the drug doxorubicin is exported much more out of the LCC6/MDR1 cell line compared to the LCC6 cell line. Therefore it was apparent that the control cell line was much more sensitive to doxorubicin as compared to the positive LCC6/MDR1 cell line, proving that the LCC6/MDR1 cell line had a stable, active and over-expressed Pgp transporter as compared to the control cell line LCC6.

Table 7. Cell Survival (%) at different concentrations of cytotoxic drug doxorubicin. Absorbance was evaluated using an ELISA reader spectrophotometer at 540 nm and the resulting data were used to evaluate the amount of cells. The absorbance directly correlates with cell number in this assay (n = 3).

Concentration nM	Cell Survival (%)	
	LCC6	LCC6/MDR1
0	100.00 ± 0.00	100.00 ± 0.00
3	83.82 ± 0.75	98.41 ± 0.95
8	75.72 ± 1.60	97.14 ± 0.28
20	42.70 ± 1.48	97.98 ± 0.35
51	31.17 ± 0.30	92.21 ± 0.81
128	34.81 ± 0.41	91.40 ± 0.45
320	29.70 ± 0.88	52.48 ± 1.23
800	17.19 ± 0.69	33.62 ± 1.10
2000	11.83 ± 0.68	29.46 ± 0.85

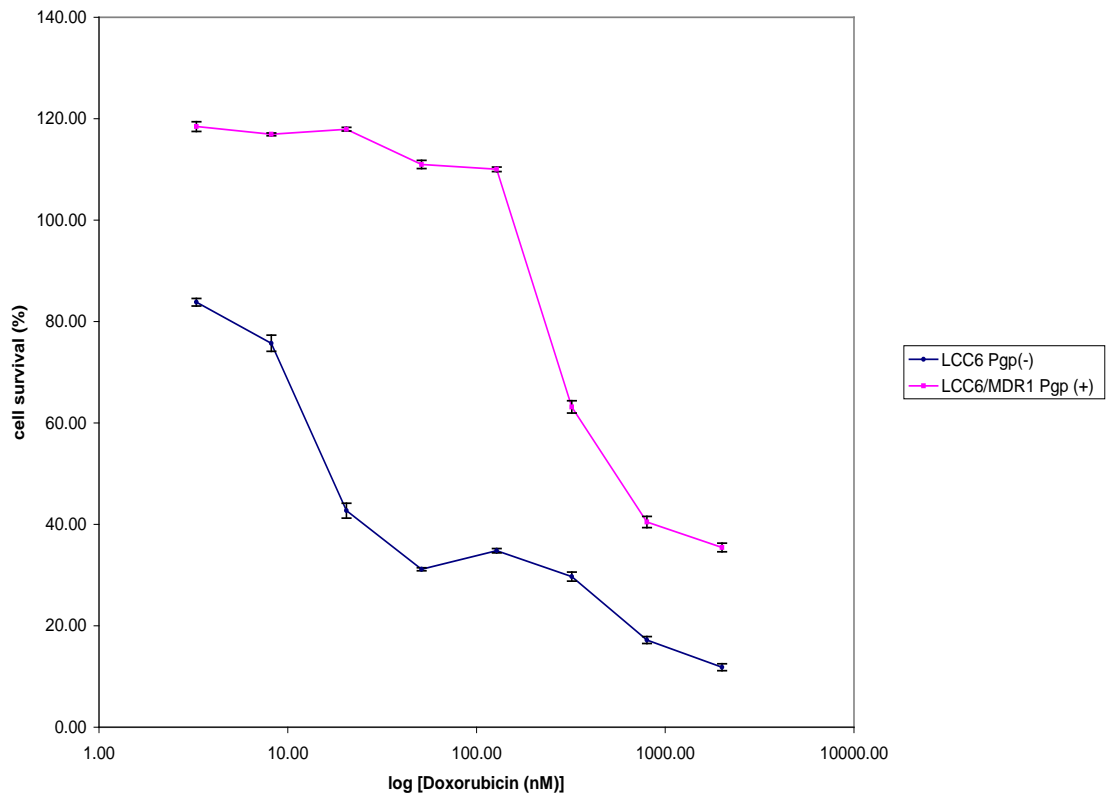


Figure 19. Plot of log [doxorubicin] (nM) vs. cell survival at different concentrations of cytotoxic drug doxorubicin for Pgp(+) cell line and the Pgp(-) cell line. The absorbance was evaluated using and ELISA reader at 540 nm and the resulting data were used to evaluate the % cell survival. The absorbance directly correlates with the cell number in this assay (n = 3). IC₅₀ values were calculated as the concentration inhibiting cell density by 50 % at the end of the treatment.

3.2.5 Conclusion

The Pgp (+) LCC6/MDR1 cell line had a twenty fold higher IC_{50} 's than the Pgp (-) LCC6 cell lines for doxorubicin. This indicated that the efflux protein Pgp was over-expressed in the LCC6/MDR1 cell line as compared to the LCC6 cell line. Therefore it has been demonstrated that there is a significantly higher concentration of Pgp in the Pgp (+) LCC6/MDR1 cell line as compared to the Pgp (-) LCC6 cell line. Thus the cell line producing the active protein Pgp was available to perform functional studies and make immobilized biopolymer columns containing Pgp. Also the control cell line had a considerably lower presence of the protein which would make it a good control cell line.

3.3 Substrate accumulation of vinblastine in Pgp (+) LCC6/MDR1 vs. Pgp(-) LCC6 Human breast cancer cells.

3.3.1 Introduction

The general aim of this study was to confirm the differential functionality of Pgp (+) vs. Pgp (-) cell lines. In a similar fashion to the previous experiment (Section 2.2) Pgp being an efflux protein, the ability of each cell line to influence the intracellular accumulation of cytotoxic drug (Figure 20) should be different depending upon the expression of the efflux Pgp transporter. For example, vinblastine diffuses through the

lipid bilayer into the intracellular space *via* passive diffusion. In the presence of the Pgp transporter the vinblastine molecule is translocated from the inner leaflet of the membrane to the outer membrane leaflet or the extracellular space. A vinblastine substrate accumulation study was carried out on the control and the positive cell line to show how each cell line accumulates varied concentration of the substrate depending upon the number of active Pgp binding sites.

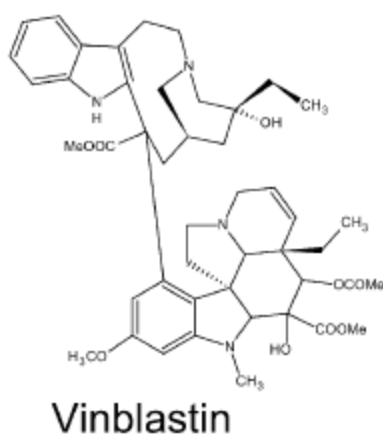


Figure 20. Molecular structure of vinblastin (Vinca alkaloid). It binds to tubuline, thereby inhibiting the assembly of microtubules. It is a substrate of Pgp with hydrophobic properties. Effective against cancers of the white blood cells such as lymphoma, non-small cell lung cancer, breast cancer and testicular cancer

3.3.2 Experimental

Pgp (+) LCC6/MDRI and Pgp (-) LCC6 human breast cancer cell lines were plated at 2.5×10^5 cell / well into 24-well culture dishes, in routine growth media, and incubated at 37°C. Forty-eight hours later, the Pgp (+) LCC6/MDRI and Pgp (-) LCC6 cell lines were treated by replacing the growth media with media containing 5 nM ^3H -vinblastine (specific activity 254 GBq) and the control wells were plated with growth media containing 5 nM cold vinblastine. After a three hour incubation, the treatment was stopped by washing each well with phosphate buffered saline (0.5 ml / well) and left to dry at room temperature. Cell monolayers were removed by trypsinization (1 ml) and diluted with 10 ml of scintillation fluid (Ecosinct A). Vinblastine accumulation was radiometrically assessed by scintillation spectrometry (n=4).

3.3.3 Results & Discussion

Pgp transporter has a ligand binding-domain, which is on the extracellular side of the protein for importers and on the cytoplasmic side for exporters. It contains a translocation pathway, which is a cavity which a specific molecule can use to travel through the protein. When an ATP molecule binds to each cassette, it induces a conformational change in both the nucleotide-binding folds and the transmembrane domains, allowing the molecule to travel through the translocation pathway. Vinblastine a Pgp substrate passes through the lipid bilayer through passive diffusion and binds to

ligand binding domain (cavity) and in presence of ATP is translocated to the outer leaflet or the extracellular space (Figure 21).

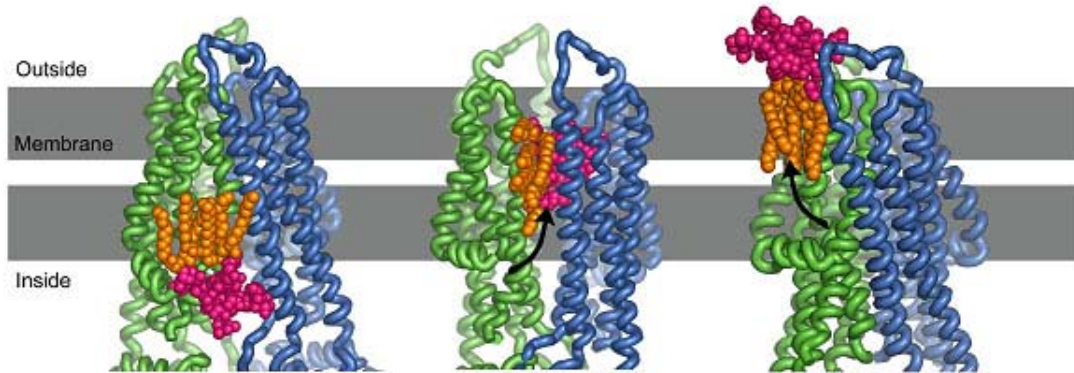


Figure 21. Vinblastine molecule bound to the ligand binding domain in the cavity of the Pgp transporter and when the nucleotide binding fold binds to an ATP molecule, a conformational change opens up the pathway and translocates the lipid to the extracellular membrane.

The vinblastine accumulation for each of the cell lines is shown in Table 8. There was a significant difference $p < 0.0001$ in the vinblastine accumulation between the two cell lines indicating that the Pgp (+) cells had overexpression of the efflux protein Pgp. Vinblastine is a Pgp substrate and therefore intracellular concentration of vinblastine should be less in cells that express Pgp as compared to cells that do not express Pgp. The Pgp (+) cell line had a six fold lower substrate accumulation of vinblastine as compared to the Pgp (-) cell line, thus indicating that there were at least six fold more active Pgp sites present on the Pgp (+) cell line as compared to the Pgp (-) cell line.

Table 8. Vinblastine accumulation was carried out on Pgp (+) and Pgp (-) cells plated on 24 well culture dishes and incubated with 5nM [³H]-vinblastine for 3 h. The cell monolayers were removed with trypsination (1ml) and then measured by scintillation counting in disintegrations per minute (DPM).

Cell Line	Vinblastine accumulation (DPM) (n = 4)
Pgp (+) LCC6/MDR1	929 ± 64
Pgp (-) LCC6	5532 ± 599

3.3.4 Conclusion

The results of the experiment proved that the substrate accumulation of vinblastine was much lower in the control cell line as compared to the test cell line. Also the Pgp protein present in the test cell lines is active as it actively effluxes vinblastine out of the cells. Thus this shows that the Pgp protein is abundantly present on the Pgp (+) cell line and therefore the cell line could now be used in the planned subsequent experiments to prepare immobilized biopolymer stationary phases. Also since the Pgp protein is over expressed in the Pgp (+) cell line as compared to the control cell line Pgp (-) which doesn't have the transfected Pgp gene, parallel experiments carried out with the Pgp (+) and Pgp (-) cell line would depict a knock-in/knock out model. The two columns have been characterised by its functionality, and the functionality is due to the Pgp and therefore there is no need to quantify the protein. This is an advantage for this method

as quantification the low amount of protein would pose a problem. Also the membranes are immobilized on the column, the number of bindings sites don't change for the column over a long period. This is seen as the retention time and K_d values remain reproducible over a period of six months.

3.4 Preparation of and frontal chromatographic studies with IAM based columns with Pgp(+) and Pgp(-) membranes

3.4.1 Introduction

As discussed earlier (Chapter 1) there are many ways in which transporters can be exploited in chromatographic systems. However, on basis of recent experience in the laboratory, it was decided to follow the example of recent work done by Moaddel *et al.*, (2000) and adopt an immobilized IAM system. Similarly the chromatographic processes would be monitored by use of radio-labeled markers.

3.4.2 Experimental

3.4.2.1 Materials

Vinblastine (Vb), dithiothreitol (DTT), 3-[3-(cholamidopropyl)dimethylammonio]-1-propane sulfate (CHAPS), glycerol, leupeptin, pepstatin, phenyl methyl sulfonyl fluoride (PMSF), EDTA, sodium hydroxide, tris[hydroxymethyl]aminomethane (Trizma) and tris[hydroxymethyl]aminomethane hydrochloride (Tris-HCl) (used to

prepare the Tris buffer), avidin, glutaric dialdehyde and aminopropyltrimethoxy silane (APTS) were purchased from Sigma (St. Louis, MO, USA). [³H]-Vinblastine (254 GBq) and [³H]-cyclosporin A (259 GBq) were purchased from Amersham Pharmacia Biotech (Piscataway, NJ, USA). 6-[(biotinoyl) amino] hexanoic acid (Biotin-X) was purchased from Molecular Probes (Eugene, OR, USA). Open tubular capillaries (100 µm i.d.) were purchased from Polymicro Technologies (Phoenix, AZ, USA).

3.4.3 Preparation of Pgp(-) and Pgp(+) membranes

3.4.3.1 Cell lines

Pgp(-) membranes were obtained from the MDA435/LCC6 (human breast cancer) cell line. The Pgp(+) membranes were obtained from the MDA435/LCC6MDR1 cell line prepared from the MDA435/LCC6 cell line by transduction with a retroviral vector carrying MDR1 cDNA (Pgp) as previously described by Leonessa *et al.*, (1996).

3.4.3.2 Solubilization of the membranes

The MDA435/LCC6 or MDA435/LCC6MDR1 cells (100×10^6 cells) were placed in 15 ml of homogenization buffer (Tris-HCl [50 mM, pH 7.4] containing 50 mM NaCl, 8 µM leupeptin, 1 µM PMSF and 8 µM pepstatin). The suspension was homogenized for 3 x 30 s at the setting of 12.5 on a Model PT-2100 homogenizer (Kinematica AG, Luzern, Switzerland). The homogenate was then centrifuged at 700 x g for 5 min and

the pellet containing the nuclear proteins was discarded. The supernatant was centrifuged at 100,000 x g for 35 min at 4°C and the resulting pellet containing the cellular membranes was collected. The pellet was then re-suspended in 10 ml of solubilization buffer (Tris HCl 50 mM pH 7.4, 250 mM NaCl, 1.5% CHAPS, 2 mM DTT, 1 µM PMSF, 8 µM pepstatin A, 10% glycerol) and the resulting mixture was rotated at 150 rpm using an orbit shaker (Lab-line Model 3520, Melrose Park, IL, USA) for 18 h at 4 °C. The resulting solution was centrifuged at 60,000 x g for 22 min and the solubilized solution was then mixed with 160 mg IAM particles and was rotated at room temperature for 3 hours at 150 rpm using an orbit shaker (Lab-line Model 3520, Melrose Park, IL, USA). The suspended particles were then dialyzed against dialysis buffer (Tris HCl [50 mM, pH 7.4], 150 mM NaCl, 1 mM EDTA, 1 mM benzamidine) for two days. The dialysed solution was centrifuged for 3 min at 4 °C at 700 x g and the supernatant was discarded. The pellet (LCC6/LCC6MDR1-IAM) was washed with running buffer A (Tris-HCL [10 mM, pH 7.4] containing 1 mM CaCl₂, 0.5 mM MgCl₂) and centrifuged. This process was repeated until the supernatant was clear.

3.4.4 Preparation of chromatographic column

The LCC6-IAM and LCC6/MDR1-IAM (180 mg) were packed into a HR 5/2 glass columns (Amersham Pharmacia Biotech, Uppsala, Sweden) using a rabbit pump at setting 5 to yield a 150 mm x 5 mm (i.d.) chromatographic beds, to produce the Pgp(+)-IAM and Pgp(-)-IAM columns.

3.4.5 Chromatographic system

The chromatographic system was composed of a Shimadzu LC-10Advp pump, 50 ml superloop (Amersham Pharmacia, Uppsala, Sweden), an IN/US system β -Ram model 3 radioflow detector (IN/US, Tampa, FL, USA) with a dwell time of 2 s and the output data was analyzed using the Laura lite 3 (IN/US) programme.

3.4.6 General procedures

In these studies, the mobile phase consisted of the marker ligand [^3H]-Vb in 5 ml of ammonium acetate (10 mM, pH 7.4) delivered at a flow rate of 0.2 ml/min. At the beginning of each experimental series, the mobile phase was run through the Pgp(+)-IAM column until an elution profile showing both front and plateau regions was observed. Increasing concentrations of the unlabelled marker or unlabelled displacer were then added to the mobile phase and the frontal chromatographic experiments were repeated. When Vb was studied, the mobile concentration of [^3H]-Vb was 0.65 nM and the added concentrations of Vb were 50, 125, 250, and 500 nM.

3.4.7 Results and Discussion

3.4.7.1 Characterisation of the immobilized Pgp-IAM column

Quantitative affinity chromatography is an extremely well documented approach used for the measurement of ligand-protein interactions (Jaulmes and Vidal-Madjar, 1989). Displacement chromatographic techniques can be used to observe binding interactions between two or more ligands binding at the same or separate sites. Thus in this manner, competitive and allosteric (cooperative or anticooperative) interactions can be readily identified.

In this study the Pgp transporter was immobilized on an immobilized artificial membrane (IAM) and used to study the binding interactions between the transporter and the ligands (Figure 22).

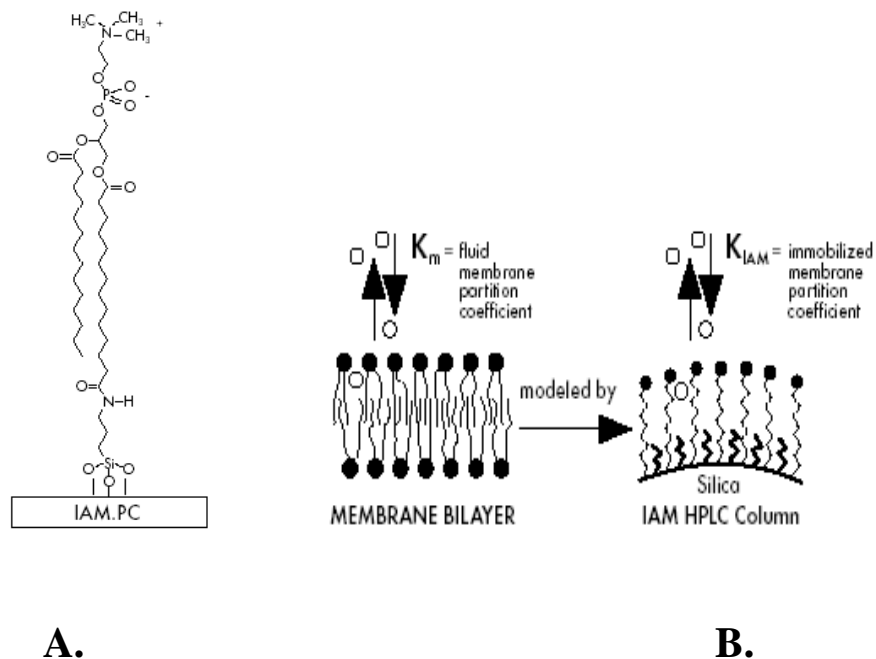


Figure 22. A. IAM chromatography packing material composed of single chain ether phospholipids containing ω -carboxyl groups in the alkyl chain immobilized on aminoopropyl silica. The phospholipids surface is stable with organic solvents and aqueous buffers between pH 2 to 8. IAM have an area per molecule of 66-104 Å². The similar area per molecule of these IAM and mobile phospholipid in liposomes indicated that the lipid environments were similar. B. IAM chromatographic surfaces prepared by covalently immobilizing cell membrane phospholipids to solid surfaces at monolayer densities. IAM surfaces mimic fluid cell membranes (lipid bilayer). This figure indicates that solute partitioning between IAM bonded phase and the aqueous mobile phase is similar to the solute partitioning between liposomes and the aqueous phase.

The activity of the Pgp transporter immobilized on IAM stationary phase Pgp(+)-IAM was determined using frontal displacement (affinity) chromatography with [³H]-Vb as the marker ligand, and Vb as the displacer. The Pgp-IAM was used to determine the binding affinities (K_d values) of Pgp substrates and inhibitors and to identify competitive, allosteric and enantioselective interactions in the ligand binding to Pgp (Figure 23).

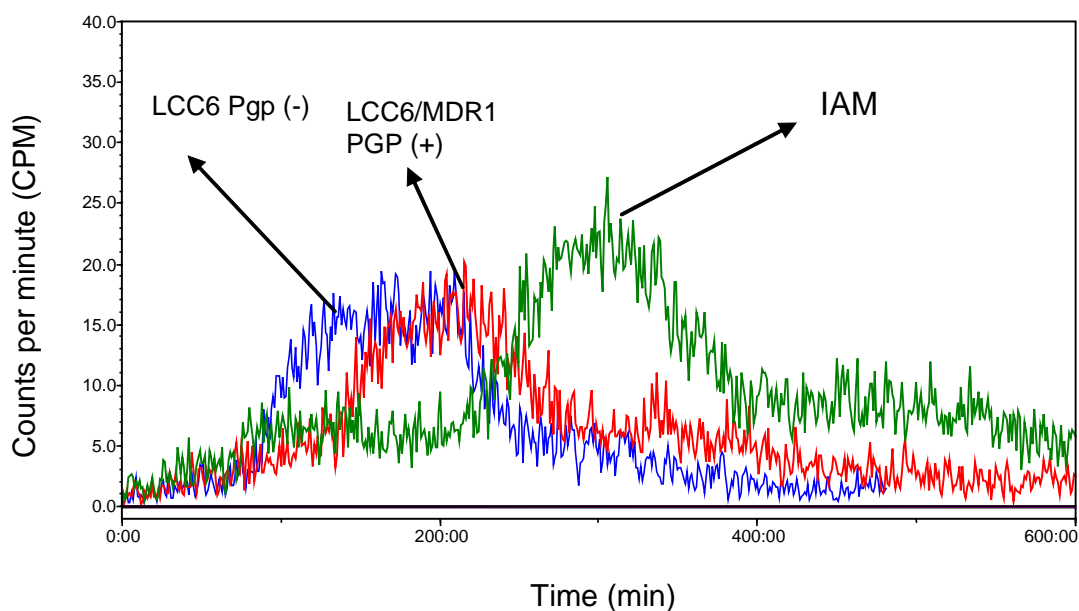


Figure 23. Comparison of the frontal chromatograms of 0.5 nM [³H]-Vb (5ml) on the LCC6/MDR1 Pgp(+)-IAM-column (red), LCC6 Pgp(-)-IAM column (blue) and IAM column (green). Elution profiles show both the front and plateau regions of the frontal chromatogram. Radioactivity was measured as counts per minute (CPM) using a liquid scintillation radioflow detector (IN/US system β -Ram model 3) and the output data is analyzed using a Laura lite programme with a dwell time of 2 s. Running buffer consisted of ammonium acetate [10 mM, pH 7.4] and the flow rate was 0.2 ml/min.

However the run times often ranged from 1 to 3 h. Also as could be seen from the elution profile of the blank IAM column, (Figure 23) a significant portion of this long run time was the result of strong lipophilic interactions between the substrate/inhibitors which are hydrophobic in nature and the IAM backbone which is very lipophilic. Due to these long retention times and accompanying long equilibration and wash times, the Pgp-IAM stationary phases were not suitable for use in the rapid determination and characterization of Pgp binding interactions. Further, the frontal chromatography of [³H]-Vb showed two distinct peaks indicating that multiple binding sites were present which made it difficult to use [³H]-Vb as the marker ligand. These multiple binding sites could also be attributed to surface of the IAM which has two binding pockets, one on the surface and another in a deep cleft.

In order to decrease the retention time of the Pgp substrates/inhibitors various methods were employed but they were not very successful. For example, varied cell number ranging from 100 million to 500 million were used in order to cover as much surface area of the IAM as possible. This produced shorter retention times but still did not allow for the rapid determinations of binding affinities. Also, 5% methanol was used to decrease the long run times, but this introduction of methanol reduced the lifetime of the column drastically, presumably the alcohol interfering with the tertiary structure of the transporter. A further problem was that the results were not reproducible indicating that the methanol could be denaturing the protein so that the protein would lose its activity and the structure of its binding site.

3.4.8 Conclusion

Although the IAM stationary phase was an ideal choice to study the nicotinic acetylcholine receptors (Moaddel, 2000), this was not the case for the Pgp transporter. Pgp substrates are predominantly lipophilic, as access to the binding pockets is located deep in the lipid bilayers. Therefore there were more non-specific interactions with the IAM stationary phase as compared to the specific interactions between ligands and the target protein.

Thus owing to the hydrophobic nature of the IAM columns and the Pgp substrates like vinblastine (very lipophilic), it became difficult to remove the non-specific interactions created by the interaction between the IAM backbone and the substrates. Therefore the use of the biopolymeric stationary phase became impractical, due to the large retention times and also long wash times (18 h). Also the use of radioactivity was a deterrent as although radioactive isotopes have higher sensitivity and help in removing for the background interference from other analytes, it has its drawbacks as it is highly hazardous and all ligands aren't readily available. Also it requires the use of special equipment and stricter safety precautions. Also certain times the commercial purity is a question mark. Thus as many of the ligands for Pgp are not readily available with radioactive tags other method of detection like mass spectrometry was carried out, giving the advantage of being able to use a more wide range of substrates for the analysis and characterization of the Pgp column.

3.5 Pgp PEEK Columns (Vanadate Trap)

3.5.1 Introduction

Given these shortcomings of these conventional IAM columns, it was necessary to find a backbone and support which would decrease the non-specific interactions and provide a faster elution profile.

The initial approach to decrease the amount of non-specific interactions with the IAM backbone was to pack the support into a peek-tubing column (762 μm i.d. x 40 cm) which had a smaller diameter. Also using this approach would also mean less utilization of the cell extract and different reagents and also IAM which is very expensive. This was an important factor as the vanadate trapping experiment could lead to a disruption of the active site of Pgp. The importance of intended vanadate trapping is that it allows for the determination of non-competitive inhibitors of this transporter. Similar effects on the transport cycle of Pgp had been observed with vanadate trapping (Rao & Nuti *et al.*, 2003) (Figure 24).

P-glycoprotein Transport Cycle

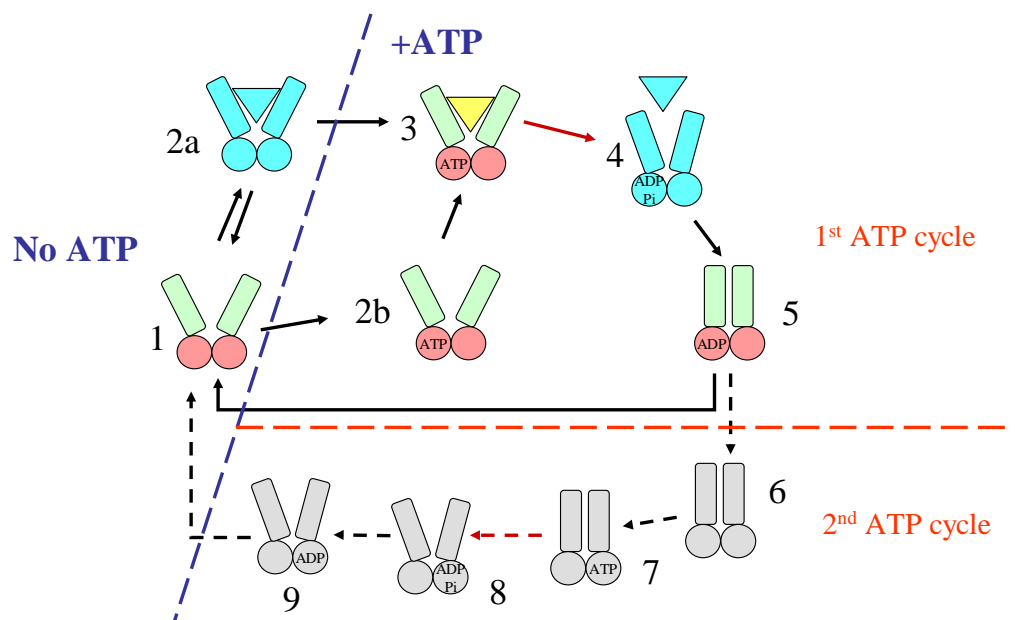


Figure 24. ATP dependant Pgp transport cycle showing Pgp transporter in its different transformational states. 2a. resting phase of Pgp, 3. pre-catalytic stage, 4. catalytic stage, 5. post-phosphate stage, 6. post ADP (adenosine triphosphate) stage. Stages 6 to 9 are for the second ATP cycle which helps Pgp get back to the original resting phase 1.

Vanadate-trapping of the Pgp transporter in state 4 is a more desirable approach than using ATP as it is cheaper, the effect lasts longer and a vanadate containing mobile phase can be used with mass spectrometry. In summary, the aim of the next phase of the research programme was not only to establish a more pragmatic approach to the frontal chromatography by using a Pgp-PEEK tubing micro-capillary column but also to apply it to the study of the effect of vanadate on the specific retention of Vb.

3.5.2 Experimental

3.5.2.1 Preparation of membranes

The preparation of Pgp (+) and Pgp(-) membranes used in this study was as described in section 3.4.3

3.5.2.2 Preparation of chromatographic column

PGP-(+)-IAM and Pgp(-)-IAM was packed into PEEK tubing column (762 μm id x 40 cm) using a rabbit pump at a flow rate at 50 $\mu\text{l}/\text{min}$ ammonium acetate [10 mM, pH 7.4] as mobile phase.

3.5.2.3 Vanadate-trapping

100 mM stock solution of sodium orthovanadate was prepared in de-ionised water by acidifying with 1M HCl. Running buffer composed of Tris [50mM pH 7.4], 150mM NH_4Cl , 5mM MgSO_4 , 0.02% NaN_3 (sodium azide), 2mM ATP and 0.3M sodium orthovanadate was prepared and run through the column for 120 min. The column was incubated at 37° C for 30 min. The immobilized Pgp transporter was trapped in the first ATP cycle using the vanadate trapping. Zonal elution studies were carried out to determine the effect of the vanadate trapping. Mobile phase containing ammonium acetate [10mM, pH 7.4], 0.1 nM vanadate was used during the study. These studies

were carried out using mass spectrometric detection on the Micromass QTOF1-MS (Waters, Milford, MA).

3.5.3 Results and Discussion

Pgp is an ATP dependent drug efflux pump, which passes through a number of phases during the transport cycle (Figure 24 {b}). The transport cycle is ATP dependent and Pgp exhibits a robust drug substrate-stimulating ATPase activity. Previous studies with the Pgp-IAM HR5/2 glass column, had suggested that when ATP was not present in the mobile phase, the Pgp transporter was frozen in state 2a (Moaddel *et al.*, 2002).

Under these conditions, the immobilized Pgp transporter binds to characterized Pgp substrates, such as Vb but there is no demonstrable affinity for non-competitive inhibitors such as CysA. The addition of ATP to the mobile phase produces a conformational shift in the immobilized Pgp resulting in its transition to state 4. In this state, the vanadate treated Pgp did not bind to Vb, but had a significant affinity for CysA.

The importance of the use of the ATP trapped (vanadate trapped) Pgp is that it allows for the determination of non-competitive inhibitors of this transporter. The results of these studies are presented in Figure 25.

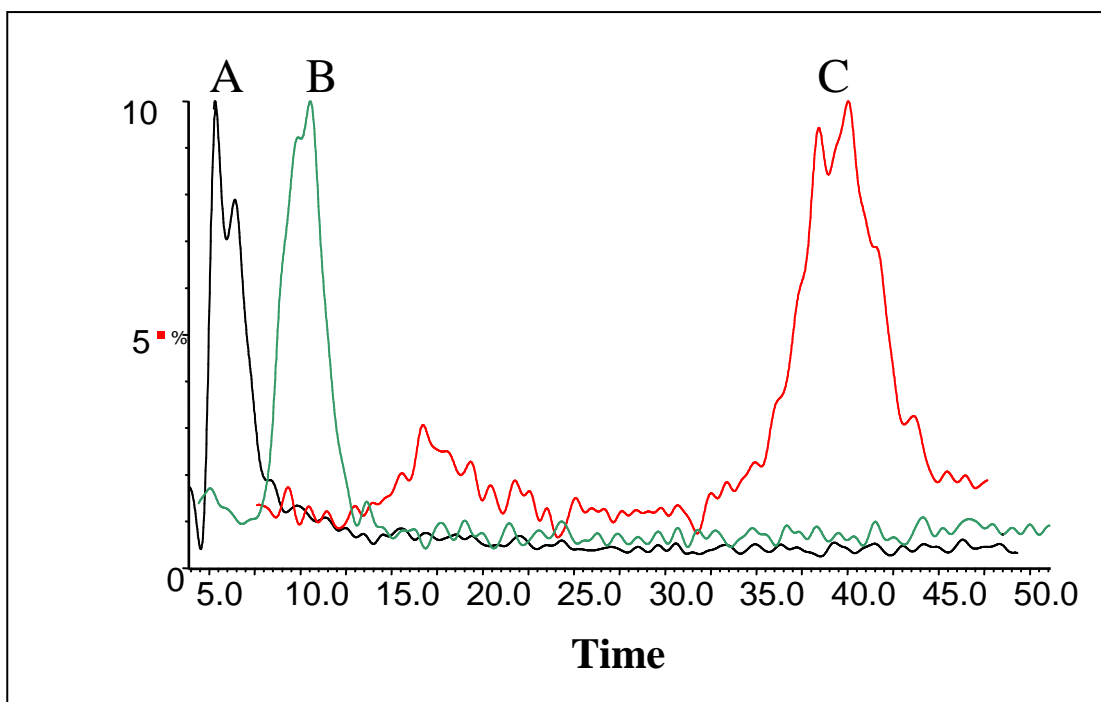


Figure 25. Effect of vanadate trapping on a the retention of Vb on a Pgp(+)-IAM PEEK tubing column where A Vb on “vanadate-trapped column”, B Vb on “ATP-saturated column” and C Vb on peek tubing column without any vanadate trapping. Running buffer consisted of ammonium acetate [10 mM, pH 7.4] and the flow rate was 50 μ l/min.

Under zonal elution conditions Vb had a retention time of 40.0 min and in the presence of 3 mM ATP, the retention time decreased to 10.4 min. With the vanadate trap the retention time of Vb was 6.0 min (Figure 7). The results of this study suggested that the Pgp transporter was trapped in the first ATP cycle using the sodium ortho vanadate. On the other hand there was a significant difference in the effect of vanadate on Vb retention. Thus the results showed that vanadate trapping caused conformational change in the Pgp binding site which lead to an inhibition (decrease) in binding of the substrate

Vb to Pgp. This could be used to screen compounds for their non-competitive inhibition activity for Pgp. However the PEEK-tubing columns generated a high back pressure at the flow rates that had been used and thus could not be used reproducibly for more than six runs. Also there was loss of column packing due to the high back pressure which resulted in poor peak shape.

3.5.4 Conclusion

As anticipated the run times were reduced. Also due to the higher proportion of Pgp to the IAM the contribution of the non-specific interaction were minimized. Therefore the reduction in the chromatographic bed to $1/3$ the size the HR5/2 column and the resulting reduction in the retention time to approx 40 min for Vb provided the means to exploit the use of these columns for studying the Pgp in its different conformational state.

Therefore, Pgp being an ATP dependent drug efflux pump, exhibited a robust drug substrate-stimulating ATPase activity and vanadate blocking effectively trapped Pgp in a non-covalent stable transition state conformation. Zonal elution studies carried out on the vanadate trapped column would help in identification of non-competitive inhibitors of Pgp.

3.6 Caco-2 permeability measurements and stimulation of membrane-based ATPase activity.

The following studies were performed as a collaborative effort with Purdue Pharma in the US. The results from their assay were used in conjunction with the results of the Pgp open tubular column to provide a comparison between the various techniques. The experimental details for the two assays are given below.

3.6.1 Materials

Human colorectal adenocarcinoma (Caco-2) cells were obtained from American Type Culture Collection. Buffer components were obtained from Baker Chemicals. Other necessary reagents and all test chemicals were obtained from Sigma Chemicals. Delbecco's Modified Eagle's Medium (DMEM) without phenol red, foetal bovine serum, trypsin/0.5% EDTA, pen/strep and Hank's buffered salt solution (HBSS) were obtained from Invitrogen Corporation (Carlsbad, CA). Electric resistance measuring device (EVOM-X) and 96-well plate electrode (STX 100M) were purchased from World Precision Instruments Inc. Multiscreen Caco-2 96-well plates were purchased from Millipore (Bedford, MA)

3.6.2 Caco-2 assay

Caco-2 permeability experiments were conducted using a previously described method (Balimane *et al.*, 2004), which was modified to meet the conditions of this study. Caco-2 cells at passage 20 were stored in liquid nitrogen upon arrival from ATCC. A cell bank was prepared and frozen at passage 23. These cells were then thawed in a 37 °C water bath (1-2 min). Freezing medium was removed by suspending the contents of one vial in 10 ml of propagation medium in a 50 ml centrifuge tube followed by centrifugation at 700 x *g* for 5 min at 4°C. The cell pellets were re-suspended in DMEM and seeded at 10^6 / T75 flask. Flasks were incubated at 37°C and 5% CO₂ for several days until reaching 60-80 % confluence.

Confluent cells were detached using a trypsin-EDTA solution followed by the addition of propagation medium to neutralize trypsin, and then the cells were pelleted by centrifugation at 700 x *g* for 5 min at 4 °C. Supernatants were removed and cell pellets were re-suspended in assay medium and counted using a hemocytometer. Cells were seeded into 96-well plates at 10^4 cells per well into apical chambers. The basolateral chambers were filled with 250 µl of DMEM. Units were assembled and placed in an incubator for at least 24 days to allow for monolayer formation, feeding three times per week.

Assay plates that were 24-30 days in culture were used in this assay. To acclimate cells to transport buffer, DMEM was removed from both the apical and basolateral chambers and replaced with apical buffer at 85 µl/well and basolateral buffer at 250 µl/well. After

30 min at 37°C and 5% CO₂ trans-epithelial electric resistance (TEER) was measured. TEER values of greater than 1500 ohms were considered acceptable for use. Usually TEER values were about 2000-3000 ohms after 24 days culture. Permeability assays were performed in both directions.

Test compounds were dissolved in DMSO to yield 10 mM stock. Compounds were further diluted to a final concentration of 30 µM in corresponding transport buffer depending on the direction of the transport assay.

In order to determine P_{appA-B} test compounds were added in apical buffer (5mM HES at pH 6.5) (85 µl/well) to apical chambers in replicates of four and blank basolateral buffer was added to basolateral chambers (5mM HEPES at pH 7.4) (250 µl/well). Plates were incubated for 2 h on an orbital shaker at a 37°C and 5% CO₂. In order to determine P_{appB-A}, test compounds in basolateral buffer (250 µl/well) were added to basolateral chambers in replicates of four and blank apical buffer was added to apical chambers (85 µl/well). Plates were incubated for 1 h on an orbital shaker in a 37 °C and 5% CO₂ incubator. After incubation, supernatants from apical and basolateral chambers were transferred to separate 96-well plates and submitted for LC-MS analysis along with neat solutions of the compounds in either buffer. Neat solutions were analyzed and used as zero-time calculations. The apparent permeability coefficients (P_{app}) were calculated in both directions as described previously (Balimane *et al.*, 2004).

3.6.3 Membrane based ATPase assay

Membrane ATPase experiments were conducted using a previously described method (Wang *et al.*, 2000; Garrigues *et al.*, 2002), that was modified to meet the conditions of this study. Potassium phosphate at 2.5, 1.25, 0.63, 0.31, 0.15, 0.75 mM and vehicle control were prepared in Tris-Mes buffer in a final assay volume of 60 μ l/well. A standard curve was plotted using Excel. The equation of the line generated was used to calculate the nmol of phosphate released in the test samples.

Stock solutions of each test compound were prepared in 100% DMSO at a concentration of 2 mM. Serial dilutions of the stock solutions were prepared using phosphate buffer, pH 7.4. The above concentrations were re-diluted in Pgp membrane solutions in the following step to yield the final test concentration.

The assay was initiated by suspending Pgp membranes in 4.5 ml of Tris-Mes Buffer then transferring 147 μ l/well of Pgp membrane solution into a 96-well plate (2.5 μ g protein per well). This was followed by the transfer of 3 μ l of test compound solution from the chemistry plate to an intermediate plate. The membrane / compound solutions prepared above were split into five 30 μ l/well aliquots and transferred into an assay plate, yielding four replicates per concentration, and discarding the remaining solution. This was followed by the addition of 10 μ l/well of sodium orthovanadate solution into background wells and 10 μ l/well of Tris-Mes buffer into test wells. ATP solution was added at 20 μ l/well to all wells. The final assay volume was 60 μ l/well. Plates were

incubated at 37 °C for 20 min after which the reaction was stopped with 30 µl/well sodium dodecyl sulphate (SDS) solution. SDS solution was also added to potassium phosphate standards. Ammonium molybdate was added at 40 µl/well followed by 160 µl/well ascorbic acid solution to test samples, background wells and standards wells. The plates were incubated for 10 min and absorbance read using a Victor2 plate reader at 690 nm. Absorbance values of signal plate were subtracted from those in the background plate. The resulting absorbance values were converted to nmol phosphate released using the phosphate standard curve equation of the best-fit line. E_{\max} values were determined using GraphPad prism.

3.7 Preparation of open tubular (OT) based columns with Pgp(+) and Pgp(-) membranes and frontal chromatographic studies with radio-labelled markers.

3.7.1 Introduction

While the Pgp-IAM stationary phase produced accurate and reproducible data, there was still scope for further improvement with respect to the chromatographic run times. A significant portion of the chromatographic retention was the result of strong lipophilic interactions between the substrates/inhibitors and the IAM backbone. Due to long retention times, the Pgp-IAM stationary phase was not suitable for use in the rapid determination and characterization of Pgp binding interactions. The objective of this study was to reduce the non-specific interactions arising from the chromatographic backbone. This could be approached through a different immobilization technique

(covalent immobilization) of cellular membranes from Pgp expressing cells Pgp (+) membranes onto the inner surface of an open tubular capillary to create a Pgp (+)-OT column.

3.7.2 Materials

Vinblastine (Vb), verapamil, imipramine, fexofenadine, ritanovir, doxorubicin, ketoconazole, prazosin, (-)-nicotine, atenolol, imipramine, loratidine, domperidone, labetalol, benzamidine, dithiothreitol (DTT), 3-[3-(cholamidopropyl)dimethylammonio]-1-propane sulfate (CHAPS), glycerol, leupeptin, pepstatin, phenyl methyl sulfonyl fluoride (PMSF), EDTA, sodium hydroxide, tris[hydroxymethyl]aminomethane (Trizma) and tris[hydroxymethyl]aminomethane hydrochloride (Tris-HCl) (used to prepare the Tris buffer), avidin, glutaric dialdehyde and aminopropyltrimethoxy silane (APTS) were purchased from Sigma (St. Louis, MO, USA). [³H]-Vinblastine (254 GBq) and [³H]-cyclosporin A (259 GBq) were purchased from Amersham Pharmacia Biotech (Piscataway, NJ, USA). Biotin-X (6-[(biotinoyl) amino] hexanoic acid) was purchased from Molecular Probes (Eugene, OR, USA). Open tubular capillaries (100 μm i.d.) were purchased from Polymicro Technologies (Pheonix, AZ, USA).

3.7.3 Preparation of Pgp(-) and Pgp(+) membranes

3.7.3.1 Cell lines

Pgp(-) membranes were obtained from the MDA435/LCC6 cell line. The Pgp(+) membranes were obtained from the MDA435/LCC6MDR1 cell line prepared from the MDA435/LCC6 cell line by transduction with a retroviral vector carrying MDR1 cDNA (Pgp) as previously described by Leonessa *et al.*, 1996.

3.7.3.2 Solubilization of the membranes

The MDA435/LCC6 or MDA435/LCC6MDR1 cells (200×10^6 cells) were placed in 10 ml of homogenization buffer (Tris-HCl [50 mM, pH 7.4] containing 50 mM NaCl, 8 μ M leupeptin, 1 μ M PMSF, and 10 μ M pepstatin). The suspension was homogenized for 3×15 s at the setting of 15 on a model PT-2100 homogenizer (Kinematica AG, Luzern, Switzerland). The homogenate was centrifuged at $450 \times g$ for 7 min and the pellet containing the nuclear proteins was discarded. The supernatant was centrifuged at $100,000 \times g$ for 35 min and the resulting pellet containing the cellular membranes was collected, resuspended in 2 ml of solubilization buffer (Tris-HCl [50 mM, pH 7.4] containing 500 mM NaCl, 15 mM CHAPS (1.5%), 2 mM DTT, 10% glycerol), and the resulting mixture was rotated at 150 rpm using an orbit shaker (Lab-line model 3520, Melrose Park, IL, USA) for 18 h at 4 °C. The resulting solution was centrifuged at $50,000 \times g$ for 25 min, the pellet was discarded and the supernatant containing the

solubilized Pgp (-) or Pgp (+) membranes was used for the immobilization onto the open tubular capillary.

3.7.4 Immobilization of the Pgp membranes on the open tubular capillary

3.7.4.1 Preparation of the capillary

A peristaltic pump (Minipulse 2, Rainin, Woburn, MA, USA) set at 50 (a flow rate of $\approx 10 \mu\text{l}/\text{min}$) was used throughout the procedure. A glass capillary (25 ~~at~~ $100 \mu\text{m}$ i.d.) was conditioned with a solution of 1 M NaOH for 30 min followed by water for 15 min and then air for 5 min. The capillary was incubated at 95°C for 1 h. An aqueous solution of 90:10 (v/v) water: APTS was passed through the capillary for 5 min then incubated in the oven at 95°C for 30 min, this was duplicated again and the capillary was left open to air overnight. The following morning, a 1% gluteraldehyde solution in phosphate buffer (50 mM, pH 7.4) was run through the capillary for 60 min followed by 250 μl of water. Then a solution of avidin (10 mg in 2 ml of phosphate buffer [50 mM, pH 7.4]) was run through the capillary for 30 min, after which both tips of the capillary were submerged in the avidin solution and the capillary was incubated for 5 days at 4°C . Subsequently, the capillary was washed for 15 min with Tris buffer (10 mM, pH 7.4) prior to continuing to the next stage.

3.7.4.2 Immobilization using biotin-X

A solution of biotin-X (14 mM in 3:1 (v/v) DMSO : phosphate buffer [50 mM, pH 7.4]) was run through the capillary for 1 h at 10 μ l / min and both tips of the capillary were then submerged in the solution overnight. The following day the solution containing the solubilized Pgp(+) or Pgp(-) membranes was run through the column for 2 h (Figure 26).

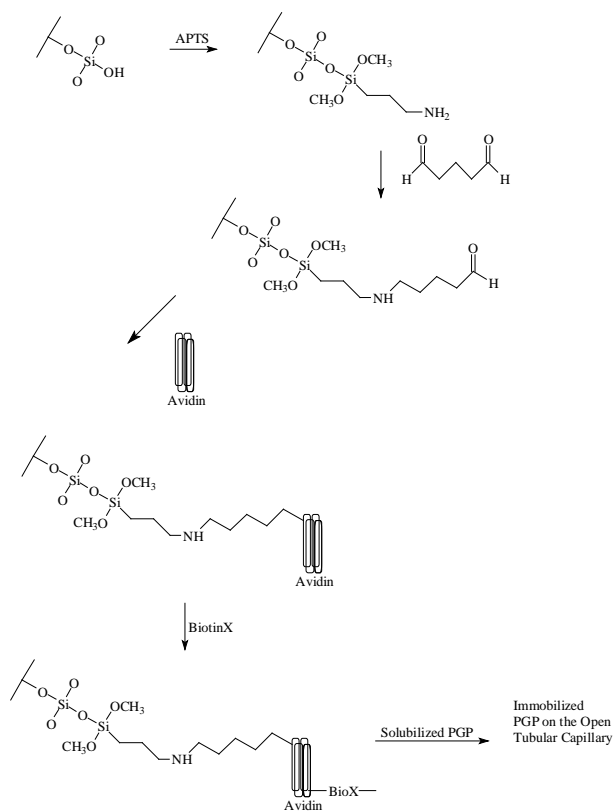


Figure 26. Schematic for the preparation of the open tubular column. The silica OT columns were first etched with NaOH. This facilitated the exposure of all the available hydroxyl groups of silica capillary. APTS was added which covalently attaches with the open tubular wall generating a free amine. This free amine then reacts with glutaric

dialdehyde through a Schiff base reactions (eliminates a molecule of water) and generates a free aldehyde. The free aldehyde is then reacted with avidin (a protein with four identical subunits). The free amino acids in the avidin react with the free aldehyde (Schiff base reaction). The resultant Schiff base is stable as the whole reaction is carried out at neutral pH. Biotin X is then added. Biotin X has a fmol binding affinity for avidin and the lipophilic arm of biotin X, will insert itself into the interstitial space of the solubilized Pgp membranes. This helps anchor the membranes onto the activated surface of the glass capillary (i.e. OT column).

3.7.4.3 Reagent removal

The open tubular capillary was capped on both ends with dialysis membrane, secured using copper wires and placed in a glass beaker containing the dialysis buffer (Tris buffer [10 mM, pH 7.4] containing 150 mM NaCl, 1.0 mM EDTA, 1.0 mM benzamidine) and dialysed at 4 °C and rotated overnight at 110 rpm using the orbit shaker. The following day, solubilized Pgp (+) or Pgp (-) membranes were again passed through the capillary for 2 h at 10 µl/ml and the dialysis was repeated. On the third day, the column was attached to a Shimadzu LC-10Advp pump (Shimadzu Corp. Columbia, MD, USA) and equilibrated by rinsing the column with ammonium acetate (10 mM, pH 7.4) for 1 h at 50 µl/min.

3.7.5 Chromatographic system

The chromatographic system was composed of a Shimadzu LC-10Advp pump, 50 ml superloop (Amersham Pharmacia, Uppsala, Sweden), an IN/US system β -Ram model 3 radioflow detector (IN/US, Tampa, FL, USA) with a dwell time of 2 s and the output data was analyzed using Laura lite 3 (IN/US) programme.

3.7.6 General procedures

In these studies, the mobile phase consisted of the marker ligand [^3H]-Vb and [^3H]-CysA in 5 ml of ammonium acetate (10 mM, pH 7.4) delivered at a flow rate of 50 $\mu\text{l}/\text{min}$. At the beginning of each experimental series, the mobile phase was run through the Pgp(+)-OT column until an elution profile showing both front and plateau regions was observed. Increasing concentrations of the unlabelled marker or unlabelled displacer were then added to the mobile phase and the frontal chromatographic experiments were repeated. When Vb was studied, the mobile phase concentration of [^3H]-Vb was 0.65 nM and the added concentrations of Vb were 50, 125, 250, and 500 nM. When cyclosporine A (Cys A) was studied, the mobile phase concentration of [^3H]-CysA was 0.6 nM and the added concentrations of [^3H]-CysA were 1 nM, 2 nM, and 3 μM .

3.7.7 Calculation of dissociation constants

Using the frontal chromatograms, the association constants of the competitive ligands (CL), K_{CL} , as well as the number of the active and available binding sites of immobilized receptors, P , were calculated using the following equations [(1) and (2)]

$$(V_{\max}-V)^{-1}=(1+[M]K_M)(V_{\min}[P]K_M)^{-1}+(1+[M]K_M)^2(V_{\min}[P]K_MK_{CL})^{-1}[\text{drug}]^{-1} \quad (1)$$

$$(V-V_{\min})^{-1}=(V_{\min}[P]K_{CL})^{-1}+(V_{\min}[P])^{-1}[M] \quad (2)$$

where, V is the retention volume of the marker ligand (M); V_{\max} the retention volume of M at the lowest concentration and in the absence of drugs; V_{\min} the retention volume of M when the specific interaction is completely suppressed. The value of V_{\min} is determined by running M in a series of concentration of drugs and plotting $1/(V_{\max}-V)$ versus $1/[CL]$ extrapolating to infinite $[CL]$. From the above plot and a plot of $1/(V-V_{\min})$ versus $[M]$, dissociation constant values, K_d , for M and CL can be obtained as can the number of active binding sites on the immobilized protein $[P]$.

3.7.8 Results and Discussion

Since the objective was to reduce the non-specific interactions between the chromatographic backbone and hydrophobic substrates/inhibitors and to achieve better reproducibility and less back pressure, an alternative approach which it was thought offered some promise was the immobilization of cellular membranes expressing Pgp(+) and Pgp(-) onto the inner surface of an open tubular (OT) capillary to create a Pgp(+)-OT and Pgp(-)-OT columns. The immobilization was carried out using biotin-streptavidin coupling as described initially in an experimental approach used by Berger & Wood (1975); and Hofmann & Kiso (1976). This biotin-streptavidin coupling can had also been used to immobilize lipid membranes using biotinylated liposomes and streptavidin-coupled gel beads (Yang *et al.*, 1998; Yang *et al.*, 2000). The latter approach was used for this immobilization.

3.7.8.1 Characterization of the immobilized Pgp(+)-OT

The activity of the Pgp transporter immobilized in the Pgp(+)-OT was determined using frontal displacement chromatography with [³H]-Vb as the marker ligand, Vb and ketoconazole as the displacers (Figure 27).

(Wang *et al.*, 2002). For both substrates, there was less than a 10-fold difference in the K_d values determined using different experimental techniques, which indicated that this method was comparable to the previously established membrane filtration assays. Thus, the results demonstrated that the immobilized Pgp retained its ability to specifically bind known Pgp substrates, and could discriminate between a solute with nM affinity for the transporter (Vb) and one with a μ M affinity for ketoconazole.

Table 9. Comparison of K_d values determined on the Pgp-OT column with those obtained on the Pgp-IAM and membrane binding studies.

	Pgp-OT		Pgp-IAM		Literature
	K_d (nM)	B_{max} or P (nmol)	K_d (nM)	B_{max} or P (nmol)	K_d (nM)
Vinblastine	97 ($r^2=0.902$)	3	71 ± 11^a 24 ± 8^b	546 ± 60^a	37 ± 10^c 36 ± 5^d
Ketoconazole	12,140 ($r^2=0.845$)	1.5	NR	NR	8,600 nM ^e

NR not reported

^a Zhang *et al.*, 2000.

^b Lu *et al.*, 2001.

^c Ferry *et al.*, 1995

^d Callaghan *et al.*, 1997.

^e Wang *et al.*, 2002.

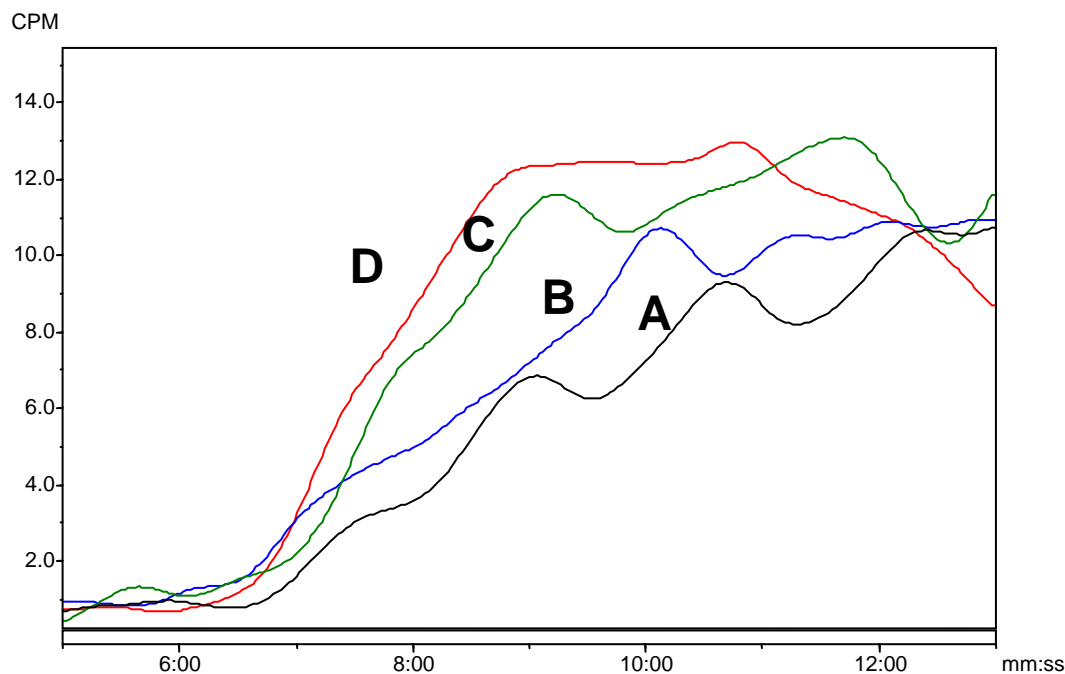


Figure 28. Frontal chromatographic study of the displacement of [^3H]-vinblastine by ketoconazole on the Pgp(+)-OT column using a mobile phase containing 0.3125 nM [^3H]-vinblastine, where: A = mobile phase; B = after the addition of 200 nM ketoconazole to the mobile phase; C = after the addition of 500 nM ketoconazole to the mobile phase; D = after the addition of 10,000 nM ketoconazole to the mobile phase.

There appeared to be a 200 fold disparity in the number of active sites (B_{max}) between the Pgp(+)-OT column and the Pgp(+)-IAM column, 3 nmol *versus* 546 nmol, respectively. This probably reflected the reduction in the total amount of membranes immobilized on the surface of the open tubular column relative to the amount immobilized on the IAM particles, and thereby, a reduction in the total amount of Pgp. One consequence of the reduced amount of available Pgp binding sites on the Pgp(+)-OT was a significant reduction in the relative capacity of the column. On the Pgp(+)-

OT, the half-height of the saturation curve was reached after the application of 500 μl of a 0.625 nM solution of [^3H]-Vb (Figure 29A), while it took 15 ml of a 1 nM solution to reach the same break-through on the Pgp-IAM column (Lu *et al.*, 2001). Since both studies used a flow rate of 50 $\mu\text{l}/\text{min}$, the experiments took 10 and 38 min, respectively. Also, since the immobilization process utilized crude membrane preparations and not the purified (or even semi-purified) Pgp protein, it was difficult to assess the total amount of material that has been immobilized on the support. One way of addressing this issue is to measure the total amount of immobilized protein as a reflection of the extent of membrane immobilization. In the previous studies with the Pgp-IAM support, the results from a bicinchoninic acid protein assay (micro-BCA) established that 17 μg of protein were immobilized per mg of support. In this study, the total amount of immobilized protein could not be measured by the micro-BCA, which has a sensitivity of 0.5 μg protein/ml. This result was consistent with the assumption that a significantly reduced amount of Pgp-containing membranes had been immobilized within the open tubular column.

Frontal studies with the Pgp (-)-OT using the same conditions as the Pgp (+)-OT, i.e. 0.625nM [^3H]-Vb, and a flow rate of 50 $\mu\text{l}/\text{min}$, produced elution profiles showing both front and plateau regions (Figure 29 B), with significant decrease in retention time as compared to the Pgp (+)-OT. Also the addition of Vb or ketoconazole to the mobile phase did not displace the curve. Thus the results from the frontal chromatographic studies with the Pgp (-)-OT demonstrated that the retention on Pgp (+)-OT was the sum of specific interactions with the Pgp transporter and other specific and non-specific

interactions arising from the components of the cellular membrane. Since the Pgp (+) and Pgp (-) membranes are obtained from the same cell lines, the only significant difference between them is the presence of the expressed Pgp in the Pgp (+) membranes. Thus, with the exception of interactions with Pgp, a compound chromatographed on the Pgp (+)-OT and Pgp (-)-OT should experience the same specific interactions with surface receptors and transporters and non-specific interactions with membrane components. Also the retention times and K_d obtained for the columns are very reproducible and the number of binding sites remain constant for a long period of time.

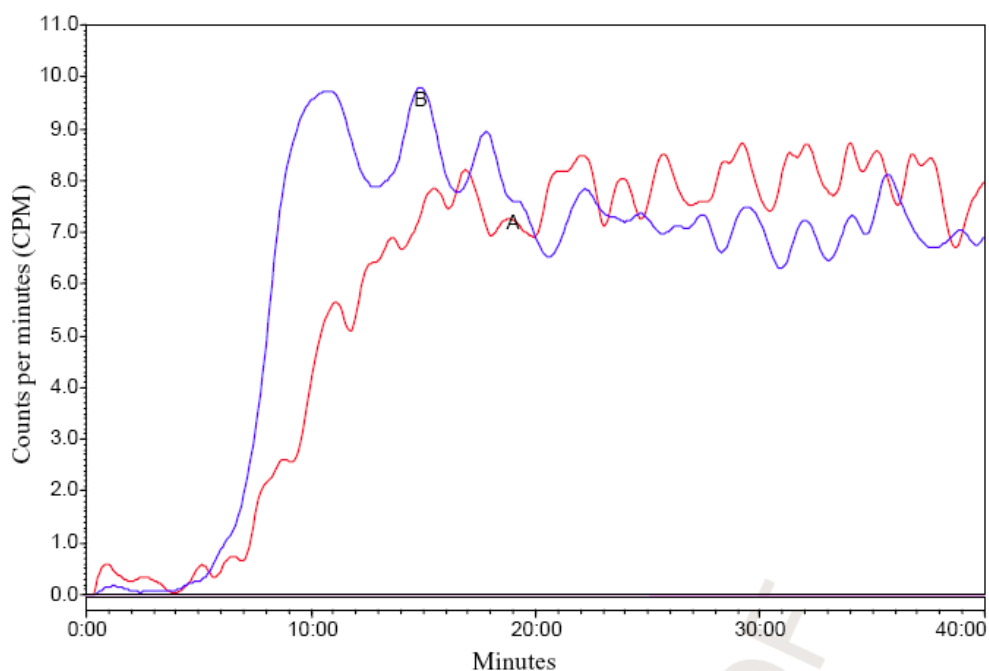


Figure 29. Frontal chromatographic study of the retention of [³H]-vinblastine on the Pgp(+)-OT column (chromatogram A) and Pgp(-)-OT column (chromatogram B) using a mobile phase containing 0.625 nM [³H]-vinblastine. Radioactive decay was measured in counts per minute and the chromatogram was summed up in 1-min intervals and smoothed using the Laura lite program..

3.7.8.2 Effect of ATP on the chromatographic properties of the Pgp(+)-OT column

Frontal chromatography with [³H]-CysA on the Pgp(+)-OT and Pgp(-)-OT gave retention times of 7.2 and 7.0 min respectively. Addition of 3mM ATP to the running buffer resulted in changes in retention for CysA, which increased from 7.2 min to 14.0 min for the Pgp(+)-OT column. No change was observed for the Pgp(-)-OT column (Table 10).

Table 10. Effect of ATP on the retention of ³H-CysA for Pgp-(+) and Pgp(-) OT columns. Retention times were extrapolated from the frontal chromatogram as half the time required for saturation. Running buffer consisted of ammonium acetate [10 mM, pH 7.4], 1mM MgCl₂, 3mM ATP and the flow rate was 50 µl/min. Elution profile with both the front and plateau regions of the frontal chromatogram were used to extrapolate the retention time k' as half the time required for saturation (plateau). Radioactivity was measured as counts per minute (CPM) using a liquid scintillation radioflow detector (IN/US system β-Ram model 3) and the output data is analyzed using a Laura lite programme with a dwell time of 2 s.

Mobile phase	Pgp(+) (min)	Pgp (-) (min)
	k'	k'
With 3mM ATP	14.0	7.2
Without 3mM ATP	7.2	7.0

The concentration of ATP was based on previously reported studies of by Sonveaux N *et al.*, 1996. Also with the addition of 3mM ATP to the running buffer, [³H-CysA] was displaced from the Pgp(+)-OT column by addition of unlabelled CysA. The results from the CysA displacement studies were used to calculate a K_d value of 0.4 nM for CysA binding to the immobilized Pgp. This was comparable to previously reported value of 18nM by Ferry *et al.*, (1995). Thus addition of ATP to the running buffer produced a cooperative allosteric interaction that increased the binding affinity of Pgp for CysA. These ATP induced changes in the chromatographic interaction between the ligand CysA and the immobilized Pgp was consistent with the shift in the tertiary structure of the transporter as reflected in earlier work by Sonveaux *et al.*, (1996) and Lu *et al.*, (2000).

3.7.9 Conclusion

The main conclusion from this study was that the immobilized Pgp liquid chromatographic stationary phase appeared to reproduce the Pgp substrate binding as determined by classical filtration binding assays. The data from this study indicated that membranes from a cell line expressing a target receptor or transporter can be immobilized on the surface of glass capillaries with retention of the target's binding activity, and that this activity can be measured using displacement frontal chromatographic techniques. The results from this study also demonstrated that since cellular membranes are immobilized, instead of the purified target, the membranes contribute specific and non-specific off-target binding to the observed chromatographic

retention. This necessitates the construction of a second open tubular capillary column using membranes from a cell line that does not express the target receptor or transporter. The target (-) column can then be used as a control for the target (+) column. This approach should be applicable for use with any membrane bound target where “knock-in” or “knock-out” cell lines are available.

The observed binding was highly sensitive to changes in the protein’s tertiary conformation caused by Pgp interactions with substrates and ATP, and reflected changes occurring in the functional cycle of Pgp. Thus this affinity based chromatography seemed to represent a promising tool in the quick identification of potential substrates / inhibitors and also showed potential as a useful probe of the transport mechanism.

3.8 Rapid-frontal chromatography with mass spectrometric detection

3.8.1 Introduction

Having characterized the Pgp-OT columns for their functionality and also proven that it is a quick means of identifying potential substrate/inhibitors and their relative K_d values, which were comparable with membrane binding assays, it was then considered that this technology could be even more versatile if mass spectrometric detection could be exploited. It was expected that this technique would provide for a rapid high throughput determination of potential substrates of Pgp and would be probably robust, quick and consume less reagents as compared to other assays. Also parallel screening capability in conjunction with MS would help as a tool for the pre-screening of potential lead candidates. Accordingly the aim of the next phase of the programme was to demonstrate the suitability of MS detection and then, hopefully, proceed to the use it to analyse a wide range of drugs

3.8.2 Chromatographic system

The chromatographic system consisted of a series 1100 liquid chromatography/mass selective detector (LC/MSD) (Agilent Technologies, Palo Alto, CA, USA) equipped with a vacuum de-gasser (G 1322 A), a binary pump (1312 A), a manual seven-port injector with a 500 μ l loop (model no. 7010, Rheodyne, Rohnert Park, CA, USA), a mass selective detector (MSD) (G1946 B) supplied with atmospheric pressure ionization electrospray (API-ES) and an on-line nitrogen generation system (Whatman,

Haverhill, MA, USA). The chromatographic system was interfaced to a 250 MHz Kayak XA computer (Hewlett-Packard, Palo Alto, CA, USA) using ChemStation software (Rev B.10.00, Hewlett-Packard).

3.8.3 Chromatographic conditions

The mobile phase was composed of ammonium acetate (10 mM, pH 7.4) and the experiments were carried out at a flow rate of 50 μ l/min at ambient temperature. The parameters on the MSD were set at 11 l/m for the drying gas flow, 350 °C for the drying gas temperature, 50 psi for nebulizer pressure, and 60 V for the fragmenter.

3.8.4 General procedures

The test ligands were Vb, labetalol, loratidine, fexofenadine, propranolol, imipramine, domperidone, verapamil, doxorubicin, ketoconazole, prazosin, ritonavir, tamoxifen, nicardipine, celecoxib, hydrocortisone and nicotine. Each compound was prepared as a 1 nM solution and a 500 μ l aliquot was applied using the injection loop on the manual injector. The compounds were monitored using single ion monitoring ($M+1$) at the following m/z values: 455.6 (verapamil); 385.1 (prazosin); 812 (Vb); 532.0 (ketoconazole); 163.2 (nicotine); 543.6 (doxorubicin). The studies were carried out in triplicate.

3.8.5 Results and Discussion

3.8.5.1 Comparison of rapid frontal chromatography using the Pgp(+)-OT and Pgp(-)-OT with Caco-2 permeability measurements and stimulation of membrane-based ATPase activity.

The determination of the interaction between lead drug candidates and Pgp has typically been conducted as part of non-clinical development, and has primarily depended on the use of a Caco-2 cell monolayer model. In this approach, a compound is identified as a substrate based on the ratio of the value of the apparent permeability coefficient (P_{app}) in the basal-to-apical direction (P_{appB-A}) to P_{app} in the apical-to-basal direction (P_{appA-B}). According to one generally accepted criterion, a compound is designated as a Pgp substrate if P_{appB-A} / P_{appA-B} exceeds 2.0 (Polli *et al.*, 2001). Caco-2 experiments may also be used to compare the value of P_{app} for a test compound in the B - A or in the A - B direction, in the absence and presence of a well-documented Pgp inhibitor such as GF120918 (Lentz *et al.*, 2000).

The Caco-2 model appears to be a reasonable and reliable method to estimate intestinal transcellular permeability or the fraction of intestinal absorption in humans and the involvement of Pgp in drug absorption. As a result, Caco-2 monolayers cultured in 12- or 24-well formats are now often included in lead optimization during drug discovery

and a 96-well format may be employed much earlier during lead selection (Balimane, 2004) when a moderate throughput is desirable.

While the Caco-2 model provides valuable information on Pgp interactions, alternative acellular techniques with higher throughput have been developed to provide information on Pgp interactions during lead selection. One of these methods is based upon substrate-stimulated ATPase activity of Pgp in isolated cell membranes, which is measured through the appearance of inorganic phosphate (Swhab *et al.*, 2003; Polli *et al.*, 2001). However, the results from the two assays do not always correlate as some compounds identified as substrates in the ATPase assay do not appear to undergo significant transmembrane permeability in Caco-2 monolayers. This is true of midazolam, which has high passive permeability, which produces a fast transcellular flux that may overcome Pgp-mediated efflux (Tolle-Sander *et al.*, 2003). Conversely, some compounds identified as substrates in the Caco-2 model (*e.g.*, vincristine, colchicine) fail to stimulate ATPase activity (Barecki-Roach *et al.*, 2003).

Clearly, it can be difficult to classify new compounds as inhibitors, non-transported substrates or substrates with a single assay (Swhab *et al.*, 2003; Polli *et al.*, 2001). The problem is further complicated by poor intra-assay reproducibility. For example, the Caco-2 model is sensitive to cell culture and experimental conditions and inhibitor selection. In addition, both assays typically use testing concentrations in the 10-50 μM range, which may exceed solubility limits in cell culture media. Furthermore, differences may also arise from differences in classification criteria and nomenclature.

Therefore, it has been recommended that for high-throughput screening for Pgp interactions a combination of methods should be used (Swhab *et al.*, 2003; Polli *et al.*, 2001). In an attempt to clarify this confusing situation, Polli *et al.*, 2001 have developed a rather complex classification system, based on the results of screening a variety of medicinal compounds in Caco-2 monolayers and for ATPase activity.

The disparity between the Caco-2 and ATPase assays is reflected in the results obtained for the 15 compounds used in this study (Table 11).

Table 11. Results from the Caco-2 permeability, ATPase membrane and chromatographic assays conducted in this study, Caco-2 cells were seeded into wells on a 96-well plate at 10^4 cells per well and cultured for 25-27 days at 37°C and 5% CO₂. Compounds were incubated with monolayers for 2 h at a final concentration of 30 μM in both directions. X denotes the assessment that the compound is a Pgp substrate, N denotes the assessment that the compound is not a Pgp substrate and ND denotes that the compound was not assessed in this study. P_{appA-B} and P_{appB-A} are the apparent permeability coefficients in the apical-to-basal and basal-to-apical directions, respectively. In the open tubular column model compounds exhibiting a value for $\Delta t \leq 0.1$ min are designated as a Pgp substrate.

4. Compound	Caco-2 Permeability Assay n = 4			Membrane ATPase Assay			Chromatographic Retention Model n = 4		
	Papp _{A-B} (cm/s × 10 ⁻⁶)	Papp _{B-A} / Papp _{A-B}	Pgp Substrate	E _{max} (nmol PO ₄)	E _{max} @ (μmol)	Pgp Substrate	Pgp(+)-OT (min)	Pgp(-)-OT (min)	Δt (min)
Domperidone	2.3	45.0 ± 27.0	X	37	250	X	23.5 ± 0.7	2.0 ± 0.0	21.5
Ritonavir	0.5	36.5 ± 12.1	X	45	1	X	13.2 ± 0.3	2.1 ± 0.0	11.1
Vinblastine	1.4	31.1 ± 18.5	X	20	6	X	14.1 ± 0.5	1.6 ± 0.2	12.5
Labetalol	3.5	8.9 ± 6.9	X	35	100	X	14.8 ± 0.4	1.9 ± 0.1	12.9
Doxorubicin	4.6	8.6 ± 5.4	X	<5	-	N	10.3 ± 0.2	9.7 ± 0.2	0.6
Prazocin	14.9	7.1 ± 6.2	X	37	100	X	10.4 ± 0.1	3.1 ± 0.4	7.3
Verapamil	24.6	3.4 ± 1.0	X	50	250	X	4.1 ± 0.4	2.9 ± 0.0	1.2
Loratadine	10.3	2.0 ± 0.5	X	45	6	X	7.4 ± 0.9	2.1 ± 0.1	5.3
Ketoconazole	29.9	2.1 ± 1.2	X	30	10	X	1.7 ± 0.0	1.6 ± 0.0	0.1
Imipramine	41.1	1.8 ± 0.7	N	30	100	X	2.1 ± 0.1	1.2 ± 0.2	0.9
Nicardipine	31.8	1.4 ± 0.7	N	30	10	X	1.9 ± 0.1	1.8 ± 0.0	0.1

Atenolol	1.1	1.4 ± 0.5	N	20	100	X	1.6 ± 0.3	1.2 ± 0.0	0.4
Fexofenadine	5.1	1.0 ± 0.9	N	10	100	N	1.8 ± 0.0	1.8 ± 0.0	0.0
Tamoxifen	ND	ND	ND	15	50	N	13.0 ± 0.0	13.1 ± 0.0	-0.1
Nicotine	ND	ND	ND	<5	-	N	2.3 ± 0.1	2.4 ± 0.4	0.0

Of the thirteen compounds assessed by both methods, one compound (doxorubicin) was identified as a Pgp substrate in the Caco-2 assay, but not in the ATPase assay, while three compounds (imipramine, nifedipine, atenolol) were identified as substrates in the ATPase assay but not by the Caco-2 method. The ATPase assay is essentially a qualitative assessment of whether a compound is a Pgp substrate, i.e. a yes/no determination, while the Caco-2 method gives both a qualitative assessment and a quantitative ranking. Thus, it was not possible to correlate the results from the two assays by linear regression. Instead, a Fisher's Exact Test was used to evaluate the relationship between the two data sets, i.e. if a compound is identified as a Pgp substrate in one test, will it be identified as a substrate in the other. The results indicated that one method could not reliably predict the results from the other, with a two-sided P value of 0.2321.

The compounds were also chromatographed on open tubular chromatographic columns, which contained immobilized cellular membranes obtained from either the MDA435/LCC6 cell line, which does not express Pgp, or from the MDA435/LCC6MDR1 cell line, which expresses Pgp. Thus, the resulting Pgp(-)-OT and Pgp(+)-OT columns were prepared from essentially the same cell line, with the difference being the presence of Pgp in the MDA435/LCC6MDR1 membranes. The columns were placed in a liquid chromatography system utilizing mass spectrometric detection and parallel rapid frontal chromatography experiments were conducted.

Chromatograms containing front and plateau regions were obtained for each compound on both columns (Figure 30). The retention times were calculated using the half-heights of the breakthrough curves, and were reproducible with an average variation of ~5% (n = 3), (Table 11 Table 13).

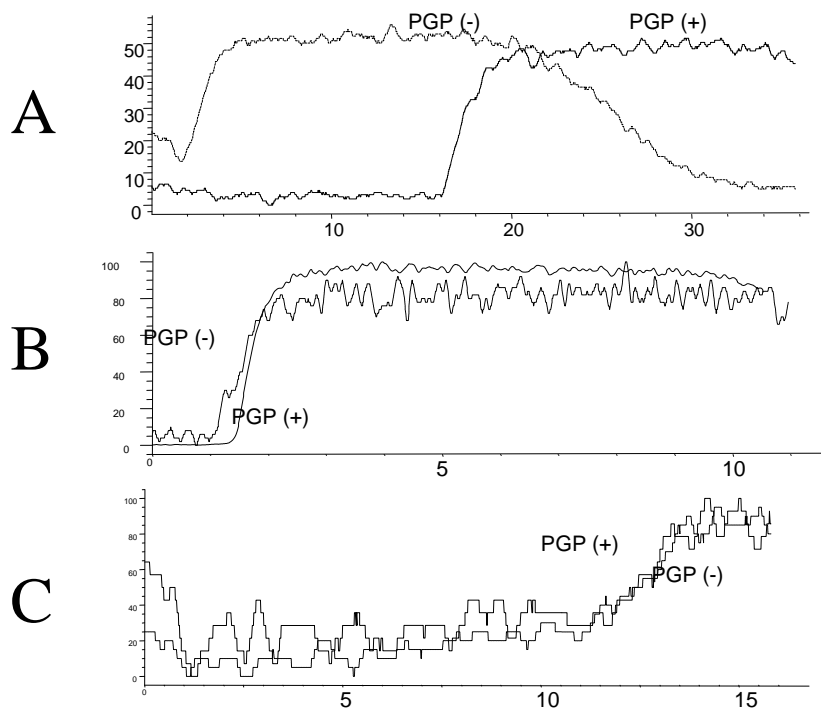


Figure 30. The frontal chromatographic traces produced by A: loratadine, B: nicardipine, C: tamoxifen, on Pgp(+)-OT and Pgp(-)-OT. Frontal chromatograms were obtained using MSD. The parameters on the MSD were set at 11 l/m for the drying gas flow, 350 °C for the drying gas temperature, 50 psi for nebulizer pressure, and 60 V for the fragmenter. A 1 ml aliquot of a 1 nM solution of each compound was injected onto the column at a flow rate of 50 μ l/min and the compounds were monitored using single ion monitoring (M+1). The experiments were carried out at room temperature using a mobile phase composed of ammonium acetate [10 mM, pH 7.4].

Chromatographic retention of a compound on a chromatographic phase containing an immobilized protein is the result of both specific and non-specific interactions. Thus, the observed retention of a compound on the Pgp(-)-OT reflects physicochemical interactions of the compound with the immobilized membranes as well specific interactions with receptors and drug importers other than Pgp, which are present in the membranes. The same interactions occur on the Pgp(+)-OT with the added specific interaction with the expressed Pgp. The specific interaction between a compound and Pgp can be identified by subtracting the retention on the Pgp(-)-OT from the retention on the Pgp(+)-OT, the Δt . The necessity of the parallel chromatographic approach is illustrated by the data obtained with ritonavir and tamoxifen. Both compounds were retained on the Pgp(+)-OT column for 13 min, which was over 3-times longer than verapamil, and initially appeared to be Pgp substrates. When the Δt values were determined, it was evident that the observed retention of ritonavir on the Pgp(+)-OT was due to interactions with the expressed Pgp, while the retention of tamoxifen was not.

Previous studies with an immobilized Pgp column had demonstrated that in the absence of ATP, the transporter binds substrates and competitive inhibitors, but not non-competitive inhibitors such as cyclosporin-A (Garrigues *et al.*, 2002). Thus, it was reasonable to assume that, under the experimental conditions utilized in this study, the specific retention observed on the Pgp(+)-OT, i.e. Δt , reflected the binding of substrates and competitive inhibitors to this transporter and that ritonavir is a Pgp substrate while tamoxifen is not.

The correlation of the Δt values with the results from the ATPase and Caco-2 studies was used to test this assumption. Since the ATPase assay is a qualitative determination, Fisher's Exact Test was used to compare the data sets. The comparison used a Δt cutoff of ≥ 0.1 min as the indication of a Pgp substrate. With this specification, there was a significant correlation ($p = 0.0088$) between the tests, indicating that the chromatographic method could be substituted for the ATPase assay.

The chromatographic and Caco-2 methods were also compared using the Fisher Exact Test to determine their relative abilities to qualitatively predict if a compound was a Pgp substrate. The parameters set at $\Delta t \leq 0.1$ min as an indicator of a $Papp_{B-A} : Papp_{A-B}$ ratio of < 2.0 . Previous studies using Caco-2 monolayers had identified tamoxifen and nicotine as Pgp-nonsubstrates with a $Papp_{B-A} : Papp_{A-B}$ ratio < 2.0 , and although their $Papp_{B-A} : Papp_{A-B}$ ratios were not determined in this study, the Δt values were (Table 11). Thus, the experimental cohort of all fifteen test compounds were analyzed using the Fisher Exact Test and a significant correlation ($P = 0.0110$) was observed between the two data sets. This indicated that the chromatographic method could be used to provide a simple yes/no answer to the question "is compound X a Pgp substrate?"

Since the Caco-2 assay provided quantitative results, the data from the Caco-2 and chromatographic studies were also compared using linear regression analysis. The data sets correlated with an $r^2 = 0.7444$ ($y = 1.911x - 0.3570$, $p = 0.0001$), indicating that the chromatographic method can be used to rank compounds relative to the extent of Pgp

transport as extensive, moderate, minimal or not at all. This result was consistent with the assumption that retention on the Pgp(-)-OT mirrors the $Papp_{A-B}$ and represents the passive absorption of a compound through the Caco-2 membranes while retention on the Pgp(+)-OT and $Papp_{B-A}$ reflected the contribution of Pgp to drug export. Thus, it was not surprising that there was a statistically significant relationship between Δt and $Papp_{A-B} : Papp_{B-A}$.

3.9 Conclusion

The main conclusion from this study was that the immobilized Pgp liquid chromatographic stationary phases could be used to study drug-protein binding for a variety of substrate/inhibitors and appeared to be comparable to the binding as determined by classical filtration binding assays. Also the immobilized Pgp columns could be used to study the proteins tertiary structure in its different conformational forms and its interactions with different substrate/inhibitors in the presence vanadate trapping. The study showed that the immobilized Pgp did have enough flexibility to have transition into one of the other conformational forms of the Pgp cell cycle. This leads to an encouraging path in designating various drugs as non-competitive inhibitors of the Pgp transporter.

The study of Pgp transporter immobilized onto open tubular columns demonstrated that the Pgp(+)-OT and Pgp(-)-OT column could be used in addition to or in place of the ATPase and/or Caco-2 assays as a screen for Pgp substrates. Using a single parallel

screening system, which permitted simultaneous chromatography on two columns (Lu L *et al.*, 2001), and a 1-hour time period (30-min frontal chromatography, 30-min wash), a single pair of columns could be used to screen at least 150 compounds a week and 600 compounds during the 4-week life time of the columns.

The method is simple, utilizes standard liquid chromatography – mass spectrometry equipment and avoids solubility problems since it utilizes nM rather than μM concentrations. Accordingly the chromatographic method represents a significant advance over the current whole cell and membrane-based assays. Also the method provides advantage over other assays as it can be run in parallel with control columns to screen out for other non-specific interactions. Also it provides more insight into the characteristic between drug-protein binding which could be further used in the development of pharmacophores for the Pgp transporter. The technique is robust, reproducible and uses fewer reagents quantities, which would be quite important when screening for large libraries of compound and also can be automated to a large extent. Therefore the immobilized Pgp columns could be used as a secondary screen for the predevelopment of lead candidates. Thus this affinity based chromatography seemed to represent a promising tool in the quick identification of potential substrates /inhibitors and also showed potential as a useful probe of the transport mechanism.

Chapter 4

4. Organic Cation Transporter (OCT)

4.1 Introduction

Having demonstrated that a stationary phase containing immobilized Pgp membranes can be used to identify substrate/inhibitors of the expressed Pgp transporter the next phase of the programme was to adapt this methodology to other target biopolymers such as human organic cation transporter 1 (hOCT1).

4.1.1 Overview

The body is continuously exposed to a variety of toxins and metabolic waste products. To rid itself of these endogenous metabolites, it is equipped with various detoxification mechanisms such as metabolizing enzymes and transport proteins, which mediates their inactivation and excretion.

Many of these compounds are positively charged and are termed as organic cations. Drugs belonging to a wide variety of clinical classes, including antihistamines, antiarrhythmics, skeletal muscle relaxants and β -adrenoceptor blocking agents- are organic cations. In addition, several endogenous bioactive amines- such as dopamine, choline and N-methylnicotinamide (NMN)- are also organic cations. Since many of the molecules are positively charged at physiological pH, membrane transporters such as the OCT are generally involved in the absorption, distribution and elimination of these

compounds. Thus together with metabolizing enzymes, transmembrane transporters are important determinants of drug metabolism and drug clearance.

Transport proteins play an essential role in the detoxification mechanisms mediating the inactivation and excretion of environmental toxins and metabolic waste products (Jonker & Schinkel, 2004). A large number of the transport proteins are found in the liver, kidney and intestines, all of which play a role in the excretory process. The largest family of transporters is the solute carrier (SLC) superfamily with 255 members in humans. Most members are highly specialized transporters. However, a number of these transporters are polyspecific, generalized transporters that play a major role in the elimination process. Of the polyspecific transporters, two have become of great interest in the drug development process, namely, SLC21 and SLC22. The SLC21 family (organic anion transporter) has nine members; these proteins transport large anionic, amphipathic compounds. The SLC22 family has twelve members in humans and rats including organic cation transporters, carnitine transporter, and several organic anion transporters. The organic cation transporters: OCT1, 2 and 3 belong to the SLC22 family of transport proteins.

The OCT1 (organic cation transporter) was the first isolated OCT in rats and was shown to have 556 amino acid protein with 12 transmembrane domains (alpha helices) (Lahjouji, 2001), and three glycosylation sites of the type NXT/S on the large hydrophilic extracellular loop between the first and second transmembrane domain (Figure 31). This was determined with specific peptide antibodies using permeabilized

and non-permeabilized stable transfected human embryonic kidney (HEK) 293 cells (Meyer-Wentrup *et al.*, 1998).

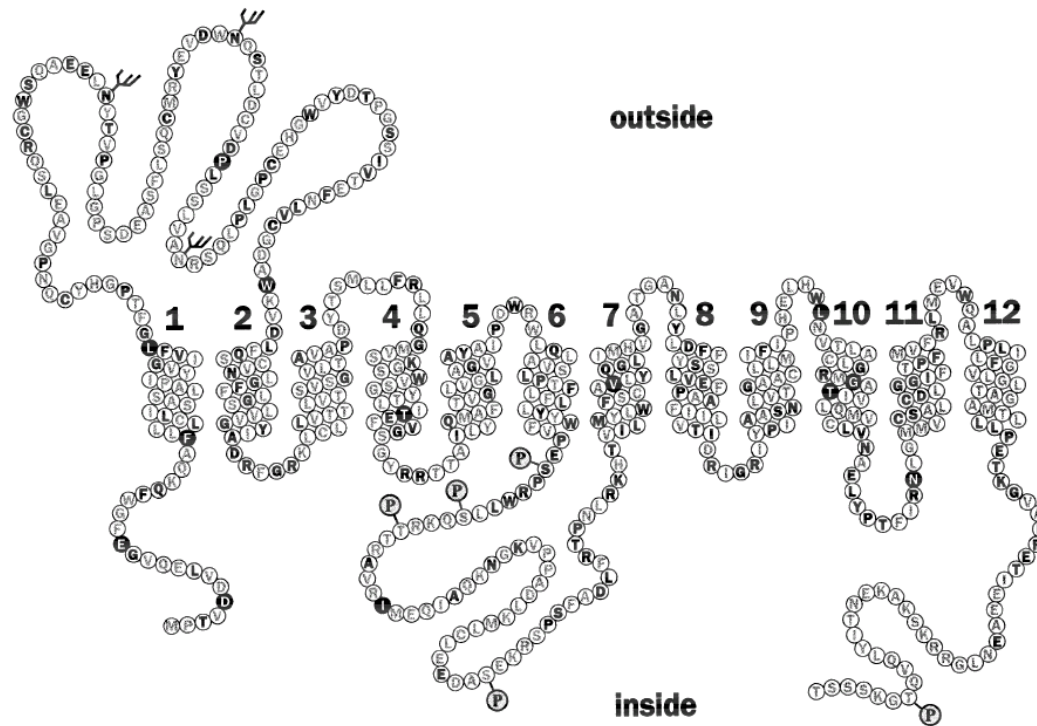


Figure 31. Schematic of the secondary structure of the OCT1 protein. The human OCT1 was shown to encode for 554 amino acids with 12 transmembrane domains and 3 glycosylation sites on the extracellular loop between the first and second transmembrane domain and had a molecular weight of 61 KDa. This was determined with specific peptide antibodies using permeabilized and non permeabilized stable transfected human embryonic kidney (HEK) 293 cells. (Meyers *et al.*, 1998; Jonker *et al.*, 2004).

The homologous cation transporters to OCT1 and OCT2 have been cloned in the rat, human, pig and rabbit. The human genes of hOCT1 and hOCT2 have been localized on chromosome 6q26 where they lie in close proximity (less than 500 kb) (Koehler *et al.*,

1997). The functional characterization of expressed OCT transporters from various species suggest that the OCT1, OCT2 and OCT3 transporters are polyspecific facilitative diffusion systems for small organic cations which operate in an electrogenic fashion and differ in respect to substrate specificity and localization. In the kidney of rat and human, OCT2 is strongly expressed. All species strongly expressed OCT1 in the liver, suggesting that OCT1 is the most important electrogenic cation transporter in the liver. Transport activities have also been determined for hOCTN1 and hOCTN2. hOCTN1 is transcribed in the kidney, bone marrow, trachea and many other organs and it mediates pH sensitive transport of tetra ethylammonium (TEA) and contains a sequence motif for nucleotide binding. hOCTN2 is strongly expressed in the heart, placenta, skeletal muscle, kidney, and pancreas and more moderately in the liver, lung and brain. The relevant function of hOCTN2 appears to be sodium-dependent, high affinity transport of carnitine

4.1.2 Conserved Amino Acids in the OCT-Family

Comparison of the twenty OCT family members suggested that forty-one amino acid residues are conserved between all members including seven proline, four glutamate, four arginine and four cysteine residues. Only ten of these conserved amino acid residues are localized in the presumed membrane spanning alpha-helices, and nine conserved amino acid residues belong to the intracellular loop which is typical for the major facilitator superfamily (Marger & Saier,1993; Gingrich *et al.*, 1992). The four cysteine residues conserved are localized in the large extracellular loop thus suggesting

the functional importance of this loop in containing disulphide bridges which may protrude into the membrane as has been described for the (Na⁺,K⁺)ATPase (Fiedler B & Schneider G, 1996; Schneider H & Schneider G, 1997). This suggests that the inhibition observed for the renal cation transport by sulphhydryl reagent could be due to the reaction with these cysteine residues (Katsura *et al.*, 1993; Sokol *et al.*, 1986a & b).

The first step in the elucidation of the molecular mechanism of the cation transport by OCTs is the identification of the cation binding sites present on the transporter. Since the involvement of electrostatic interactions is probable, conserved negatively charged, aromatic and polar amino acids within transmembrane alpha-helices or on extracellular loops may participate in binding domains. Therefore acidic amino acid residues or amino acid residues with negative partial charge that are conserved in the cation transporters but not in the anion transporters should be identified. There are seven acidic amino acids that are conserved in the electrogenic cation transporters of the OCT1/OCT2 subfamily but not in the anion transporters and the OCTN1/OCTN2 cation transporter subfamily: two glutamate and three aspartate residues in the large extracellular loop, one aspartate residue in TM8 and other one in TM11. In the cation transporters, hOCTN1, hOCTN2 and in the anion transporters this latter aspartate residue is replaced by arginine. The π -electrons of tryptophan, as well as partial negatively charges on the serine and threonine residues, may participate in electrostatic cation binding, it is therefore relevant that five threonine, three tryptophan and four serine residues are conserved in the OCT1/OCT2/OCT3 transporter subgroup but not in the anion transporters. Also further mutagenesis experiments would help in elucidating

as to which of the negatively charged or polarized domains on the large extracellular loop and in the transmembrane alpha-helices are involved in cation binding and transport.

4.1.3 Functional properties of expressed cation transporters

Cation transport by the OCT transporters has been studied in a variety of expression systems like oocytes, human embryonic kidney cells, HeLa cells and also insect cells. Tracer uptake studies in these systems showed that the uptake of small organic cations like TEA and 1-methyl-4-phenylpyridinium (MPP) was induced by most of the OCT transporters, and could be inhibited by a variety of organic cations with varied molecular structures, including high affinity inhibitors like quinine, quinidine, cyanine 863 and decynium 22. This data suggested that the OCT1 and OCT2 type transporters from different species operate in a similar fashion, i.e. they all appear to electrogenic facilitative diffusion systems for small organic cations that work independently of the sodium and proton gradients. However the OCT1 and OCT2 subtypes do exhibit differential substrate specificities that are species specific. In general these transporters have substrates with cations smaller in size and more hydrophilic suggesting that they are identical to substrates of a type 1 cation transporter which can be distinguished from a type 2 cation transporter which in the same membrane would transport more hydrophobic cations such as quinine and d-tubocurarine (Elferink *et al.*, 1995; Mol *et al.*, 1988; Steen *et al.*, 1991; 1992)

Bush *et al.*, (1996) showed that the apparent K_m values for TEA and choline decreased with increasing potential in rOCT1 subtype indicating that the transport system had to be electrogenic and that the cation binding site involved in the transport may be localized within the electrical field of the membrane potential. Also preliminary experiments performed on the rOCT1 and hOCT2 transporters showed that efflux of organic cations could be demonstrated directly by measuring the release of [^3H]-MPP from oocytes and HEK 293 cells. Also transporter mediated MPP efflux was observed even when no cations were present in the bath (i.e.trans-zero state), thus showing that the OCT1 and OCT2 transporters could function as uniporters.

Koepsell *et al.*, (1999) measured rOCT1 mediated [^{14}C]TEA influx experiments at different TEA concentrations in the presence of various concentrations of NMN a transported cation and quinine a nontransported inhibitor, in order to elucidate whether non-transported inhibitors interact at the same cation binding site. The results showed a competitive inhibition for NMN whereas quinine proved to be a non-competitive inhibitor, thus suggesting that an allosteric cation binding site might be present. This site could be localized close to the cation transport site but is not protected by transporter cations. Recently it has been observed that cation transport can be inhibited by the organic anion probenecid which is known to be a classical high affinity inhibitor of the renal anion transporter (Roch-Ramel *et al.*, 1992). This can be explained since the two transporters the anion and the cation transporters belong to the same family thus indicating that there might be a presence of degenerated probenecid binding site (Hsyu *et al.*,1988; Cacini *et al.*, 1982; Sheikh *et al.*,1976).

Comparison of the K_i values of various organic cation inhibitors (transported and nontransported) suggests that these cations may reflect organic cation binding affinities of two allosterically interacting cation binding sites, thus when modeling the binding sites of these transporters each group of cations should be considered separately. Also the comparison of the K_i values for several of the expressed members of the OCT1/2 subfamily suggests that there is a difference in the affinity patterns in both inter and intra species (Ullrich *et al.*, 1991; 1992; 1993; 1997). rOCT1 has much higher affinity for some cations (mepiperphenidol and procainamide), a similar affinity for others (decynium 22 and quinidine) and lower affinity for corticosterone as compared to rOCT2. Also the cation specificity pattern of the human subtype's hOCT1 and hOCT2 are distinctly different from their rat counterparts. There is no systemic pattern of the OCT1/2 subtypes from the human and the rat. Trying to summarize the species difference between human and rat, it may be stated that for several ligands hOCT1 has lower affinity than rOCT1 (exceptions are corticosterone and desipramine). Stereospecificity for quinine and quinidine was determined for rOCT1 but not for rOCT2 and hOCT1. All in all the data from various experiments shows that there is distinct difference in substrate specificities of OCT1/2 type transporters which are species specific and cannot be used to predict the overall homology of these transporters. This suggests that the development of an immobilized mammalian expression system (hOCT1, hOCT2, hOCTN1/2) to facilitate the study of drug interactions and transport *in vitro* and the development of drugs that specifically target cells that express each of these OCTs would be useful.

Zhang L & Giacomini M, (1999) developed a mammalian expression system for hOCT1 and tried to functionally characterize the transporter based on various substrate/inhibitor interactions. Different TEA uptake studies showed that organic cations including clonidine, quinine, quinidine and verapamil significantly inhibited TEA uptake. They also found that K_i values of several compounds interacting with the hOCT1 differed substantially from the corresponding rat OCT, rOCT1, and the human kidney-specific OCT, hOCT2, determined in other studies. They showed that the multivalent cation vecuronium interacted with the hOCT1 in the micromolar concentrations ($K_i = 232 \mu\text{M}$), suggesting that the nature of hydrophobic moiety played an important role in the potency of interactions of multivalent cations with hOCT1. Also they determined the effect of neutral molecules like corticosterone and midazolam on the transport of TEA *via* hOCT1. It had been previously thought that corticosterone entered the cell through simple diffusion but their most recent studies demonstrated that corticosterone is a potent inhibitor of TEA uptake mediated by hOCT1 which is consistent with the findings of Grundemann *et al.*, (1994, 1997) that showed that corticosterone also interacts with the rOCT1. Studies on the neutral compound midazolam showed that the K_i of the compound in inhibiting the TEA transport in hOCT1 is in the same range of its K_m of metabolism by CYP3A. Also since hOCT1 is primarily expressed in the liver, which is the major metabolism site for midazolam, it is possible that the transport rate limits the metabolism of midazolam. Collectively the data suggests that hOCT1 is polyspecific not only for organic cations but also for various neutral compounds. This implies that the positive charge(s) of a molecule may not be the only structural requirement for interaction with the hOCT1 transporter.

Blaschke and Giacomini, (1987); Drayer, (1986); Levy and Boddy, (1991), have shown that the differences in the pharmacological activities of stereoisomeric compounds and that stereoselective metabolism of these compounds play an important role in understanding the nature of the function of this transporter. Giacomini *et al.*, examined the potency of various isomers in inhibiting TEA uptake in hOCT1 transfected cells. The diastereomers of quinine and quinidine did not show a significant difference in IC₅₀ values, whereas S-(+)-disopyramide was approximately 2 fold less potent than R-(-)-disopyramide ($29.9 \pm 8.5 \mu\text{M}$ vs. $15.4 \pm 11.0 \mu\text{M}$). Further experiments with other stereoisomers would therefore be needed to establish the possibility of enantioselectivity of this transporter.

Zhang & Giacomini *et al.*, (1998), studied the interaction of a series of a series of n-tetraalkylammonium (n-TAA) compounds (alkyl chain length, N, ranging from 1 to 6 carbons) with hOCT1 in a transiently transfected human cell line, HeLa. A systematic determination of the effect of hydrophobicity on inhibition potencies of compounds interacting with hOCT1 was found. Furthermore, the effect of hydrophobicity on the rate of transport by hOCT1 was also determined. A reversed correlation of IC₅₀ values with alkyl chain lengths or partition coefficients (log P) was observed. Tran-stimulation and trans-inhibition studies revealed that with increasing alkyl chain lengths (N>2), n-TAA compounds were more poorly translocated by hOCT1 although their potency of inhibition was increased. Similar results were also observed for the nonaliphatic hydrocarbons. In summary, the longer the alkyl chain length i.e., the more hydrophobic and bulkier, the higher the affinity of the TAA compounds for hOCT1, and

slower the rate of transport (i.e. poorer substrate) by hOCT1. The correlation observed between the IC_{50} and the P values could be used to predict the IC_{50} of various N-TAA compounds interacting with hOCT1. Thus a balance between hydrophobic and hydrophilic properties is required for efficient transport of organic cations by hOCT1.

4.1.4 OCT1 and OCT2 type distribution

Renal secretion is a major pathway of elimination for many clinically used organic cations. In addition, transport of toxic organic cations into the kidney may lead to nephrotoxicity. Over the past decade, the mechanism of renal organic cation transport has been investigated in a number of different tissue preparations and cell culture models.

The studies have shown that multiple organic cation transporters exist in the basolateral membrane (BLM) and BBM of the kidney. These transporters are found primarily in the proximal tubule and, to a lesser extent, in the distal tubule. Several potential-sensitive organic cation transport mechanisms have been described at the BLM region, indicating that the transport across the BLM is down the electrochemical gradient.

In contrast, at the BBM, organic cation-proton antiport mechanisms have been described. In this case, organic cations are transported from inside the cell into the

tubule lumen in exchange for a luminal proton. These two systems working together result in net secretion of organic cations from the blood to the tubule fluid.

Although renal cation transport systems in the basolateral and luminal membranes of proximal tubules have been characterized in great detail, a localization of the cloned transporters on the basis of functional *in vivo* data remains speculative. *In situ* hybridization with specific probes, RT-PCR experiments with dissected tubuli and immunohistochemical experiments with specific antibodies are required to localize the cloned transporters. In addition, distinct species differences concerning the tissue distribution and histochemical localization of the OCT1 and OCT2 transporters have been observed. For example the rOCT1 from rat is expressed in the kidney and liver, whereas human hOCT1 is only expressed in the liver. On the other hand the tubular localization and membrane localization of hOCT2 has not been unequivocally determined. *In situ* hybridization and immunohistochemistry revealed that hOCT2 is mainly expressed in the distal convoluted tubules and localized at the luminal membrane.

Overall it may be said that the OCT1 has wide tissue distribution with primary expression in the kidney and liver. To date five organic cation transporters have been cloned; OCT1, OCT2, OCT3, OCTN1 and OCTN2. Based on their functional characteristics, namely sensitivity of membrane potential OCT1/2/3 are likely to be found within the BLM of epithelial cells in the kidney. Hence these transporters are most likely to be involved in the first step in the renal secretion of drugs. However, so

far, only rOCT1 has been convincingly localized to the BLM of the kidney. Therefore caution is warranted until definitive localization studies for the other isoforms are reported. In contrast, OCTN1 is thought to transport organic cations in exchange for protons, which is consistent with a renal BBM transporter. However localization and further studies are still needed to confirm these speculations. Although OCTN2 transports the small zwitterion carnitine in a sodium dependent fashion, it is different from other organic cation transporters which transport cations in a sodium-independent manner.

The OCTs are believed to mediate the bidirectional transport of small hydrophilic compounds (50-350 amu) with usually one charged amine moiety. Not all of the compounds that have been shown to have an effect on the OCT are transported by the OCT. Compounds that have been identified as being transported by the OCT include, but are not limited to: tetraethylammonium, 1-methyl-4-phenyl pyridinium (MPP), verapamil, quinine, quinidine, antidiabetics, dopamine's and norepinephrine.

Therefore with the identification of the OCT family a new age in the elucidation of renal cation excretion and reassertion has begun. Review of the research till today suggests that the OCT family contains subfamilies of different polyspecific transporters that may translocate cations and anions. The OCT1/OCT2 subfamily contains polyspecific facilitated diffusion systems for small organic cations. Out of the two other known subfamilies of OCT, one may be related to rOCT3. This may also mediate the

transport of polyspecific electrogenic cations but may show a different membrane localization and substrate specificity as the OCT1/OCT2 subfamily. A third subfamily of transporters known as the OCTN1/OCTN2 may be high affinity sodium co transporters of zwitterionic solutes.

Thus in order to understand the role of the cation transport in the kidney all transporters must be identified, localized and functionally characterized. Also since the polyspecific transporters for the cations, anions and non-charged solutes have overlapping substrate specificities, it is very important that while studying the interactions of drugs and their renal toxicity all the different types of polyspecific transporters are considered.

Overall, it is clear that the future holds a demanding challenge in elucidating the molecular mechanisms of these polyspecific electrogenic cation transporters. Therefore it is vital that these proteins be crystallized, their tertiary structure determined by X-ray crystallography and the cation binding sites characterized by affinity labeling, site-directed mutagenesis and biochromatography and QSAR modeling; Also because OCT exhibits marked species variance it is of high importance that we identify, clone, characterize and localize all the human cation transporters. The expression systems with these transporters i.e. immobilized protein based stationary phases, will help us in identifying new drugs with optimized secretion properties. Also the knowledge regarding the structure-activity relationship of these cation binding sites and their transport mechanism will help to design drugs that modulate transporter activities.

4.2 Drug Uptake studies for hOCT1 & MDCK cell lines

4.2.1 Experimental

4.2.1.1 Materials

Phosphate buffer saline 1X (PBS), Ecoscint A, MEM, foetal bovine serum, NaOH and N-[³H]-methyl-4-phenyl pyridinium acetate ([³H]-MPP) (9.7 MBq) were purchased from American Radiolabeled Chemicals, Inc (St.Louis, MO). [³H]-Dopamine (1.67 TBq), [³H]-propranolol (1.22 TBq), [³H]-verapamil (9.25 MBq) and [³H]-nicotine (3.2 TBq) were purchased from Amersham Biosciences Inc (Piscataway, NJ, USA) and [³H]-methamphetamine was obtained from the National Institute of Drug Abuse

4.2.1.2 Method

The Madin-Darby canine kidney cells (MDCK) and the hOCT1 cell line were plated at 2.5×10^5 cells/well into 24 well culture dishes, in routine growth media [MEM Eagle's with Earle's balanced salt solution supplemented with 100 units/ml penicillin, 100ug/ml streptomycin (transfected cells are antibiotic resistant thus the antibiotics help in stopping infections), and 10% (v/v) foetal bovine serum (FBS)], and incubated at 37°C. After 48 h, the cells were treated by replacing the growth media with 0.5 ml media containing 1 μ M of the following ligands: [³H]-N-methyl-4-phenylpyridinium (MPP), [³H]-dopamine, [³H]-propranolol, [³H]-verapamil and [³H]-nicotine. All treatments were

carried out in triplicate. After 90 min incubation, the treatment was stopped. The supernatant was collected and diluted with 3ml of scintillation fluid (Ecoscint A). Subsequently, the plates were washed with cold phosphate buffered saline (0.5ml/well) twice and left to dry at room temperature. Cell monolayers were removed with 0.5ml NaOH (0.2N) and diluted with 3 ml of scintillation fluid (Ecosinct A). Drug accumulation was radiometrically assessed by a liquid scintillation counter (Beckman Model).

4.3 Preparation of IAM based columns with MDCK and hOCT1 membranes

4.3.1 Materials

(R,S)-verapamil (9.25 MBq), (R,S)-psuedoephedrine, (R,S)-atenolol, (R,S)-propranolol, (R,S)-alpha methylbenzylamine, [³H]- N-methyl-4-phenyl pyridinium iodide (MPP), [¹⁴C]- tetraethyl ammonium (TEA), quinine, quinidine, nicotine, dopamine, vinblastine, benzamidine, sodium chloride, magnesium chloride, cholate, leupeptin, phenyl methyl sulfonyl fluoride (PMSF), EDTA, Trizma, CHAPS were purchased from Sigma Chemical (St. Louis, MO) and metamphetamine was obtained from the National Institute of Drug Abuse. HPLC grade methanol, ammonium acetate and 0.1 M ammonium hydroxide solution were purchased from Fisher Scientific (Pittsburgh, PA). N-[³H]-methyl-4-phenyl pyridinium acetate ([³H]-MPP) (9.7 MBq), [¹⁴C]-tetraethyl ammonium ([¹⁴C]-TEA) (6.3 Bq), [³H]-nicotine (3.2 TBq), [³H]-dopamine (1.67 TBq), [³H]-verapamil (9.25 MBq) and [³H]-propranolol (1.22 TBq) were purchased from

American Radiolabeled Chemicals, Inc (St Louis, MO). Immobilized artificial membrane PC stationary phase (IAM-PC, 12 micron particle size, 300Å pore size) was purchased from Regis Chemical Co. (Morton Grove, IL, USA). A HR 5/2 glass column was purchased from Amersham Pharmacia Biotech (Uppsala, Sweden).

4.3.2 Preparation of hOCT1(-) and hOCT1(+) membranes

4.3.2.1 Cell lines

hOCT1(-) (MDCK) and the hOCT1(+) cell lines were obtained from K.Giacomini from the University of California San Francisco. Madin-Darby canine kidney cells (MDCK) and the transfected MDCK with mutant hOCT1 cDNA inserts were maintained in MEM Eagle's with Earle's balanced salt solution supplemented with 100 units/ml penicillin, 100 µg/ml streptomycin, and 10% (v/v) FBS in 5% CO₂ / 95% air.

4.3.3 Solubilization of the membranes

The MDCK or hOCT1-MDCK cells (100×10^6 cells) were placed in 15 ml of homogenization buffer (Tris-HCl [50 mM, pH 7.4] containing 50 mM NaCl, 8 µM leupeptin, 1 µM PMSF and 8 µM pepstatin). The suspension was homogenized for 3 x 30 s at the setting of 12.5 on a Model PT-2100 homogenizer (Kinematica AG, Luzern, Switzerland). The homogenate was then centrifuged at 700 x g for 5 min and the pellet

containing the nuclear proteins was discarded. The supernatant was centrifuged at 100,000 x g for 35 min at 4°C and the resulting pellet containing the cellular membranes was collected. The pellet was then re-suspended in 10 ml of solubilization buffer (Tris HCl 50 mM pH 7.4, 250 mM NaCl, 1.5% CHAPS, 2 mM DTT, 1 µM PMSF, 8 µM pepstatin A, 10% glycerol) and the resulting mixture was rotated at 150 rpm using an orbit shaker (Lab-line Model 3520, Melrose Park, IL, USA) for 18 h at 4°C.

4.3.4 Immobilization of the solubilized membranes

The resulting solution was centrifuged at 60,000 x g for 22 min and the solubilized solution was then mixed with 160 mg IAM particles and was rotated at room temperature for 3 h at 150 rpm using an orbit shaker (Lab-line Model 3520, Melrose Park, IL, USA). The suspended particles were then dialyzed Tris HCl [50 mM, pH 7.4] containing 150 mM NaCl, 1 mM EDTA, 1 mM benzamidine for 2 days. The dialyzed mixture was centrifuged for 3 min at 4 °C at 700 x g and the supernatant was discarded. The pellet (hOCT1/MDCK-SP) was washed with running buffer A (Tris-HCl [10 mM, pH 7.4] containing 1 mM CaCl₂, 0.5 mM MgCl₂) and centrifuged. This process was repeated until the supernatant was clear.

4.4 Frontal chromatography with radio-labeled markers

4.4.1 Chromatographic system

The chromatographic system was composed of a Shimadzu LC-10Advp pump, 50 ml superloop (Amersham Pharmacia, Uppsala, Sweden), an IN/US System β -Ram Model 3 radioflow detector (IN/US, Tampa, FL, USA) with a dwell time of 2 s and the output data was analyzed using Laura lite 3 (IN/US) running on a PC.

4.4.2 Determination of binding affinities using frontal chromatography

The hOCT1 (+) and hOCT1 (-)-IAM (180 mg) was packed into a HR 5/2 glass column to yield a 150 mm x 5 mm (ID) chromatographic bed. The column was then connected to a LC-10AD isocratic HPLC pump (Shimadzu, Columbia, MD, USA). The mobile phase consisted of running buffer A delivered at 0.2 ml/min at room temperature. Detection of the [^3H]-MPP was accomplished using an on-line scintillation detector (IN/US system, β -ram Model 3 (Tampa, FL, USA) with a dwell time of 2 s using Laura lite 3.

4.4.3 Chromatographic studies:

The marker ligand used in these studies was [³H]-MPP (20 pM). In the chromatographic studies, a 50-ml sample Superloop (Amersham Pharmacia Biotech) was used to apply the marker ligand and a series of displacer ligands: (R,S) verapamil (1, 2, 3, 5, 10 μM), R-verapamil (5 nM, 10 nM, 25 nM, 50 nM, 100 nM, 200 nM), S-verapamil (1, 2, 5, 10, 15, 20 μM), quinine (1, 4, 10, 15 μM), quinidine (1, 3, 5, 20, 40 μM), nicotine (1, 2, 4, 6, 10, 15, 20, 30 μM), dopamine (50, 100, 175, 250, 500 μM), vinblastine (0.5, 1, 2, 5, 10 μM), MPP high (2.5, 5, 7.5, 10, 20 pM) and MPP low (0.5, 1, 2, 5 μM) through the hOCT1-IAM column to obtain elution profiles showing a front and plateau regions.

4.4.4 Data analysis

The dissociation constants, K_d , for the marker and displacer ligands were calculated using a previously described approach (Moaddel *et al.*, 2002]. The experimental approach is based upon the effect of escalating concentrations of a competitive binding ligand on the retention volume of a marker ligand that is specific for the target receptor. For example, if the hOCT1 receptor is the target, MPP can be used as the marker ligand (Dresser *et al.*, 2001; Koepsell *et al.*, 1999). Then the association constants of MPP, K_{MPP} , and the test drug, K_{drug} , as well as the number of the active binding sites of the immobilized hOCT1 receptor, P , can be calculated using Eqn 1.

$$(V - V_{\min})^{-1} = (V_{\min} [P] K_{MPP})^{-1} + (V_{\min} [P]^{-1} [MPP]) \quad (\text{Eqn 1})$$

where, V is retention volume of MPP; V_{\min} , the retention volume of MPP when the specific interaction is completely suppressed (this value can be determined by running [^3H]-MPP in a series of concentration of drugs and plotting $1/(V_{\max} - V)$ versus $1/[\text{drug}]$ extrapolating to infinite [drug]). From the above plot and a plot of $1/(V - V_{\min})$ vs. [MPP], dissociation constant values, K_d , for [^3H]-MPP and the drugs can be obtained. The data was analyzed by non-linear regression with a sigmoidal response curve using Prism 4 software (Graph Pad Software, Inc., San Diego, CA, USA) running on a personal computer.

4.5 Membrane Binding Assays

The membrane binding assays were carried out as previously described (Ferry, 1995; Lu, 2001b). Briefly, 50 μl of [^{14}C]-TEA (1 μM) was incubated with hOCT1 (+) and hOCT1 (-) membranes (150 $\mu\text{g}/\mu\text{l}$) and 50 μl of cold vinblastine (0.5, 1, 5, 10, 50, 100, 500 μM) in solubilizing buffer (Tris-HCl [50 mM, pH 7.4] containing 250 mM NaCl, 1.5% CHAPS, 2 mM dithiothreitol, 2 μM leupeptin, 2 μM PMSF, 2 μM pepstatin, 10 % glycerol) at room temperature for 2 h, before bound and free drug were separated by rapid filtration through Whatman GF/C filters (pre-wetted with solubilizing buffer with 0.1% BSA). The filters were dried and then placed in liquid scintillation vials containing 3 ml of scintillation liquid for counting on the liquid scintillation counter. The data was analyzed by non-linear regression with a sigmoidal response curve using

Prism 4 software (Graph Pad Software, Inc., San Diego, CA, USA) running on a personal computer.

4.6 Pharmacophore – Methods

Molecular modelling employed in pharmacophore development was done using HyperChem V 6.0 software (HyperCube Inc., Gainesville, FL). Chemical structure of every processed compound was modelled using the same procedure. At first the model was constrained manually with special attention being paid to correct stereochemistry. Then the structure was subjected to procedure >build< employed in HyperChem to obtain reasonable spatial geometry. In the last step a short minimization of the system energy was done using AM1 semi-empirical method (200 steps or root-mean-square of the gradient less than 0.5 kcal/mole).

In the case of chiral molecules, the procedure >invert< was used to obtain both enantiomers as real mirror images and both enantiomers were at the stereogenic center. The molecules were overlaid and analyzed in relation to their chromatographically determined K_d values and the structural attributes common to the pharmacophore were identified. HyperChem software was employed to measure distances and angles between these attributes.

4.7 Results and Discussion

4.7.1 Characterization of the hOCT1 and MDCK cell lines

In order to check for whether the hOCT1 transporter is active and is expressed in the MDCK-hOCT1 cell line efflux studies were carried out on the hOCT1 and MDCK cell lines. This study would help in the characterization of the cell lines for further use in the immobilization onto HR 5/2 columns based on an IAM backbone. The results of the efflux studies are presented in Figure 32 and demonstrate that there was a significant efflux of [¹⁴C]-TEA from the pre-incubated hOCT1-MDCK cells but not from the MDCK cells. The data indicated that the hOCT1-MDCK cells accumulated [¹⁴C]-TEA, but not the MDCK and that the hOCT1 was functioning in the hOCT1-MDCK cells. Thus the transfected cell line can be now used to create columns where the hOCT1 protein can be immobilized onto a chromatographic backbone made up of IAM.

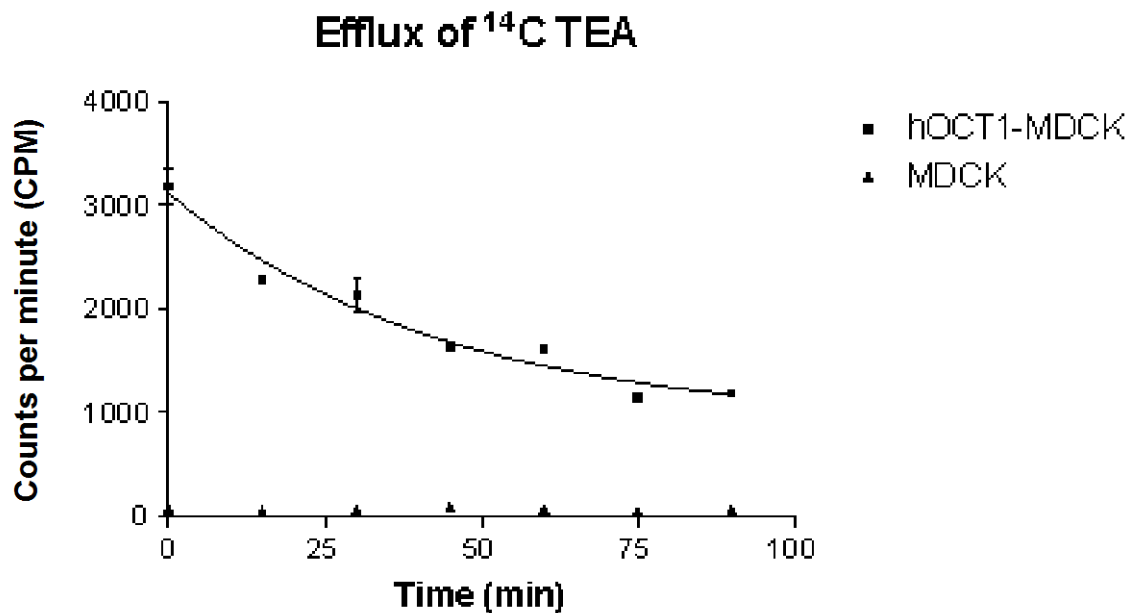


Figure 32. [¹⁴C]-TEA efflux studies carried out on hOCT1-MDCK (+) cell line and MDCK (-) cell line. 50 μ l of [¹⁴C]-TEA (1 μ M) was incubated with each cell membranes and varied concentrations of cold vinblastine were added. The bound and free drug were separated by rapid filtration through Whatman GF/C filters and place in liquid scintillation vials for counting on the liquid scintillation counter (n = 3). The data was analysed by non-linear regression with a sigmoidal response curve obtained using Graph Pad Prism 4 software.

4.7.2 Characterization of the immobilized hOCT1(+)-IAM

Having proved that the MDCK-hOCT1 cells expressed the hOCT1 transporter in its active form, as compared to the control cell line which does not express the transporter, the cell lines could now be used to prepare chromatographic biopolymeric stationary phases. The hOCT1 transporter was successfully immobilized on the IAM stationary

phase; this was initially shown by comparing the retention time of [³H]-MPP on the hOCT1(+)-IAM and comparing it with MDCK-IAM (hOCT1(-)) (Figure 33). MPP is a known substrate of hOCT1 transporter with a K_i of 12.3 μM (Giacomini *et al.*, 1998). In order to characterize the hOCT transporter it is necessary to use known substrates like MPP and TEA as it helps correlate the results of the chromatographic studies with those obtained with cellular studies (from literature). The elution profiles contained both front and plateau regions on both columns. The midpoint of the breakthrough curve occurred at 10 min on the hOCT1(-)-IAM column and 17 min on the hOCT1(+)-IAM column, representing breakthrough volumes of 2.0 ml and 3.4 ml respectively (Figure 33). Since the void volume elution time of the chromatographic system, column and detector was 0.7 min, the results indicated that the [³H]-MPP was retained on both columns. However there was significant increase in retention time of MPP for the hOCT1(+)-IAM as compared to the MDCK-IAM column. This differential retention indicated that the hOCT1 transporter was functionally immobilized on the IAM based column. Also the IAM backbone did not interfere with the substrate-protein binding in this case as generally the substrates for the hOCT1 transporter are all hydrophilic and generally charged. Thus the non-specific interactions caused due to the strong lipophilic properties of the IAM, which led to long retention times in the Pgp based columns were not an issue for the OCT transporter.

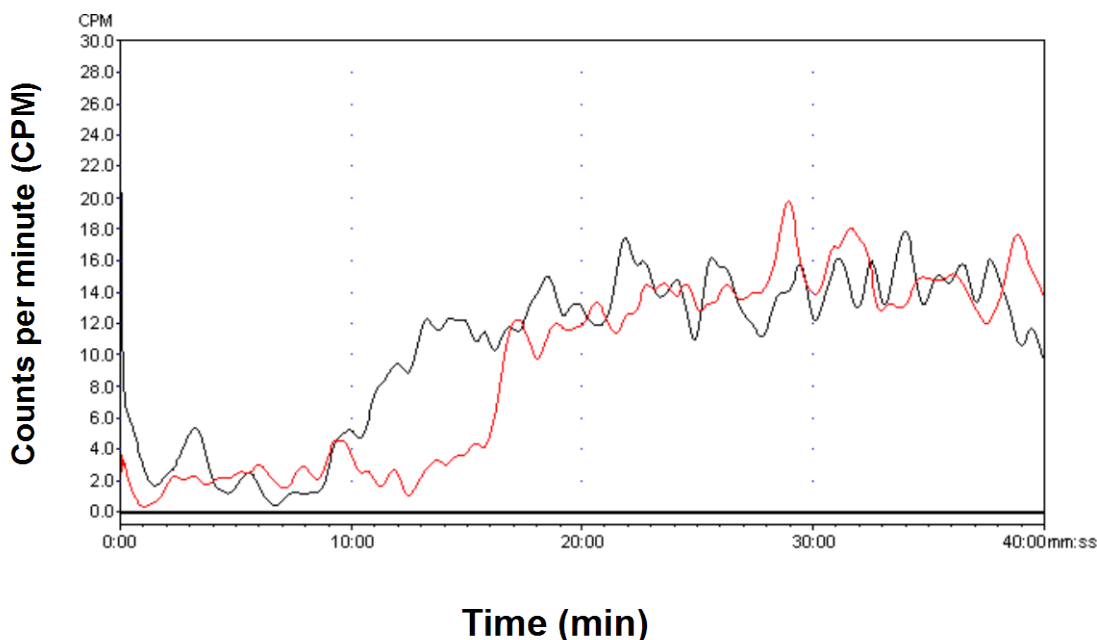


Figure 33. Comparison of the frontal chromatograms of 20 pM [^3H]-MPP on the hOCT1-column (red) and on the MDCK-column (hOCT1-(-)) (black) showing the front and plateau regions for each column. The detection of [^3H]-MPP was accomplished using an on-line liquid scintillation detector (IN/US system, β -ram model 3) with a dwell time of 2s using Laura Lite 3 program. The breakthrough curves occurred at 10.0 min for hOCT1-(-) and 17.0 min for the hOCT1-(+). Running buffer consisted of Tris [10 mM, pH 7.4] 1 mM CaCl_2 , 0.5 mM MgCl_2 and the flow rate was 0.2 ml/min.

The retention of MPP on both the hOCT1(+)-IAM and hOCT1(-)-IAM columns was consistent with the observation that MPP accumulates in both the hOCT1 (+) and hOCT (-) cell lines. However the intracellular concentration of MPP was 10-fold higher in the hOCT1(+) cell line. This suggested that MPP interacted with membranes from the

MDCK cell at specific and non-specific sites, other than exclusively at the hOCT1, and at the same site plus the hOCT1 with membranes from the hOCT1-MDCK.

These differences in the combination of specific and non-specific interactions between the control and the expressed cell lines and the resulting effect on the chromatographic retention had also been previously demonstrated with the Pgp(+)-OT and the Pgp(-)-OT. The studies with the Pgp transporter had demonstrated that the specific interactions with the expressed Pgp could be measured using displacement chromatography and Pgp-specific markers.

The activity of the immobilized hOCT1 transporter was further confirmed in this study, by the addition of 30 μM nicotine, a competitive inhibitor of the hOCT1 (Dresser *et al.*, 2001), to the running buffer. It had no effect on the retention of [^3H]-MPP on the hOCT1(-)-IAM column. However, addition of 10 μM and 20 μM nicotine on the hOCT1(+)-IAM column produced significant and concentration dependent decreases in retention of [^3H]-MPP. The results indicated that on the hOCT1(-)-IAM column, the retention of [^3H]-MPP occurred at sites other than the hOCT1 and that the binding affinity of the immobilized hOCT1 could be further probed using affinity displacement chromatography.

Binding activity of the immobilized hOCT1 transporter was therefore determined using frontal displacement chromatography with [^3H]-MPP as the marker ligand and MPP, verapamil, vinblastine, quinine, dopamine, nicotine and quinidine as displacers. Frontal

displacement was seen between all the ligands tested and MPP in a competitive manner, the chromatogram of nicotine is shown in Figure 34. Using this approach, the affinity of the displacer for the immobilized hOCT1, expressed as the dissociation constant (K_d) and number of available binding sites (B_{max}) were calculated using equation 1, (Table 12). A representative analysis is shown in Figure 35.

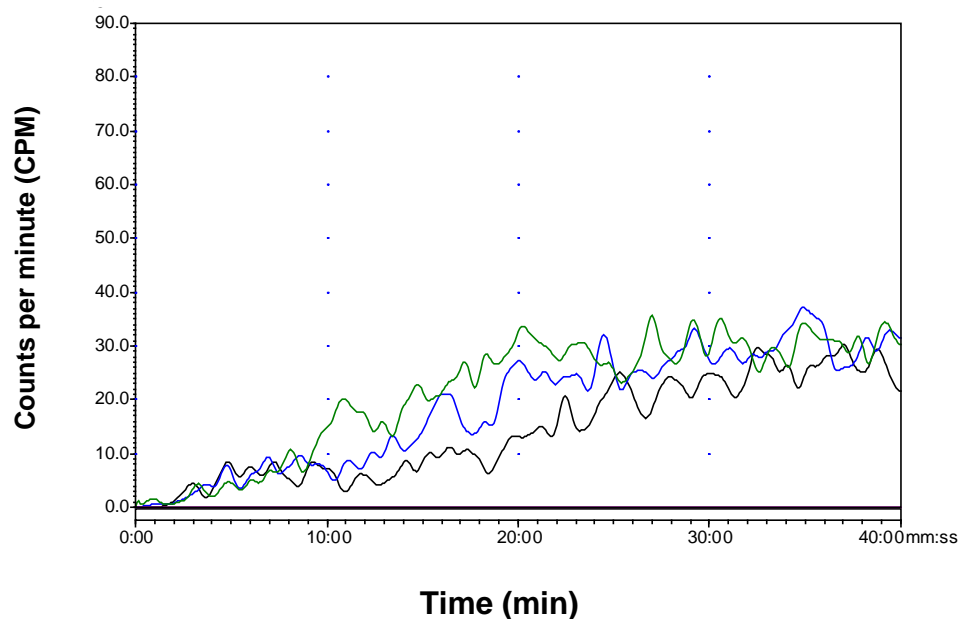


Figure 34. The effect of the addition of increasing concentrations of nicotine on the chromatographic retention of 20 pM $[^3\text{H}]\text{-MPP}^+$ on the hOCT1(+)-IAM column from no nicotine in the mobile phase (black trace), to 10 μM cold nicotine in the mobile phase (blue trace) to 20 μM cold nicotine in the mobile phase (green trace). The detection of $[^3\text{H}]\text{-MPP}$ was accomplished using an on-line liquid scintillation detector (IN/US system, β -ram model 3) with a dwell time of 2 s using Laura Lite 3 program). Running buffer consisted of Tris [10 mM, pH 7.4] 1 mM CaCl_2 , 0.5 mM MgCl_2 and the flow rate was 0.2 ml/min.

K_d determination of Nicotine

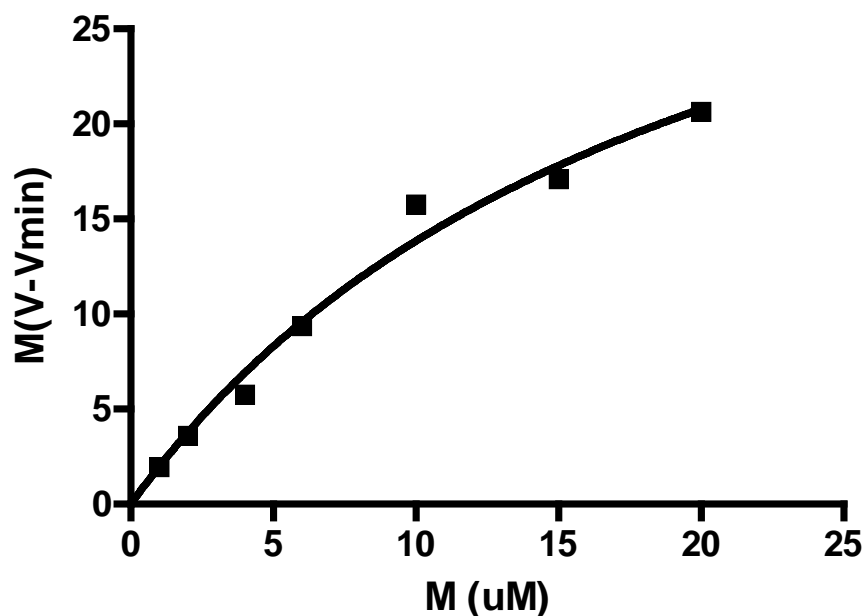


Figure 35. The relationship between chromatographic retention volume expressed as $(V - V_{\min})$ and increasing mobile phase concentrations of nicotine on the hOCT1(+)-IAM column. Running buffer (Tris [10 mM, pH 7.4], 1mM CaCl₂, 0.5 mM MgCl₂) at room temperature at 0.2 ml/min. 10 ml samples of 20 pM [³H]-MPP supplemented with a range of concentrations of cold nicotine (10, 20 and 30 μM) was run and the signal was recorded every 2 s. The elution volume data was used to calculate the dissociation constant of the ligand ($n = 3$). The K_d value of nicotine was calculated by non linear regression with Prism (GraphPad Software) using one site binding equation to be $(20.15 \pm 6.06) \mu\text{M}$.

Table 12. Binding affinities expressed as K_d values (μM) calculated by frontal affinity chromatography using the immobilized hOCT1(+)-IAM column, compared to K_i 's calculated by uptake studies (Dresser *et al.*, 2000). All compounds selected were known hOCT1 substrates/inhibitors and were selected as their inhibition rate constants (K_i) were published in the literature which would help to compare the literature values with the data obtained from frontal displacement chromatography. (n = 2)

Compounds	K_d (μM)	B_{max} (nmoles)	K_i (μM)
Verapamil	2.80 ± 1.09	3.14 ± 0.59	2.9^{a}
Quinidine	6.33 ± 1.48	10.42 ± 1.02	$17.5^{\text{a}}, 5.4^{\text{b}}$
Methyl Phenyl Pyridinium	1.80 ± 1.28 $(6.06 \pm 2.87) \times 10^{-6}$	0.513 ± 0.207 $(10.48 \pm 2.35) \times 10^{-6}$	12.3^{a}
Quinine	10.18 ± 2.06	8.10 ± 0.94	22.9^{a}
Nicotine	20.15 ± 6.06	208 ± 38	53.2^{b}
Dopamine	198 ± 112	840 ± 256	487.2^{b}
Vinblastine	7.28 ± 6.93	2.63 ± 1.67	21.5

a: Zhang *et al.* 1998

b: Bednarczyk, *et al.* 1989.

A linear regression analysis was carried out between the binding affinities obtained by frontal chromatography on the hOCT1 column with those obtained by membrane binding studies reported in the literature (Zhang *et al.*, 1998; Bednarczyk, *et al.*, 1989) to determine if differences represent a qualitative difference or a quantitative difference. A linear relationship was observed with an r^2 value of 0.9987 ($p < 0.001$, very significant) with all the tested ligands except for vinblastine (no cellular uptake data available), which was analyzed in this study and was calculated to have a K_d of 21.48 μM . To ensure that the r^2 observed was not an artifact, since the K_d for dopamine is at least 40 fold different from the remaining tested ligands, the correlation analysis was carried out without dopamine resulting in an r^2 of 0.9363 ($p = 0.0016$, significant). This indicated that the binding to the immobilized hOCT1 was consistent with those from the membrane binding assays and had only a relative difference.

The number of available binding sites for all the ligands was similar (1-10 nmoles) except for nicotine (208 nmoles) and dopamine (840 nmoles). These compounds were also tested on the MDCK column to determine if there was any specific binding occurring to any other protein other than the hOCT1 transporter. No displacement was seen with nicotine or dopamine at concentrations of 30 μM and 500 μM , respectively. The significant increase in the amount of available binding sites for nicotine and dopamine can be explained in terms of affinity and specificity. It is believed that at a reduced affinity, these ligands bind to numerous sites *en route* to the specific binding site on the hOCT1 protein.

An interesting result obtained with the hOCT1 column, that had not been reported elsewhere, was the discovery of a second high-affinity site for MPP on the hOCT1 transporter, i.e. 6 pM (Table 12). Subsequently, the displacer ligand was increased and a second site which had an affinity for MPP of 1.80 μ M was found. The latter site is consistent with the binding affinity values for MPP reported elsewhere. However, the former high affinity site had not been reported to date and this was the first time that two binding sites for MPP had been identified. It should be noted that although with the methods used here a pM binding at the high affinity site was observed, qualitatively this could have been out by an order of magnitude. In order to calculate binding affinities in frontal chromatography there are two assumptions that must be held. The one which was not held in this case was that the concentration of the marker ligand should be significantly lower than the binding affinity of the marker. In the case of the high affinity MPP site, the concentration of the marker was 20 pM and the reported affinity was 6 pM. In spite of the limitations of frontal chromatography, the column had successfully identified a second high affinity site for MPP. On the basis of the results found in this study it may be concluded that the immobilized hOCT1 transporter can be used to screen for know substrate/inhibitors in a rapid and precise manner.

4.7.3 Enantioselectivity on the hOCT1 column

Previous studies on the hOCT1 had demonstrated that diisopyramide enantioselectively inhibited hOCT1 mediated uptake of TEA (Zang *et al.*, 1998). In these studies, the IC₅₀ value of (R)-diisopyramide was about 2 fold lower than that of (S)-diisopyramide, 15.4 μM and 29.9 μM, respectively. An interesting result was observed for the hOCT1 column which showed differences in the affinity for the enantiomers of verapamil (Table 13).

In the frontal chromatography studies, low concentrations of (R)-verapamil produced significant displacements of [³H]-MPP⁺ while significantly higher concentrations of (S)-verapamil were required to displace the marker (Figure 36).

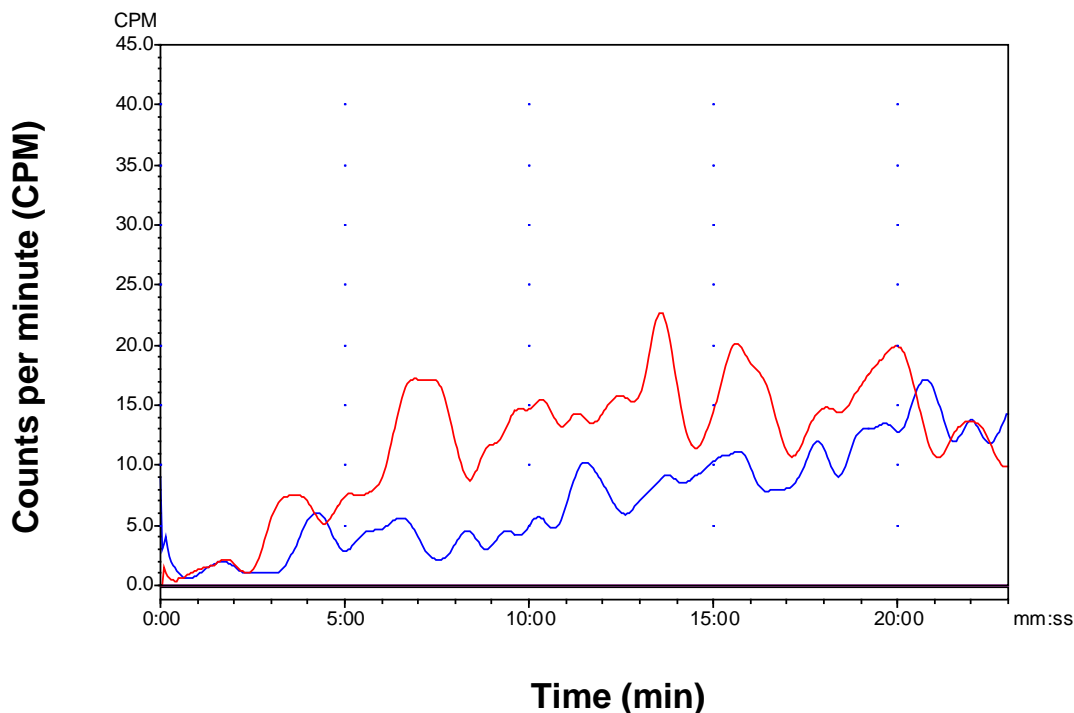


Figure 36. Frontal affinity chromatography showing enantioselectivity for the enantiomers of verapamil. The chromatogram shows the displacement of 20 pM [^3H]-MPP $^+$ on the hOCT1(+)-IAM column by 0.1 μM (R)-verapamil (red trace) and 1.0 μM (S)-verapamil (blue trace) which were added to the mobile phase. The detection of [^3H]-MPP was accomplished using an on-line liquid scintillation detector (IN/US system, β -ram model 3) with a dwell time of 2 s using Laura Lite 3 program). The mobile phase consisted of Tris [10 mM, pH 7.4] 1 mM CaCl_2 , 0.5 mM MgCl_2 and the flow rate was 0.2 ml/min.

The results demonstrated that (R)-verapamil had a 58-fold lower K_d value than (S)-verapamil, 0.06 and 3.46 μM , respectively (Table 13). Since enantiomers have the same physiochemical properties, the observed difference had to be due to specific interactions with immobilized biopolymers. Since no enantioselectivity was observed

on the column containing the control membranes, the difference between (R)- and (S)-verapamil must be a result of specific interactions with the immobilized hOCT1. Thus, the immobilized transporter retained the ability to enantioselectively bind to substrates and inhibitors. Further experiments were carried out to study the enantioselective properties of the hOCT1 transporter. Enantiomers of propranolol, atenolol, α -methylbenzylamine and psuedoephedrine were studied on the hOCT1 and it was observed that the transporter showed enantioselectivity for these compounds (Table 13, Figure 37).

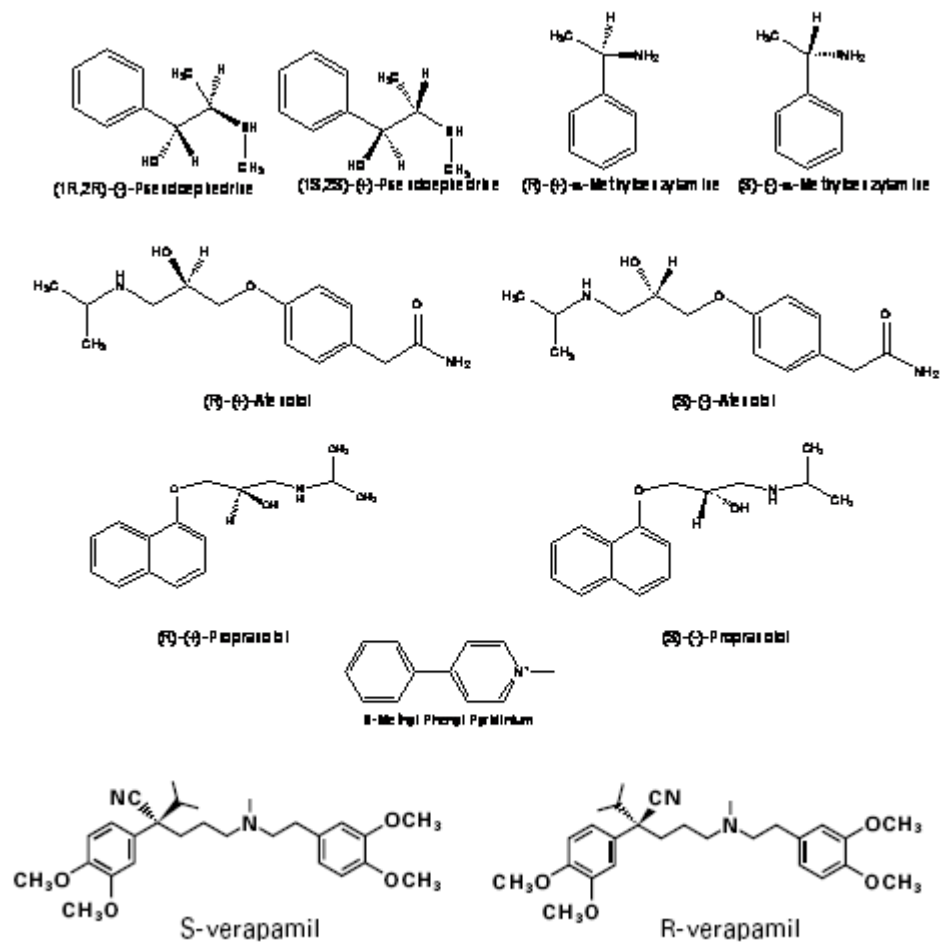


Figure 37. The structure of the enantiomers of propranolol, atenolol, pseudoephedrine, α -methylbenzylamine and verapamil used in this study. All compounds have chiral centres and they were used to characterize the hydrogen bonding receptor sites to demonstrate enantioselectivity of the hOCT1 transporter.

In this competitive displacement study, increasing concentrations of a competing ligand were added to the mobile phase and the effects on the retention volume of the marker, measured at the mid-point of the breakthrough curves, were determined and the K_d values calculated using Eqn 1, as had been previously described (Moaddel *et al.*, 2005). In this study, both of the enantiomers of propranolol displaced MPP^+ when they were added to the mobile phase. However, (-)-(S)-propranolol produced a greater displacement than (+)-(R)-propranolol. For example, the addition of 1 μ M of (+)-(R)-propranolol to the mobile phase reduced the mid-point of the breakthrough curve of MPP^+ by 3 min (Figure 38), Trace B, while the same concentration of the (S)-enantiomer reduced the mid-point of the breakthrough curve by 7 min to 13 min, (Figure 38) Trace C.

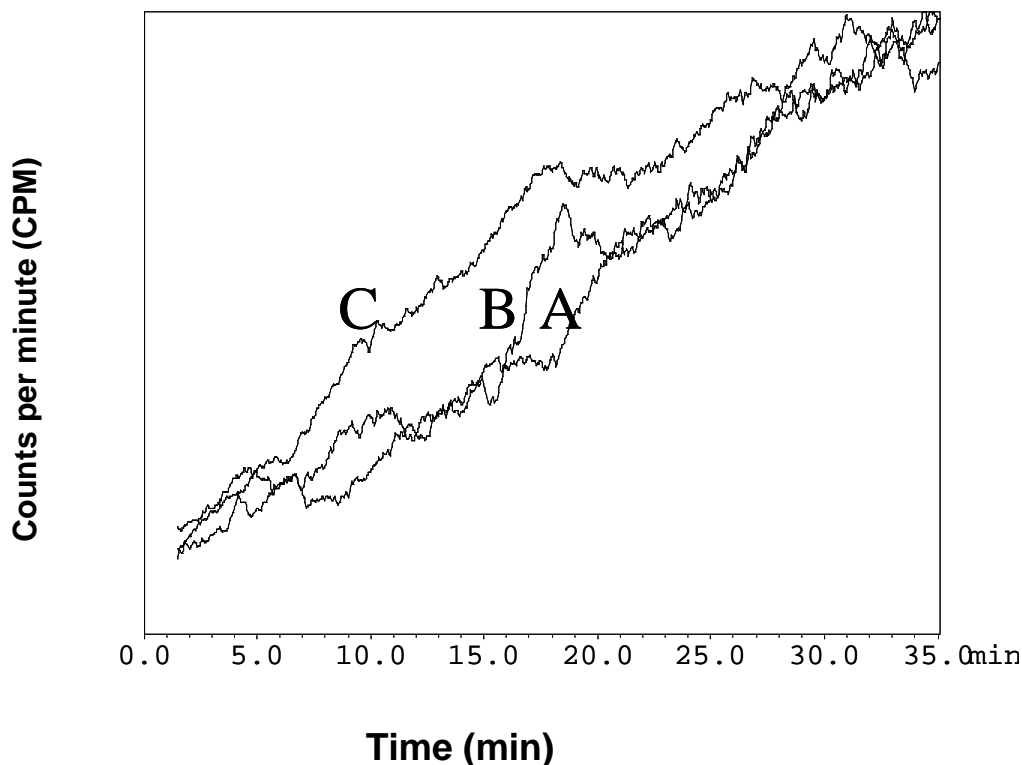


Figure 38. The chromatographic traces from the frontal competitive displacement of 10 pM [^3H]-MPP, where: Trace A [^3H]-MPP alone; Trace B after the addition of 1 μM (+)-(R)-propranolol to the mobile phase; Trace C after the addition of 1 μM (-)-(S)-propranolol to the mobile phase. The experiments were carried out using a stationary phase containing immobilized membranes obtained from the hOCT1-MDCK cell line that express a human organic cation transporter. The detection of [^3H]-MPP was accomplished using an on-line liquid scintillation detector (IN/US system, β -ram model 3) with a dwell time of 2 s using Laura Lite 3 program). The mobile phase consisted of Tris [10 mM, pH 7.4] 1 mM CaCl_2 , 0.5 mM MgCl_2 and the flow rate was 0.2 ml/min.

Similar results were observed with atenolol, and pseudoephedrine. However, the addition of up to 5 μM of (R)- or (S)- α -methylbenzylamine to the mobile phase produced no displacement of the marker ligand. This result indicated that, under the experimental conditions used in this study, α -methylbenzylamine did not compete with MPP^+ for binding to the immobilized hOCT1.

The displacement data was analyzed using Eqn. 1 and a K_d value for each compound was calculated from the non-linear binding curve, as depicted for (R)-propranolol in Figure 39.

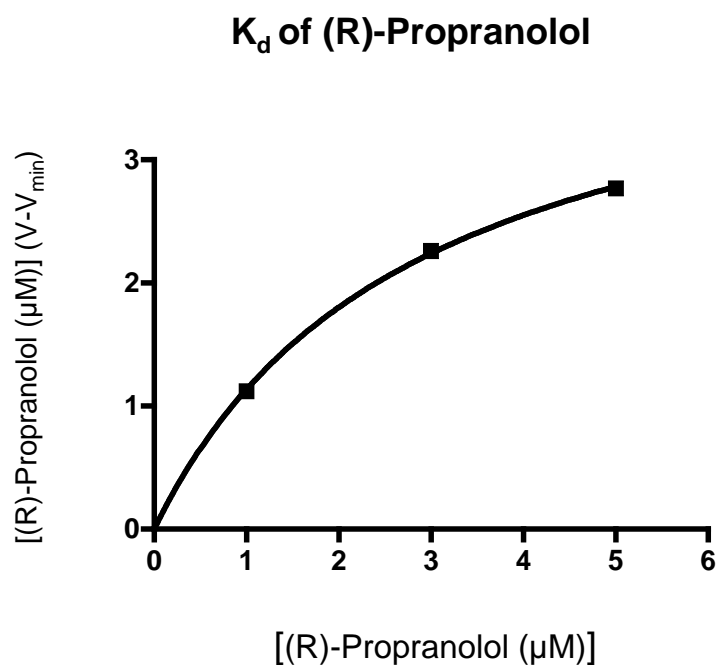


Figure 39. Determination of the binding affinity, K_d value, of (+)-(R)-propranolol for the immobilized human organic cation transporter calculated using Eqn. 1 and the effect of the addition of increasing concentrations of (+)-(R)-propranolol on the chromatographic retention of [^3H]-N-methyl 4-phenyl pyridinium.

As previously demonstrated for the immobilized hOCT1 column (Moaddel *et al.*, 2005) and for other immobilized receptor and transporter studies, only a single series of displacement studies is required to calculate reproducible K_d values which are comparable and consistent with affinities produced using other experimental approaches.

A significant enantioselectivity was observed for propranolol where the (S)-enantiomer had a lower K_d value, and, therefore higher affinity, and there was an excellent fit to the non-linear curve, $r^2 = 0.999$ for each enantiomer (Table 13).

Table 13. The binding affinities (K_d) of the compounds used in this study for the immobilized human organic cation transporter obtained using frontal displacement chromatography with [3 H]-MPP⁺ as the marker ligand.

Compound	K_d (μ M)	Ratio
(+)-(R)-Propranolol	2.85 ± 0.19	2.98
(-)-(S)-Propranolol	0.95 ± 0.01	
(+)-(R)-Atenolol	0.98 ± 0.42	2.11
(-)-(S)-Atenolol	0.46 ± 0.25	
(+)-(1S;2S)-Pseudoephedrine	1.71 ± 0.67	1.53
(-)-(1R;2R)-Pseudoephedrine	1.12 ± 1.08	
(+)-(R)-Verapamil	0.05	86.5
(-)-(S)-Verapamil	3.46	
(+)-(R)- α -Methylbenzylamine	ND ^a	1.00 ^a
(+)-(S)- α -Methylbenzylamine	ND ^a	

^a ND: No displacement of the marker up to 5 μ M concentration of the displacer

The same enantioselectivity was observed for atenolol, where (S)-atenolol had a higher affinity for the immobilized hOCT1, but the magnitude and the curve fit were significantly lower than those observed for propranolol (Table 13). The chromatographically calculated K_d value of (1R;2R)-pseudoephedrine was 53% lower than the corresponding value for the (1S;2S)-enantiomer (Table 13). However, even though excellent curve fits were obtained for both enantiomers, the calculated 1.5-fold enantioselectivity while representing a reproducible trend, cannot be considered as statistically significant.

None of the compounds used in this study have been previously identified as substrates or inhibitors of hOCT1. In order to determine if the data from this study reflected actual pharmacological activity, a competitive inhibition study was conducted using [14 C]-TEA as the substrate and (-)-(S)-propranolol and (+)-(R)-propranolol as the competitive inhibitors. The data demonstrated that propranolol enantioselectively inhibited the cellular uptake of [14 C]-TEA. (Figure 40)

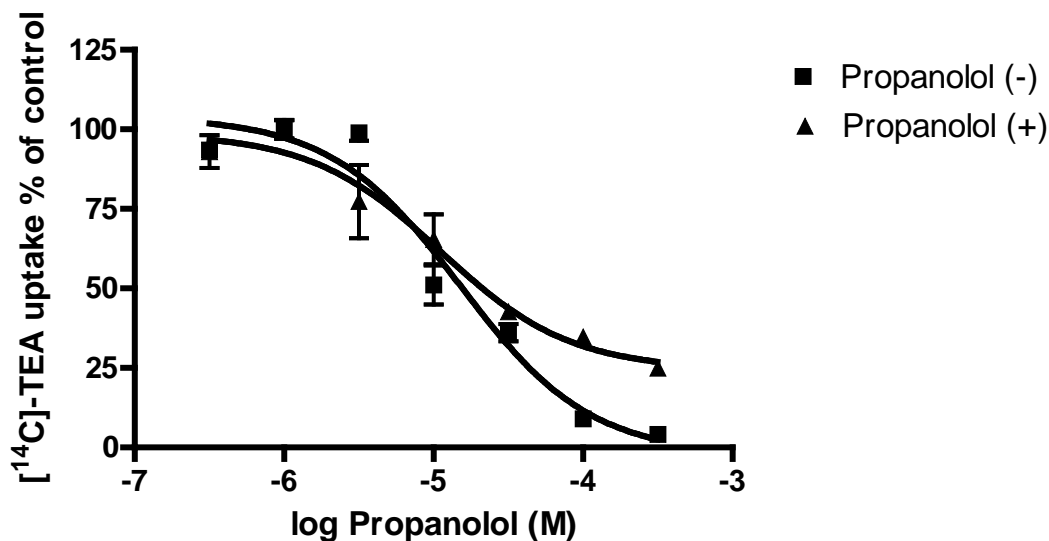


Figure 40. The inhibition of the intercellular uptake of [¹⁴C]-tetraethyl ammonium by increasing concentrations of (-)-(S)-propranolol {■} or (+)-(R)-propranolol {▲} in the hOCT1-MDCK cell line. (n = 3)

There was a 2.75-fold difference between the calculated IC₅₀ values of (-)-(S)-propranolol (15.1 μM) ($r^2 = 0.9629$) and (+)-(R)-propranolol (41.7 μM) ($r^2 = 0.9786$). These results were essentially the same as the difference in the chromatographically determined affinities ($K_{d(+)-(R)\text{-propranolol}} / K_{d(-)-(S)\text{-propranolol}} = 2.98$). This indicated that for the compounds used in this study, the chromatographically determined affinities and enantioselectivities reflected pharmacologically relevant properties.

Molecular models of propranolol, atenolol and pseudoephedrine were constructed and the enantiomers with the lowest K_d values, i.e. the highest affinity, were used to construct a preliminary pharmacophore. The stereogenic centres containing the hydroxyl moiety were used to position the molecules relative to the pharmacophore.

Under this constraint, the configuration around the centres were identical for (S)-propranolol, (S)-atenolol and (1R;2R)-pseudoephedrine. The calculated distances between the hydrophobic, ion pair and hydrogen bonding moieties of the compounds used in this study are presented in Table 14 (n = 3).

Table 14. The calculated distances between the middle of the aromatic ring (Ar), the amine nitrogen atom (N) and the oxygen atom of the hydroxyl group (O) for the compounds used in this study (n = 3).

Ligands	Distances [\AA]		
	Ar-N	Ar-O	N-O
α -Methylbenzylamine	3.7	--	--
Pseudoephedrine	5.1	3.5	2.7
N-Methyl-4-phenyl pyridinium	5.7	--	--
Atenolol	6.9	5.9	2.9
<i>Propranolol</i>	6.9	5.9	2.9

The resulting pharmacophore contained hydrophobic and ion pair interaction sites and the calculated distance between these sites was $\sim 5\text{\AA}$. This distance is consistent with the previously described hOCT1 pharmacophore in which the calculated distances between three hydrophobic areas and a positive ionizable site ranged from 4.2\AA to 5.3\AA (Bednarczyk *et al.*, 2003). Although the previous work included chiral compounds in

the experimental cohort used to calculate the reported pharmacophore, enantioselective interactions were not considered and, consequently, additional binding sites were not identified. In this study, the consideration of the enantioselectivity of the binding led to the identification of a third site, a hydrogen bond donor site, located 4.3Å from the hydrophobic site and 2.2Å from the ion pair interaction site. These interactions are illustrated by the inclusion of (-)-(S)-propranolol in the proposed pharmacophore. (Figure 41)

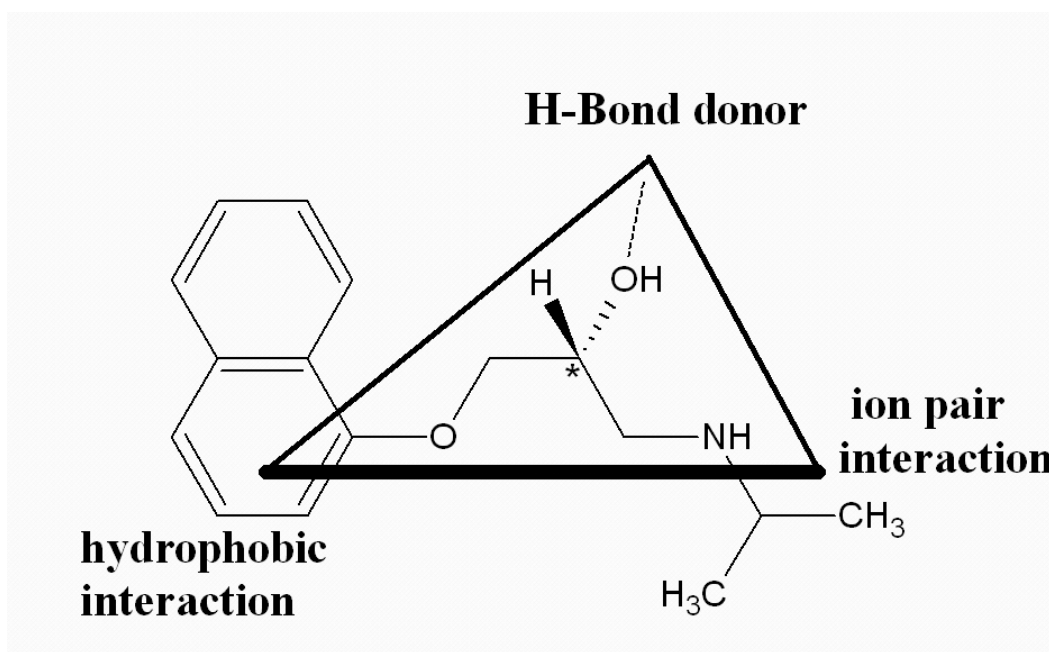


Figure 41. Preliminary pharmacophore that describes the enantioselective binding interactions observed in this study.

Based upon the data obtained in this study, a new pharmacophore is being constructed in this laboratory (Dr IW Wainer, National Institute on Aging), using a larger set of chiral and achiral compounds and considering enantioselective interactions. The results of this study will be reported elsewhere.

The data from the study suggested that the initial binding to the immobilized hOCT1 occurs via an ionic interaction between an ammonium moiety on the ligand and an anionic site on the extracellular portion of the hOCT1, which is followed by the second interaction between a hydrophobic moiety on the ligand and a hydrophobic pocket within the lumen of the hOCT1. Both interactions are necessary for significant binding to occur between the ligand and the hOCT1, and position the ligand for the enantioselective hydrogen bonding interaction.

It is important to note that the presence of a hydrogen bond acceptor is not necessary for a compound to act as a substrate or inhibitor of the hOCT1. Indeed, the marker ligand used in this study, MPP⁺, does not contain a hydroxyl moiety (Figure 41). What is key to the interaction between a potential ligand and the hOCT1 is the distance between the ion pair and hydrophobic moieties. For MPP⁺, this distance is 5.7 Å (Table 14), which is compatible with the pharmacophore developed in this study as well as the previously reported pharmacophore (Bednarczyk *et al.*, 2003).

The suggested binding mechanism and the preliminary pharmacophore derived in this study, as well as the previously described pharmacophore, provide an explanation for the lack of significant binding of α -methylbenzylamine to the immobilized hOCT1. It can be assumed that an ionic interaction occurs between the ammonium moiety on the α -methylbenzylamine and the anionic site on the hOCT1, which tethers the compound to the transporter. However, the second interaction does not occur because the distance between the ammonium moiety and the phenyl ring, 3.7 Å (Table 14), is not long enough for the phenyl ring to reach the hydrophobic pocket. The proposed binding mechanism is currently under investigation using liquid chromatographic stationary phases containing point-mutation variants of the hOCT1. The results will be reported elsewhere. Also the nature of binding of enantiomers of verapamil shows significant enantioselectivity. Although it is believed that verapamil binds to the same site, where the nitrile group binds to the hydrogen bonding site, it is likely that it also tethers to a fourth site, which would be a hydrophobic site resulting in the strong enantioselectivity of verapamil. Evidence to support this model for verapamil was generated in further work by the Wainer group after this research project was completed.

4.7.4 Drug transport on the hOCT1 column

Drug uptake studies were also carried out using the hOCT1 cell line and the MDCK cell line to evaluate whether any of the substrate/inhibitors which showed binding affinity for the hOCT1 transporter on the IAM based columns, were transported by it or not. A series of known ligands like propranolol, verapamil, dopamine, MPP, metamphetamine

and nicotine were studied and the results indicated that MPP and propranolol were transported whereas verapamil, dopamine, nicotine and metamphetamine were not transported through the cell membrane (Figure 42).

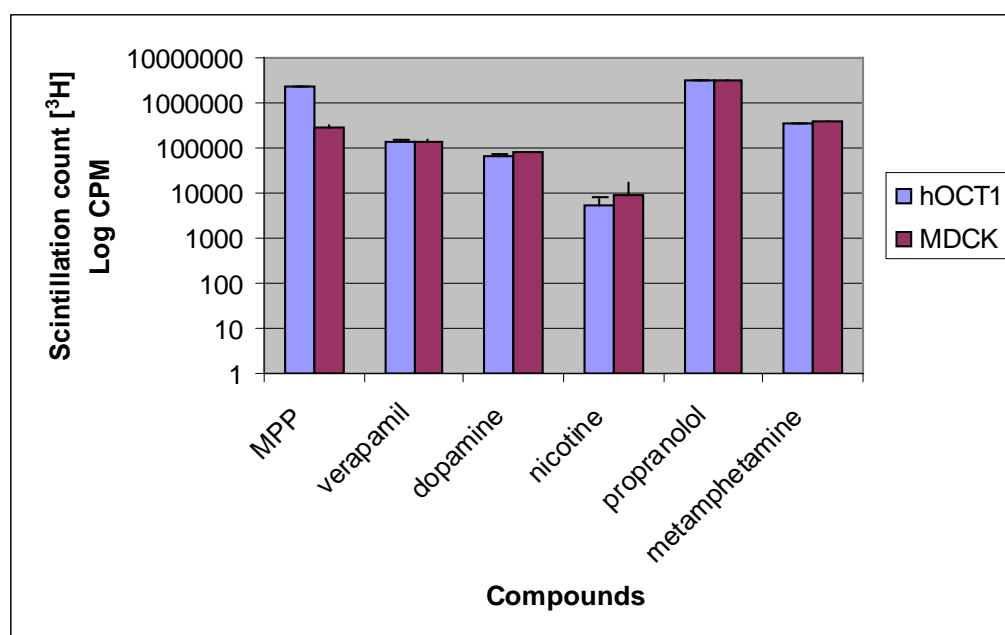


Figure 42. Drug uptake studies on the hOCT1(+) and MDCK cell lines where each cell line was treated with 1 μm of the following ligands: [^3H]-propranolol, [^3H]-verapamil, [^3H]-dopamine, [^3H]-MPP, [^3H]-metamphetamine and [^3H]-nicotine. The monolayer was removed and the drug accumulation was radioametrically assessed by a liquid scintillation counter (Beckman Model) (n = 3).

This showed that even though a lot of these substrate/inhibitors do bind to the transporter they are not transported by it. They can be termed as competitive inhibitors of the hOCT1. The results from this data also corroborated previous studies where it

had been shown that verapamil is a known inhibitor of the hOCT1 transporter. Thus the use of immobilized hOCT1 columns as a possible screen for target lead optimization is a promising tool for Drug Discovery and also in the studying the characteristics of drug-protein binding which would help in the development of a suitable pharmacophore depicting the characteristics of the active site of the protein.

4.8 Conclusion

Quite clearly the main aim of this part of the programme had been achieved. The data from this study indicated that membranes from the hOCT1(+) and MDCK (hOCT1(-)) cell lines had been immobilized on IAMs (12 micron, 300 Å). Further the columns were fully characterized by conducting displacement chromatographic studies and binding affinities were calculated for a series of ligands. Importantly a linear regression analysis was carried out between the binding affinities obtained by frontal chromatography on the hOCT1 column with those obtained by membrane binding studies reported in the literature (Zhang *et al.*, 1998; Bednarczyk *et al.*, 1989) to determine if differences represent a qualitative difference or a quantitative difference.

Further, the column demonstrated enantioselectivity showing that both the ionic and hydrophobic interactions are necessary for significant binding to occur between the ligand and the hOCT1, and position the ligand for the enantioselective hydrogen bonding interaction. This data was further confirmed by demonstrating that propranolol

enantioselectively inhibited the cellular uptake of [^{14}C]-TEA. Therefore it indicated that for the compounds used in this study, the chromatographically determined affinities and enantioselectivities also reflected pharmacologically relevant properties.

Molecular models of enantiomers of propranolol, atenolol and pseudoephedrine were used to construct a preliminary pharmacophore which showed that the configuration around the centers were identical for (S)-propranolol, (S)-atenolol and (1R;2R)-pseudoephedrine. The resulting pharmacophore contained hydrophobic and ion pair interaction sites and the calculated distance between these sites was $\sim 5\text{\AA}$ which was consistent with the previously described hOCT1 pharmacophore in which the calculated distances between three hydrophobic areas and a positive ionizable site ranged from 4.2\AA to 5.3\AA (Bednarczyk *et al.*, 2003). Also some new and exciting results led to the identification of a third site, a hydrogen bond donor site, located 4.3\AA from the hydrophobic site and 2.2\AA from the ion pair interaction site. Conclusion from these data does indicate that immobilized biopolymeric hOCT1 transporter columns provide an excellent tool in studying for the drug-protein binding and gives us both qualitative and quantitative data which is comparable to other methods. Also further work with more ligands will help in the proper characterization of the active sites of this transporter and enable in the validation of the pharmacophore for this transporter.

Chapter 5

5. Conclusion and Suggestion for Future Work

Membrane bound receptors and trans-membrane transporters and ion channels are difficult to characterize and to utilize in Drug Discovery unless you have a marker ligand. The parallel screening technique demonstrated by the Pgp(+) and Pgp(-) OT columns is a new and important approach to this problem. It will be particularly important in characterizing orphan receptors, ion channels and transporters. To put this use into focus, G-protein coupled receptors (GPCRs) are the target for over 50% of the marketed drugs. The human genome contains about 1,000 genes which encode for approximately 10,000 GPCRs and only a few 100 GPCRs have been characterized.

The data from this research programme indicated that membranes from a cell line expressing a target receptor or transporter could be immobilized on the surface of glass capillaries with retention of the target's binding activity, and that this activity could be measured using displacement frontal chromatographic techniques. The results from the programme also demonstrated that since cellular membranes were immobilized, instead of the purified target, the membranes contributed specific and non-specific off-target binding to the observed chromatographic retention. This necessitated the construction of a second open tubular capillary column using membranes from a cell line that does not express the target receptor or transporter. The target (-) column could then be used as a control for the target (+) column. This approach should be applicable for use with any membrane bound target where "knock-in" or "knock-out" cell lines are available. In this study, Pgp (+)-OT and Pgp (-)-OT columns were used in 30-min parallel frontal

chromatographic experiments to qualitatively rank compounds based upon their relative affinities for the immobilized Pgp transporter. The Pgp(+)-OT / Pgp(-)-OT approach permitted the ranking of up to 200 compounds per week and, as the columns are active for between 3 and 4 weeks, each pair could be used to screen a minimum of 800 compounds. This capacity would be comfortable enough for the primary role envisaged for this technology, i.e. as a secondary screen for profiling predevelopment candidates. The chromatographic approach should be a significant advance over the current approach to the determination of a Pgp substrate/inhibitor, which involves the use of multiple Pgp assays and a complex classification system of transported and non-transported substrates and inhibitors. A comparative inter-assay assessment is currently being conducted with a larger cohort of compounds and will be reported elsewhere (Moaddel & Wainer, starting 2005).

The success of these experiments would help to generate affinity chromatography models for other proteins. There should now be a more effective route into meeting the important, exciting, but demanding challenges of elucidating the molecular mechanisms of these solute carrier transporters. For example, the ultimate manifestation of this technology could be an arrangement of such transporter protein and other columns that would allow the study of all the significant drug protein interactions taking place in the brain.

In order to extract the maximum potential out of these possibilities that arise from this research programme there are a number of further studies that would be useful. It is vital that these proteins be crystallized, their tertiary structure determined by X-ray crystallography and their binding sites characterized by affinity labeling, site-directed mutagenesis and biochromatography and QSAR modeling. Also since these transporters exhibits marked species variance it is of high importance that all the human transporters are identified, cloned, characterized and localized. The expression systems with these transporters i.e. immobilized protein based stationary phases, will help in identifying new drugs with optimized secretion properties. Also the knowledge regarding the structure-activity relationship of these binding sites and their transport mechanism will help to design drugs that have modulated transporter activities.

Also this technique with its versatility in determining binding constants of drugs or active compounds to pharmaceutical biological targets, offers an interesting opportunity in the characterization of the ligand binding sites. The immobilized biopolymers can be used in on-line pharmacological studies and as rapid screen for the isolation and identification of lead drug candidates from complex biological mixtures. Besides it can also be applied to determine apparent equilibrium constants (association constants, dissociation constants, binding constants) using very small amount of biopolymer and ligand. Also these affinity chromatographic methods are of particular relevance in monitoring interactions between exogenous or endogenous compounds in binding to different drug receptors. This would lead to the understanding of their pharmacological and/or toxicological activities.

Therefore in conclusion the use of affinity chromatographic methods are valid for high throughput screening of compound libraries, for the development of new drugs and for their safe use, the activity of a drug not being fully understood without understanding its binding to target proteins. Thus affinity chromatography provides a unique contribution and moves the field along from conventional use of purified proteins.

Chapter 6

6. References

Albuquerque EX, Alkondon M, Pereira EF, Castro NG, Schratzenholz A, Barbosa CT, Bonfante-Cabarcas R, Aracava Y, Eisenberg HM, Maelicke A. Properties of neuronal nicotinic acetylcholine receptors: pharmacological characterization and modulation of synaptic function. *J Pharmacol Exp Ther*, 280(3):1117-1136, 1997.

Arias HR. Binding sites for exogenous and endogenous non-competitive inhibitors of the nicotinic acetylcholine receptor. *Biochim Biophys Acta*, 1376(2):173-220, 1998.

Augustijns PF, Bradshaw TP, Gan LSL, et al. Evidence for a polarized efflux system in Caco-2 cells capable of modulating cyclosporine A transport. *Biochem Biophys Res Commun*, 197: 360-365, 1993.

Balimane PV, Patel K, Marino A and Chong S. Utility of 96 well Caco-2 cell system for increased throughput of P-gp screening in drug discovery. *Eur J Pharmacokin Biopharmaceut* 58: 90-105, 2004.

Balimane PV, Patel K, Marino A and Chong S (2004) Utility of 96 well Caco-2 cell system for increased throughput of P-gp screening in drug discovery. *Eur J Pharmacokin Biopharmaceut* 58, 90-105.

Barecki-Roach M, Wang E-J and Johnson WW (2003) Many p-glycoprotein substrates do not inhibit the transport process across cell membranes. *Xenobiotica* 33, 131-140.

Barrand MA, Bennett GC, Taylor CJ, et al. Immunohistochemical localization in rat brain microvessels of transporters involved in solute and water movements across the blood-brain barrier [abstract]. IVth International Conference: Cerebral Vascular Biology, Blood-Brain Barrier, Apr 1-5; Cambridge, UK, 2001.

Baynham MT, Patel S, Moaddel R & Wainer IW. Multidimensional on-line screening for ligands to the $\alpha 3\beta 4$ neuronal nicotinic acetylcholine receptor using an immobilized nicotinic receptor liquid chromatographic stationary phase. *J Chrom B*, 772:155-161, 2002.

Beaulieu E, Demeule M, Ghitescu L, et al. P-glycoprotein is strongly expressed in the luminal membranes of the endothelium of blood vessels in the brain. *Biochem J*, 326:539-544, 1997.

Bednarczyk D, Ekins S, Wikel JH, Wright SH. Influence of Molecular Structure on Substrate Binding to the Human Organic Cation Transporter, hOCT1. *Mol Pharmacol*, 63:489-498, 2003.

Bendayan R, Lee G & Bendayan M. Functional expression and localization of p-glycoprotein at the blood brain barrier. *Microscopy Research and Technique*, 57:365-380, 2002.

Biedler JL and Riehm H. Cellular resistance to actinomycin D in Chinese hamster cells in vitro: cross-resistance, radioautographic, and cytogenetic studies. *Cancer Res*. 30:1174-1184, 1970.

Biegel D, Spencer DD, Pachter JS, et al. Isolation and culture of human brain microvessel endothelial cells for the study of blood-brain barrier properties in vitro. *Brain Res*, 692:183-189, 1995.

Borst P, Evers R, Kool M & Wijnholds J. A family of drug transporters: the multidrug resistance-associated proteins. *J. Natl. Cancer Inst.* 92:1295-1302, 2000.

Boumendjel A, Pietro AD, Dumontet C & Barron D. Recent advances in the discovery of flavonoids and analogs with high-affinity binding to p-glycoprotein responsible for cancer cell multidrug resistance. *Medicinal Res. Rev*, 22(5):512-529, 2002.

Bruggemann EP, Germann UA, Gottesman MM, et al. Two different regions of phosphoglycoprotein are photoaffinitylabeled by azidopine. *J Biol Chem*, 264:15483, 1989.

Buccafusco JJ. Neuronal nicotinic receptor subtypes: defining therapeutic targets. *Molecular Interventions*, 4(5):285-293, 2004.

Busch AE, Quester S, Ulzheimer JC, Waldegger S, Gorboulev V, Arndt P, Lang F, Koepsell H. Electrogenic properties and substrate specificity of the polyspecific rat cation transporter rOCT1. *J Biol Chem*, 271:32599-32604, 1996.

Callaghan R, Berridge G, Ferry D.R, Higgins CF, Biochem. The functional purification of P-glycoprotein is dependent on maintenance of a lipid-protein interface. *Biophys. Acta* 1328:109, 1997.

Cailleau R, Young R, Olive M, Reeves WJ. Breast tumor cell lines from pleural effusions. *J. Natl Cancer Inst*, 53: 661-674, 1974.

Cailleau R, Olive M, Cruciger QVA. Long-term human breast carcinoma cell lines of metastatic origin:preliminary characterization. *In Vivo*, 14: 911-915, 1978.

Changeux JP, Galzi JL, Devillers-Thiery A, Bertrand D. The functional architecture of the acetylcholine nicotinic receptor explored by affinity labelling and site-directed mutagenesis. *Q Rev Biophys*, 25(4):395-432, 1992.

Chaudhary PM & Roninson IB. Induction of multidrug resistance in human cells by transient exposure to different chemotherapeutic drugs. *J National Cancer Institute*, 85:632-639, 1993.

Chiba P, Ecker G, Schmid D, et al. Structural requirements for activity of propafenone-type modulators in P-glycoprotein-mediated multidrug resistance. *Mol Pharmacol*, 49:1122-1130, 1996.

Chiba P, Holzer W, Landau M, et al. Substituted 4-acylpyrazoles and 4-acylpyrazolones: synthesis and multi-drug resistance-modulating activity. *J Med Chem*, 41: 4001-4011, 1998.

Chui WK, Wainer IW. Enzyme based HPLC supports as probes of enzyme activity and inhibition: The immobilization of trypsin and α -chymotrypsin on an immobilized artificial membrane HPLC support. *Anal. Biochem*, 201:237-245, 1992.

Cordon-Cardo C, O'Brien JP, Boccia J, et al. Expression of the multidrug resistance gene product (P-glycoprotein) in human normal and tumor tissues. *J Histochem Cytochem*, 38:1277-1287, 1990.

Dano K. Cross resistance between vinca alkaloids and anthracyclines in Erlich ascites tumor in vivo. *Cancer Chemother. Rep.* 56:701-708, 1972.

Dano K. Active outward transport of daunomycin in resistant Ehrlich ascites tumor cells. *Biochim. Biophys. Acta* 323:466-483, 1973.

Dean M, Rzhetsky A, Allikmets R. The human ATP-binding cassette (ABC) transporter superfamily. *Genome Res.* 11:1156-1166, 2001.

Dey S, Ramachandra M, Pastan I, Gottesman MM, Ambudkar SV. Evidence for two nonidentical drug interaction sites in the human P-glycoprotein. *Proc Natl Acad Sci USA*, 94:10594-10599, 1997.

Domenici E, Bertucci C, Salvadori P, Felix G, Cahagne I, Motellier S, Wainer IW. Synthesis and chromatographic properties of an HPLC chiral stationary phase based upon human serum albumin. *Chromatographia* 29:190-176, 1990.

Dresser MJ, Leabman MK, Giacomini KM. Transporters involved in the elimination of drugs in the kidney: Organic anion transporters and organic cation transporters. *J of Pharmaceutical Sci*, 90:397-421, 2001.

Dwoskin LP, Crooks PA. Competitive neuronal nicotinic receptor antagonists: a new direction for drug discovery. *J Pharmacol Exp Ther*, 298(2):395-402, 2001.

Early Breast Cancer Trialists' Collaborative Group. Polychemotherapy for early breast cancer: an overview of the randomised trials. *Lancet*, 352:930-942, 1998.

Ecker G, Huber M, Schmid D, et al. The importance of a nitrogen atom in modulators of multidrug resistance. *Mol Pharmacol*, 56: 791-796, 1999.

Elferink R, Meijer D, Kuipers F, Jansen P, Groen A, Groothuis G. *Biochim Biophys Acta*, 1241:215-268, 1995.

Eytan GD, Regev R, Oren G, Hurwitz CD, Assaraf YG. Efficiency of P-glycoprotein mediated exclusion of rhodamine dyes from multidrug resistance cells is determined by their passive transmembrane movement rate. *Eur J Biochem*, 248:104-112, 1997.

Faber KN, Muller M, Jansen PLM. Drug transport proteins in the liver. *Advanced Drug Delivery Rev*, 55: 107-124, 2003.

Ferry DR, Malkandi PJ, Russel MA and Kerr DJ. Allosteric regulation of [³H] vinblastine binding to P-glycoprotein of MCF-7 ADR cells by dexniguldipine. *Biochem Pharmacol*, 49:1851-1861, 1995.

Fiedler B, Scheiner-Bobis G. Transmembrane topology of alpha- and beta-subunits of Na⁺, K⁺-ATPase derived from beta-galactosidase fusion proteins expressed in yeast. *J Biol Chem*, 271:29312-29320, 1996.

Ferry D.R, Malkhandi P.J, Russell M.A, Kerr D. Allosteric regulation of [³H]-vinblastine binding to P-glycoprotein of MCF-7 ADR cells by dexniguldipine. *J. Biochem. Pharmacol*, 49:1851, 1995.

Fojo AT, Ueda K, Slamon DJ. Expression of a multidrug resistance gene in human tumors and tissues. *Proc Natl Acad Sci USA*, 84:265-269, 1987.

Fricke G, Drewe J, Huwyler J, et al. Relevance of P-glycoprotein for the enteral absorption of cyclosporine A: in vitro-in vivo correlation. *Br J Pharmacol*, 118:1841-1847, 1996.

Furuya R, Oka K, Watanabe I, Kamiya Y, Itoh H, Andoh T. The effects of ketamine and propofol on neuronal nicotinic acetylcholine receptors and P2x purinoceptors in PC12 cells. *Anesth Analg*, 88(1):174-180, 1999.

Cacini W, Keller MB, Grund VR. Accumulation of cimetidine by kidney cortex slices. *J Pharmacol Exp Ther*, 221:342-346, 1982.

Garrigues A, Nugier J, Orlowski S and Ezan E (2002) A high-throughput screening microplate test for the interaction of drugs with P-glycoprotein. *Anal Biochem* 305, 106-114

Garrigues A, Nugier J, Orlowski S and Ezan E. A high-throughput screening microplate test for the interaction of drugs with P-glycoprotein. *Anal Biochem* 305:106-114, 2002.

Gingrich JA, Andersen PH, Tiberi M, El Mestikawy S, Jorgensen PN, Fremeau RT, Jr, Caron MG. Identification, characterization, and molecular cloning of a novel transporter-like protein localized to the central nervous system. *FEBS Lett*, 312:115-122, 1992.

Gottesman MM, Pastan I. Biochemistry of multidrug resistance mediated by the multidrug transporter. *Annu Rev Biochem*, 62:395-427, 1993.

Gottschalk I, Lagerquist C, Zuo S.-S, Lundqvist A, Lundahl P. Immobilized-biomembrane affinity chromatography for binding studies of membrane proteins. *J Chromatogr. B*, 768: 31-40, 2002.

Greenberger LM. Major photoaffinity drug labeling sites for iodoaryl azidoprazosin in P-glycoprotein are within or immediately C-terminal to transmembrane domains 6 and 12. *J Biol Chem*, 268:11417-25, 1993.

Gros P, Croop J & Housman D. Mammalian multidrug resistance gene: complete cDNA sequence indicates strong homology to bacterial transport proteins. *Cell* 47 371-380, 1986.

Gundish D. Nicotinic acetylcholine receptor ligands as potential therapeutics. *Expert Opin Ther Patents*, 15(9):1221-1239, 2005.

Hage D & Austin J. High-performance affinity chromatography and immobilized serum albumin as probes for drug- and hormone-protein binding. *J Chrom B* 739:39-54, 2000.

Hait WN & Aftab DT. Rational design and pre-clinical pharmacology of drugs for reversing multidrug resistance. *Biochem Pharmacol.*, 43:103-107, 1992.

Hegewisch-Becker S. MDR1 reversal: criteria for clinical trials designed to overcome the multidrug resistance phenotype, *Leukemia* 10(Suppl. 3):532-538, 1996.

Hernandez SC, Bertolino M, Xiao Y, Pringle KE, Caruso FS, Kellar KJ. Dextromethorphan and its metabolite dextrorphan block $\alpha 3\beta 4$ neuronal nicotinic receptors. *J Pharmacol Exp Ther*, 293(3):962-967, 2000.

Higgins CF & Gottesman MM. Is the multidrug transporter a flippase? *Trends Biochem. Sci.* 17:18-21, 1992.

Hijazi Y, Bolon M, Boulieu R. Stability of ketamine and its metabolites norketamine and dehydronorketamine in human biological samples. *Clin Chem*, 47(9):1713-1715, 2001.

Hochman JH, Yamazaki M, Ohe T and Lin JH (2002) Evaluation of drug interactions with P-glycoprotein in drug discovery: in vitro assessment of the potential for drug-drug interactions with P-glycoprotein *Curr Drug Metab* 3, 257-273.

Holladay MW, Dart MJ and Lynch JK. Neuronal nicotinic acetylcholine receptors as targets for drug discovery. *J. Med. Chem.*, 40: 4169-4177, 1997.

Hucho F, Tsetlin VI, Machold J. The emerging three-dimensional structure of a receptor. The nicotinic acetylcholine receptor. *Eur J Biochem*, 239(3):539-557, 1996.

Hung LW, Wang IX, Nikaido K et al. Crystal structure of the ATP-binding subunits of an ABC transporter. *Nature*, 396:703-707, 1998.

Hunter J, Jepson MA, Tsuruo T, et al. Functional expression of P-glycoprotein in apical membranes of human intestinal Caco-2 cell layers: kinetics of vinblastine secretion and inter-action with modulators. *J Biol Chem*, 268: 14991-14997, 1993a.

Hunter J, Hirst BH, Simmons NL. Drug absorption limited by P-glycoprotein-mediated secretory drug transport in human intestinal epithelial Caco-2 cells. *Pharm Res*, 10: 743-749, 1993b.

Hsyu PH, Gisclon LG, Hui AC, Giacomini KM. Interactions of organic anions with the organic cation transporter in renal BBMV. *Am J Physiol*. 254:F56-F61, 1988.

Jadaud P, Thelohan S, Schonbaum GR & Wainer IW. The Stereochemical Resolution of Enantiomeric Free and Derivatized Amino Acids Using an HPLC Chiral Stationary Phase based on Immobilized α -Chymotrypsin. *Chirality* 1: 38-44, 1989.

Jozwiak K, Ravichandran S, Collins JR, Wainer IW. Interaction of noncompetitive inhibitors with an immobilized $\alpha 3\beta 4$ nicotinic acetylcholine receptor investigated by affinity chromatography, quantitative-structure activity relationship analysis, and molecular docking. *J Med Chem*, 47(16):4008-4021, 2004.

Juliano RL & Ling V. A surface glycoprotein modulating drug permeability in Chinese hamster ovary cell mutants. *Biochim. Biophys. Acta*, 455: 152-162, 1976.

Julien M, Kajiji S, Kaback RH & Gros P. Simple purification of highly active biotinylated p-glycoprotein: Enantiomer specific modulation of drug stimulated ATPase activity. *Biochemistry*, 39:75-85, 2000.

Kaliszan R & Wainer IW. Combinaton of biochromatography and chemometrics: A potential new research strategy in molecular pharmacology and drug design. In: Chromatographic separations based on molecular recognition. Wiley-VCH, Inc.USA, 1997.

Karlin A. Emerging structure of the nicotinic acetylcholine receptors. *Nat Rev Neurosci*, 3(2):102-114, 2002.

Katsura T, Takano M, Tomita Y, Yasuhara M, Inui K.-i, Hori R. *Biochim Biophys Acta*, 1146:197-202, 1993.

Kerr KM, Sauna ZE & Ambudkar SV. Correlation between steady-state ATP hydrolysis and vanadate induced ADP trapping in human p-glycoprotein. *J Bio Chem*, 276(12):8657-8664, 2001.

Klein I, Sarkadi B & Varadi A. An inventory of the human ABC proteins. *Biochim. Biophys. Acta* 1461 237-262, 1999.

Klepstad P, Maurset A, Moberg ER, Oye I. Evidence of a role for NMDA receptors in pain perception. *Eur J Pharmacol*, 187(3):513-518, 1990.

Koehler MR, Wissinger B, Gorboulev V, Koepsell H, Schmid M. The two human organic cation transporter genes SLC22A1 and SLC22A2 are located on chromosome 6q26. *Cytogenet Cell Genet*, 79:198-200, 1997.

Koepsell H, Gorboulev V and Arndt P. Molecular pharmacology of organic cation transporters in kidney. *J Membrane Biol*, 167:103-117, 1999.

Kolbah TA, Wainer IW. Application of an enzyme-based stationary phase to the determination of enzyme kinetic constants and types of inhibition: A new HPLC approach utilizing an immobilized artificial membrane chromatographic support. *J Chrom. A*, 653:122-129, 1993.

Korzekwa KR, Krishnamachary N, Shou M, Ogai A, Parise RA, Rettie AE, Gonzalez FJ, Tracy TS. Evaluation of atypical cytochrome P450 kinetics with two substrate models:evidence that multiple substrates can simultaneously bind to cytochrome P450 active sites. *Biochemistry*, 37:4137-4147, 1998.

Lahjouji K, Mitchell GA and Qureshi IA. Carnitine transport by organic cation transporters and systemic carnitine deficiency. *Mol Genetics and Metabolism*,73: 287-297, 2001.

Lee CG, Ramachandra M, Jeang KT, Martin MA, Pastan I & Gottesman MM. Effect of ABC transporters on HIV-1 infection: inhibition of virus production by the MDR1 transporter. *FASEB J*, 14:516-522, 2000.

Lee W and Kim RB. Transporters and renal drug elimination. *Annu Rev Pharmacol Toxicol*, 44:137-166, 2004.

Lentz KA, Polli JW, Wring SA, Humphreys JE and Polli JE (2000) Influence of passive permeability on apparent p-glycoprotein kinetics. *Pharmaceut Res* 17, 1456-1460.

Leonessa F & Clarke K. ATP binding cassette transporters and drug resistance in breast cancer. *Endocrine-Related Cancer*, 10:43-73, 2003.

Leonessa F, Kim JH, Ghiorghis A, Kulawiec RJ, Hammer C, Talebian A & Clarke R. C-7 analogues of progesterone as potent inhibitors of the p-glycoprotein efflux pump. *J Med Chem*, 45:390-398, 2002.

Lin JH & Yamazaki M. Role of p-glycoprotein in pharmacology. *Clin Pharmacokinet*, 42(1):59-98, 2003.

Ling V & Thompson LH. Reduced permeability in CHO cells as a mechanism of resistance to colchicine. *J. Cell Physiol*. 83 103-116, 1974.

Litman T, Zeuthen T, Skovsgaard T, Stein WD. Competitive, noncompetitive and cooperative interactions between substrates of P-glycoprotein as measured by its ATPase activity. *Biochim Biophys Acta*, 1361:169-176, 1997.

Lloyd KG and Williams M. Reactions to total dose infusion of iron dextran in rheumatoid arthritis. *J. Pharmacol. Exp. Ther*, 292: 461-469, 1999.

Loo TW & Clarke DM. Rapid purification of human p-glycoprotein mutants expressed transiently in HEK 293 cells by nickel-chelate chromatography and characterization of their drug stimulated ATPase activities. *J Bio Chem*, 270(37):21449-21452, 1995.

Loo TW & Clarke DM. Identification of residues in the drug_binding site of human P_glycoprotein using a thiol_reactive substrate. *J Biol. Chem.* 272:31945-31948, 1997.

Loo TW & Clarke DM. Identification of residues in the drug_binding domain of human P_glycoprotein. Analysis of transmembrane segment 11 by cysteine_scanning mutagenesis and inhibition by dibromobimane. *J. Biol. Chem.* 274:35388-35392, 1999a.

Loo TW & Clarke DM. Determining the structure and mechanism of the human multidrug resistance P_glycoprotein using cysteine_scanning mutagenesis and thiol_modification techniques. *Biochim. Biophys. Acta* 1461:315-325, 1999b.

Loo TW & Clarke DM. Identification of residues within the drug_binding domain of the human multidrug resistance P_glycoprotein by cysteine_scanning mutagenesis and reaction with dibromobimane. *J. Biol. Chem.* 275:39272-39278, 2000.

Loo TW & Clarke DM. Determining the dimensions of the drug_binding domain of human P_glycoprotein using thiol cross_linking compounds as molecular rulers. *J. Biol. Chem.* 276:36877-36880, 2001a.

Loo TW & Clarke DM. Cross-linking of human multidrug resistance P-glycoprotein by the substrate tris-(2-maleimidoethyl)amine, is altered by ATP hydrolysis. *J. Biol. Chem.* 276:31800-31805, 2001b.

Loo TW & Clarke DM. Vanadate trapping of nucleotide at the ATP_binding sites of human multidrug resistance P_glycoprotein exposes different residues to the drug_binding site. Proc. Natl. Acad. Sci. USA 99:3511-3516, 2002.

Lough WJ. Chiral Liquid Chromatography. In: WH DE Camp: ed. Immobilized proteins as HPLC chiral stationary phases. New York: Chapman and Hall, 1989, pp 130.

Lough WJ & Wainer IW. Chirality in natural and applied science. Blackwell Science Ltd, Oxford, 2002.

Loun B & Hage D. Characterization of thyroxine – albumin binding using high-performance affinity chromatography. J. Chromatogr B 579 (2): 225-235, 1992.

Lu L, Leonessa F, Clarke R & Wainer IR. Competitive and allosteric interactions in ligand binding to p-glycoprotein as observed on an immobilized p-glycoprotein liquid chromatographic stationary phase. Mol Pharmacol, 59:62-68, 2001.

Lu L, Leonessa F, Clarke R and Wainer IW (2001) Competitive and allosteric interactions in ligand binding to P-glycoprotein as observed on an immobilized P-glycoprotein liquid chromatographic stationary phase. Molec. Pharmacol. 658, 1-7.

Marger MD, Saier MH Jr. A major superfamily of transmembrane facilitators that catalyse uniport, symport and antiport. Trends biochem Sci, 18:13-20, 1993.

Marle I, Erlandsson P, Hansson L, Isaksson R, Pettersson C, Pettersson G. Separation of enantiomers using cellulase (CBH I) silica as a chiral stationary phase. J Chromatogr 589:233-248, 1991.

Marle I, Karlsson A & Pettersson C. Separation of enantiomers using α -chymotrypsin-silica as a chiral stationary phase. J Chrom 604(2):185-196, 1992.

Marietta MP, WAY WL, Castagnoli N Jr, Trevor AJ. On the pharmacology of the ketamine enantiomorphs in the rat. J Pharmacol Exp Ther, 202(1):157-165, 1977.

Martin C, Higgins CF & Callaghan R. The vinblastine binding site adopts high- and low-affinity conformations during a transport cycle of p-glycoprotein. *Biochemistry*, 40:15733-15742, 2001.

Meyer-Wentrup F, Karbach U, Gorboulev V, Arndt P, Koepsell H. Membrane localization of the electrogenic cation transporter rOCT1 in rat liver. *Biochem Biophys Res Commun*, 248:673-678, 1998.

Meschter CL, Connolly JM, Rose DP. Influence of regional location of the inoculation site and dietary fat on the pathology of MDA-MB-435 human breast cancer cell-derived tumors, growing in nude mice. *Clin. Exp Metastasis*, 10:167-173, 1992.

Moaddel R, Lu Lili, Baynham M & Wainer IW. Immobilized receptor- and transporter-based liquid chromatographic phases for on-line pharmacological and biochemical studies: a mini-review. *J Chrom B*, 768:41-53, 2002.

Moaddel R, Bullock P and Wainer IW. Development and characterization of an open tubular column containing immobilized p-glycoprotein for rapid on-line screening for p-glycoprotein substrates. *J Chromat B* 799, 255-263, 2004.

Moaddel R & Wainer IW. Immobilized nicotinic receptor stationary phases: going with the flow in high-throughput screening and pharmacological studies. *J Phar Biomedical Analysis*, 30:1715-1724, 2003.

Moaddel R, Jozwiak K, Whittington K, Wainer, IW. Conformational mobility of immobilized $\alpha 3\beta 2$, $\alpha 3\beta 4$, $\alpha 4\beta 2$, $\alpha 4\beta 4$ □ nicotinic receptor stationary phases, *Anal. Chem*, 77:895-901, 2005.

Moaddel R, Yamaguchi R, Ho P, Patel S, Hsu C-P, Subrahmanyam V, Wainer, I.W. Development and characterization of an immobilized human organic cation transporter based liquid chromatographic stationary phase. *J. Chromatogr. B*, 818:263-268, 2005.

Mol W, Fokkema G, Weert B, Meijer D. Mechanisms for the hepatic uptake of organic cations. Studies with the muscle relaxant vecuronium in isolated rat hepatocytes. *J Pharmacol Exp Ther*, 244:268-274, 1988.

Nelson EJ, Zinkin NT, Hinkle PM. Fluorescence methods to assess multidrug resistance in individual cells. *Cancer Chemother Pharmacol*, 42:292-299, 1998.

Newhouse P, Singh A, Potter A. Nicotine and nicotinic receptor involvement in neuropsychiatric disorders. *Curr Top Med Chem*, 4(3):267-282, 2004.

Noctor TAG, Diaz-Perez MJ, Wainer IW. Use of a human serum albumin-based stationary phase for high-performance liquid chromatography as a tool for the rapid determination of drug-plasma protein binding. *J Pharm Sci* 82:675-676, 1993.

Osterberg T, Norinder U. Theoretical calculation and prediction of P-glycoprotein-interacting drugs using MolSurf parametrization and PLS statistics. *Eur J Pharm Sci*, 10:295-303, 2000.

Oye I, Paulsen O, Maurset A. Effects of ketamine on sensory perception: evidence for a role of N-methyl-D-aspartate receptors. *J Pharmacol Exp Ther*, 260(3):1209-1213, 1992.

Pan B-F, Dutt A, Nelson JA. Enhanced transepithelial flux of cimetidine by Madin-Darby canine kidney cells overexpressing human P-glycoprotein. *J Pharmacol Exp Ther*, 270:1-7, 1994.

Panwala CM, Jones JC, Viney JL. A novel model of inflammatory bowel disease: mice deficient for the multiple drug resistance gene, *mdr1a*, spontaneously develop colitis. *J Immunol*, 161:5733-5744, 1998.

Pascaud C, Garrigos M, Orłowski S. Multidrug resistance transporter P-glycoprotein has distinct but interacting binding sites for cytotoxic drugs and reversing agents. *Biochem J*, 333:351-358, 1998.

Price JE, Polyzos A, Zhang RD, Daniels LM. Tumorigenicity and metastasis of human breast carcinoma cell lines in nude mice. *Cancer Research*, 50:717-721, 1990.

Ramachandra M, Ambudkar SV, Chen D, Hrycyna CA, Dey S, Gottesman MM, Pastan I. Human p-glycoprotein exhibits reduced affinity for substrates during a catalytic transition state. *Biochemistry*, 37:5010-5019, 1998.

Raviv Y, Pollard HB, Bruggemann EP, Pastan I & Gottesman MM. Photosensitized labeling of a functional multidrug transporter in living drug-resistant tumor cells. *J. Biol. Chem.* 265:3975-3980, 1990.

Reich DL, Silvay G. Ketamine: an update on the first twenty-five years of clinical experience. *Can J Anaesth*, 36(2):186-197, 1989.

Riehm H & Biedler JL. Cellular resistance to daunomycin in Chinese hamster cells in vitro. *Cancer Res.* 31:409-412, 1971.

Rocchi E, Khodjakov A, Volk EL, Yang CH, Litman T, Bates SE & Schneider E. The product of the ABC half-transporter gene ABCG2 (BCRP/MXR/ABCP) is expressed in the plasma membrane. *Biochem. Biophys. Res. Commun.* 271 42-46, 2000.

Rodriguez ME, Patel S & Wainer IW. Determination of the enantiomers of ketamine and norketamine in human plasma by enantioselective liquid chromatography-mass spectrometry. *J Chrom B*, 794:99-108, 2003.

Roninson IB, Abelson HT, Housman DE, Howell N & Varshavsky A. Amplification of specific DNA sequences correlates with multi-drug resistance in Chinese hamster cells. *Nature* 309 626-628, 1984.

Roninson IB, Chin JE, Choi KG, Gros P, Housman DE, Fojo A, Shen DW, Gottesman MM & Pastan I. Isolation of human mdr DNA sequences amplified in multidrug-resistant KB carcinoma cells. *Proc. Natl. Acad. Sci. USA* 83 4538-4542, 1986.

Rosenberg MF, Callaghan R, Ford RC & Higgins CF. Structure of the multidrug resistance P_glycoprotein to 2.5 nm resolution determined by electron microscopy and image analysis. *J. Biol. Chem.* 272 10685-10694, 1997.

Sakaeda T, Nakamura T & Okumura K. MDR1 genotype-related pharmacokinetics and pharmacodynamics. *Biol Pharm Bull.* 25(11):1391-1400, 2002.

Sarkadi B, Price EM, Boucher RC, Germann UA, Scarborough GA. Expression of the human multidrug resistance cDNA in insect cells generates a high activity drug stimulated membrane ATPase. *J Biol Chem*, 267:4854-4858, 1992.

Sauan ZE & Ambudkar SV. Evidence for a requirement for ATP hydrolysis at two distinct steps during a single turnover of the catalytic cycle of human p-glycoprotein. *PNAS*, 97(6):2515-2520, 2000.

Sauan ZE & Ambudkar SV. Characterization of the catalytic cycle of ATP hydrolysis by human p-glycoprotein: The two ATP hydrolysis events in a single catalytic cycle are kinetically similar but affect different functional outcomes. *J Bio Chem*, 276(15):11653-11661, 2001.

Sauna ZE, Muller M, Peng ZH & Ambudkar SV. Importance of the conserved walker B glutamate residues, 556 and 1201, for the completion of the catalytic cycle of ATP hydrolysis by human p-glycoprotein (ABCB1). *Biochemistry*, 41:13989-14000, 2002.

Schneider H, Scheiner-Bobis G. Involvement of the M7/M8 extracellular loop of the sodium pump alpha subunit in ion transport. Structural and functional homology to P-loops of ion channels. *J Biol Chem*, 272:16158-16165, 1997.

Schwab D, Fischer H, Tabatabaei A, Poli S & Huwyler J. comparison of in vitro p-glycoprotein screening assays: Recommendations for their use in drug discovery. *J Med Chem*, 46:1716-1725, 2003.

Schwab D, Fischer H, Tabatabaei A, Poli S and Huwyler J (2003) Comparison of in vitro P-glycoprotein screening assays recommendations for their use in drug discovery. *J Med Chem* 46, 1710-1725.

Seelig A. How does P-glycoprotein recognize its substrates? *Int J Clin Pharmacol Ther* 1998; 36: 50-54, 1998.

Seelig A, Landwojtowicz E. Structure-activity relationship of P-glycoprotein substrates and modifiers. *Eur J Pharm Sci*, 12:31-40, 2000.

Senior AE, Gadsby DC. ATP hydrolysis cycles and mechanism in p-glycoprotein and CFTR. *Semin Cancer Biol*, 8:143-150, 1997.

Shapiro AB & Ling V. The mechanism of ATP-dependent multidrug transport by P-glycoprotein. *Acta Physiol Scand Suppl*, 643:227-234, 1998.

Sheikh MI. Renal handling of phenol red. II. The mechanism of substituted phenolsulphophthalein (PSP) dye transport in rabbit kidney tubules in vitro. *J Physiol*, 256:175-195, 1976.

Shirai A, Naito M, Tatsuta T, et al. Transport of cyclosporin A across the brain capillary endothelial cell monolayer by P-glycoprotein. *Biochim Biophys Acta*, 1222: 400-404, 1994.

Singh C. Rational use of in vitro P-glycoprotein assays in drug discovery. *J Exp Therap* 399:620-628, 2001.

Sonveaux N, Shapiro AB, Goormaghtigh E and Ling V. Secondary and tertiary structure changes of reconstituted P-glycoprotein. *J Biol Chem* 271:24617-24624, 1996.

Stephens JC, Schneider JA, Tanguay DA, Choi J, Acharya T, Stanley SE, Jiang R, Messer CJ, Chew A, Han JH, Duan J, Carr JL, Lee MS, Koshy B, Kumar AM, Zhang G, Newell WR, Windemuth A, Xu C, Kalbfleisch TS, Shaner SL, Arnold K, Schulz V,

Drysdale CM, Nandabalan K, Judson RS, Ruano G, Vovis GF. *Science*, 293:489-493, 2001.

Steen H, Merema M, Meijer D. A multispecific uptake system for taurocholate, cardiac glycosides and cationic drugs in the liver. *Biochem Pharmacol*, 44:2323-2331, 1992.

Steen H, Oosting R, Meijer D. Mechanisms for the uptake of cationic drugs by the liver: a study with tributylmethylammonium (TBU⁺MA). *J Pharmacol Exp Ther*, 258:537-543, 1991.

Sukhai M & Piquette-Millaer M. Regulation of the multidrug resistance genes by stress signals. *J Pharmacy & Pharmaceutical Sciences*, 3:268-280, 2000.

Sun J, He Z-G, Cheng G, Wang S-J, Han X-H and Zou M-J (2004) Multidrug resistance P-glycoprotein: crucial significance in drug disposition and interaction. *Med Sci Monit* 10, RA5-14.

Svensson JO, Gustafsson LL. Determination of ketamine and norketamine enantiomers in plasma by solid-phase extraction and high-performance liquid chromatography. *J Chromatogr B Biomed Appl*, 678(2):373-376, 1996.

Taguchi Y, Kino K, Morishima M, et al. Alteration of substrate specificity by mutations at the His61 position in predicted transmembrane domain 1 of human MDR1/P-glycoprotein. *Biochemistry*, 36: 8883-8889, 1997a.

Taguchi Y, Morishima M, Komano T, et al. Amino acid substitutions in the first transmembrane domain (TM1) of P-glycoprotein alter substrate specificity. *FEBS Lett*, 413:142-146, 1997b.

Takeda M, Narikawa S, Hosoyamada M, Cha SH, Sekine T, Endou H. Characterization of organic anion transport inhibitors using cells stably expression human organic anion transporters. *European J Pharmacol*, 419:113-120, 2001.

Tan B, Piwnica-Worms D, Ratner L. Multidrug resistance transporters and modulation, *Curr. Opin. Oncol.* 12 450–458, 2000.

Tang-Wai DF, Brossi A, Arnold LD, et al. The nitrogen of the acetamido group of colchicine modulates P-glycoprotein-mediated multidrug resistance. *Biochemistry*, 32: 6470-6476, 1993.

Tassonyi E, Charpantier E, Muller D, Dumont L, Bertrand D. The role of nicotinic acetylcholine receptors in the mechanisms of anesthesia. *Brain Res Bull*, 57(2):133-150, 2002.

Tatsuta T, Naito M, Oh-hara T, et al. Functional involvement of P-glycoprotein in blood-brain barrier. *J Biol Chem*, 267: 20383-20391, 1992.

Thelohan S, Jadaud PH, Wainer IW. Immobilized Enzymes as Chromatographic Phases for HPLC: The Chromatography of Free and Derivatized Amino Acids on Immobilized Trypsin. *Chromatographia* 28(11-12):551-555, 1989.

Thiebaut F, Tsuruo T, Hamada H, et al. Cellular localization of the multidrug resistance gene product P-glycoprotein in normal human tissues. *Proc Natl Acad Sci U S A*, 84: 7735-7738, 1987.

Tiberghien F & Loo R. Ranking of P-glycoprotein substrates and inhibitors by a calcein-AM fluorometry screening assay. *Anticancer Drugs*, 7:568-578, 1996.

Tolle-Sander S, Rautio J, Wring S, Polli JW and Polli JE. Midazolam exhibits characteristics of a highly permeable p-glycoprotein substrate. *Pharmaceut Res* 20:757-764, 2003.

Tsuji A, Terasaki T, Takabatake Y, et al. P-glycoprotein as the drug efflux pump in the primary cultured bovine brain capillary endothelial cells. *Life Sci*, 51: 1427-37, 1992.

Tsuji A, Tamai I, Sakata A, et al. Restricted transport of cyclosporine A across the blood-brain barrier by a multidrug transporter, P-glycoprotein. *Biochem Pharmacol*, 46:1096-1099, 1993.

Ueda K, Okamura N, Hirai M, et al. Human P-glycoprotein transports cortisol, aldosterone, and dexamethasone, but not progesterone. *J Biol Chem*, 267: 24248-24252, 1992.

Ueda K, Taguchi Y, Morishima M. How does P-gp recognize its substrates? *Semin Cancer Biol*, 8:151-159, 1997.

Ullrich KJ, Papavassiliou F, David C, Rumrich G, Fritzsche G. *Pfluegers Arch*, 419:84-92, 1991.

Ullrich KJ, Rumrich G, David C, Fritzsche G. Bisubstrates: substances that interact with both, renal contraluminal organic anion and organic cation transport systems. II. Zwitterionic substrates: dipeptides, cephalosporins, quinolone-carboxylate gyrase inhibitors and phosphamide thiazine carboxylates; nonionizable substrates: steroid hormones and cyclophosphamides. *Pfluegers Arch*, 425:280-299, 1993.

Ullrich KJ, Rumrich G. Luminal transport system for choline⁺ in relation to the other organic cation transport systems in the rat proximal tubule. Kinetics, specificity: alkyl/aryl amines, alkyl amines with OH, O, SH, NH₂, ROCO, RSCO and H₂PO₄-groups, methylaminostyryl, rhodamine, acridine, phenanthrene and cyanine compounds. *Pfluegers Arch*, 432:471-485, 1996.

Ullrich KJ, Rumrich G, Neiteler K, Fritzsche G. Contraluminal transport of organic cations in the proximal tubule of the rat kidney. II. Specificity: anilines, phenylalkyl amines (catecholamines), heterocyclic compounds (pyridines, quinolines, acridines). *Pfluegers Arch*, 420:29-38, 1992.

Urbatsch IL, al SM, Senior AE. Characterization of the ATPase activity of purified Chinese hamster P-glycoprotein. *Biochemistry*, 33:7069-7076, 1994.

Urbatsch IL, Gimi K, Mounts SW, Marmarosh NL, Rousseau ME, Gross P & Senior AE. Cysteines 431 and 1074 are responsible for inhibitory disulfide cross-linking between the two nucleotide-binding sites in human p-glycoprotein. *J Bio Chem*, 276(29):26980-26987, 2001.

Wainer IW. Drug stereochemistry. Analytical methods and pharmacology. 2nd edn. Marcel Dekker, New York, 1993.

Wainer IW, Zhang Y, Xiao Y, Kellar KJ. Liquid chromatographic studies with immobilized neuronal nicotinic acetylcholine receptor stationary phases: effects of receptor subtypes, pH and ionic strength on drug-receptor interactions. *J Chrom B*, 724(1):65-72, 1999.

Wainer IW. Drug Stereochemistry: Analytical Methods and Pharmacology. 2nd Ed. Marcel Dekker, N.Y., 1993, pp 167-172.

Wandel C, Kim RB, Kajiji S, Guengerich P, Wilkinson GR & Wood AJJ. P-glycoprotein and cytochrome P-450 3A inhibition: Dissociation of inhibitory potencies. *Cancer Research*, 59:3944-3948, 1999.

Wang E, Casciano CN, Clement RP and Johnson WW. Two transport binding sites of P-glycoprotein are unequal yet contingent: initial rate kinetic analysis by ATP hydrolysis demonstrates intersite dependence. *Biochim Biophys Acta* 1481: 63-74, 2000.

Wang E, Casciano CN, Clement RP and Johnson WW (2000) Two transport binding sites of P-glycoprotein are unequal yet contingent: initial rate kinetic analysis by ATP hydrolysis demonstrates intersite dependence. *Biochim Biophys Acta* 1481, 63-74.

Wang, E, Lew. K, Casciano C.N. , Clement R.P. , Johnson W.W. Antimicrobial. *Agents Chemother.* 46 (2002) 160. [15] S. Dey, M. Ramachandra, I. Pastan, M.M. Gottesman, S.V. Ambudkar, *Proc. Natl. Acad. Sci. U.S.A.* 94 (1997) 10594.

Wang EJ, Casciano CN, Clement RP, Johnson WW. Active transport of fluorescent p-glycoprotein substrates: evaluation as markers and interaction with inhibitors. *Biochem Biophys Res Commun*, 289:580-585, 2001.

Wang R, Casciano CN, Clement RP & Johnson WW. Two transport binding sites of p-glycoprotein are unequal yet contingent: initial rate kinetic analysis by ATP hydrolysis demonstrates intersite dependence. *Biochimica et Biophysica Acta*, 1481:63-74, 2000.

White PF, Ham J, Way WL, Trevor AJ. Pharmacology of ketamine isomers in surgical patients. *Anesthesiology*, 52(3):231-239, 1980.

White PF, Way WL, Trevor AJ. Ketamine--its pharmacology and therapeutic uses. *Anesthesiology*, 56(2):119-136, 1982.

Wu C-Y, Benet LZ, Hebert MF, et al. Differentiation of absorption and first-pass gut and hepatic metabolism in humans: studies with cyclosporine. *Clin Pharmacol Ther*, 58:492-497, 1995.

Wu Q, Bounaud P, Kudul S, et al. Identification of the domains of photoincorporation of the 3- and 7-benzophenone analogues of taxol in the carboxyl-terminal half of murine mdrlb P-glycoprotein. *Biochemistry*, 37: 11272-9, 1998.

Xiao Y, Meyer EL, Thompson JM, Surin A, Wroblewski J, Kellar KJ. Rat alpha3/beta4 subtype of neuronal nicotinic acetylcholine receptor stably expressed in a transfected cell line: pharmacology of ligand binding and function. *Mol Pharmacol*, 54(2):322-333, 1998.

Yamakura T, Chavez-Noriega LE and Harris RA. Subunit-dependent inhibition of human neuronal nicotinic acetylcholine receptors and other ligand-gated ion channels by dissociative anesthetics ketamine and dizocilpine. *Anesth.*, 92: 1144-1162, 2000.

Yanagihara Y, Ohtani M, Kariya S, Uchino K, Aoyama T, Yamamura Y, Iga T. Stereoselective high-performance liquid chromatographic determination of ketamine and its active metabolite, norketamine, in human plasma. *J Chromatogr B Biomed Sci Appl*, 746(2):227-31, 2000.

Zhang YX, Xiao YX, Kellar KJ, Wainer IW. Immobilized nicotinic receptor stationary phase for on-line liquid chromatographic determination of drug-receptor affinities. *Anal Biochem*, 264:22-25, 1998.

Zhang Y, Leonessa F, Clarke R, Wainer IW. Development of an immobilized P-glycoprotein stationary phase for on-line liquid chromatographic determination of drug-binding affinities. *J Chromatogr B Biomed Sci Appl*, 739(1):33-37, 2000

Zhang L, Schaner ME and Giacomini KM. Functional characterization of an organic cation transporter (hOCT1) in a transiently transfected human cell line (HeLa). *J Pharmacol and Exp Therapeutics*, 286: 354-361, 1998.

Zhang L, Brett CM and Giacomini KM. Role of organic cation transporters in drug absorption and elimination. *Annu Rev Pharmacol Toxicol*, 38:431-460, 1998.

Zhang L, Gorset W, Dresser MJ and Giacomini KM. The interaction of n-tetraalkylammonium compounds with a human organic cation transporter, hOCT1. *J of Pharmacol and Environmental Therapeutics*, 288:1192-1198, 1999.

Zhang Y, Leonessa F, Clarke R, Wainer IW. Development of an immobilized P-glycoprotein stationary phase for on-line liquid chromatographic determination of drug-binding affinities. *J. Chromatogr. B* 739:33-37, 2000.

CHAPTER 7

7. Appendices

7.1 Papers

1. Michael T. Baynham, Sharvil Patel, Ruin Moaddel, Irving W. Wainer. Multidimensional on-line screening for ligands to the alpha3beta4 neuronal nicotinic acetylcholine receptor using an immobilized nicotinic receptor liquid chromatographic stationary phase. *Journal of Chromatography B*, 772 (2002) 155–161.
2. Maria Esther, Sharvil Patel, Irving W. Wainer Determination of the enantiomers of ketamine and norketamine in human plasma by enantioselective liquid chromatography-mass spectrometry. *Journal of Chromatography B*, 794 (2003) 99–108.
3. Ruin Moaddel, Rika Yamaguchi, Paul Ho, Sharvil Patel, C-P Hsu, V Subrahmanyam, IW Wainer. Development and characterization of an immobilized human organic cation transporter based liquid chromatographic stationary phase. *In Press*.
4. Ruin Moaddel, Sharvil Patel, Krystof Jozwiak, Rika Yamaguchi, Paul Ho, IW Wainer. Enantioselective binding to the human cation transporter -1 (hOCT1) determined using an immobilized hOCT1 liquid chromatographic stationary phase. *In press*.

7.2 Chapters

1. Sharvil Patel, William J Lough, IW Wainer. Affinity-based chiral stationary phases. In: Handbook of Affinity Chromatography (David Hage, editor), Marcel Dekker Inc, NY, *In Press*.
2. Sharvil Patel, William J Lough, IW Wainer. Chromatographic studies of molecular recognition and solute binding to immobilized enzymes & plasma protein. In: Handbook of Affinity Chromatography (David Hage, editor), Marcel Dekker Inc, NY, *In Press*.

7.3 Abstracts & Presentations

1. Poster presentation at National Institute on Aging Intramural Research Program Annual Retreat. Evaluation of P-glycoprotein substrate binding and transport cycle by affinity chromatography. S Patel, R Moaddel, IW Wainer, F Leonessa. Laboratory of Clinical investigations, Bioanalytical Chemistry Section, Gerontology research center, National Institute on Aging, Baltimore MD.

7.4 Conferences

1. Organizing committee for First Ramanbhai Foundation International Symposium on Drug Development held in Ahmedabad, India on January 22-25, 2003. The theme of the symposium is “Recent Advances in Medicinal Chemistry”, with an emphasis on chirality and drug development, including the regulatory process.
2. HPLC 2002, Montreal, Canada.